The Effects of Macroscopic Heterogeneities of Pore Structure and Wettability on Residual Oil Recovery Using the Gravity-Assisted Inert Gas Injection (GAIGI) Process

by

Rafat Parsaei

A thesis
presented to the University of Waterloo
in fulfillment of the
thesis requirement for the degree of
Doctor of Philosophy
in
Chemical Engineering

Waterloo, Ontario, Canada, 2011

I hereby declare that I am the sole author of this thesis. This is a true copy of the thesis, including any required final revisions, as accepted by my examiners.

I understand that my thesis may be made electronically available to the public.

Rafat Parsaei

Abstract

To recover oil remaining in petroleum reservoirs after waterflooding, the gravitationally stable mode of gas injection is recognized as a promising tertiary oil recovery process. Understanding the phenomena occurring over the course of the gravity-assisted inert gas injection (GAIGI) process is thus important. Extensive studies on both secondary and tertiary modes of gravity drainage have shown promising results in recovering oil from homogeneous water-wet glass bead packs, sand packs, and sandstone cores, respectively. However, it is not realistic to anticipate similar flow mechanisms and recovery results in all types of reservoirs because the natural hydrocarbon reservoirs are all heterogeneous in terms of their permeability, porosity, and wettability. Such heterogeneities cause irregular displacement patterns, and nonuniform fluid distribution. The impact of heterogeneity of the porous media on the GAIGI process has not been fully addressed in the experimental studies carried out to date; therefore, this thesis aims to fill in the gap of knowledge on this area.

The impact of reservoir wettability and pore structure heterogeneities at the macroscopic scale on the recovery efficiency of the GAIGI process was investigated through a systematic experimental study for tertiary recovery of waterflood residual oil. To obtain heterogeneous (in terms of wettability) packings, isolated inclusions of oil-wet consolidated glass beads were embedded in a continuum of unconsolidated water-wet glass beads. Similarly, the heterogeneous porous media exhibiting permeability heterogeneity consisted of large-pore-size isolated regions randomly distributed in a small-pore-size continuum.

Upon waterflooding, significantly higher waterflood residual oil saturation was established in both cases of heterogeneous media in comparison to water-wet homogeneous porous media. The amount of waterflood residual oil varied linearly with the volume fraction of heterogeneities in the packings. Experimental results obtained from tertiary gravity drainage experiments demonstrated that the continuity of water-wet portions of the heterogeneous porous media facilitates the residual oil recovery through the film flow mechanism, provided that the oil spreading coefficient is positive. In addition, owing to the high waterflood residual oil content of the heterogeneous media tested, the oil bank formation occurred earlier and grew faster than that in homogeneous media, resulting in a higher oil recovery factor. However, the favorable wettability conditions in both the homogeneous and heterogeneous porous media exhibiting permeability heterogeneity resulted in slightly lower reduced

residual oil saturation after the GAIGI process compared to that in the heterogeneous media with wettability heterogeneity under the same condition of withdrawal rate. In addition, the oil recovery factor at gas breakthrough was found to be inversely related to the production rate due to the functionality of gravity and viscous forces over the course of gravity drainage. These two forces were combined into a dimensionless form, defined as the gravity number ($N_{gv}=K\Delta\rho_{og}g/\mu_o V_{pg}$). It was discovered that there is a correlation between the oil recovery factor at gas breakthrough and the gravity number for both the heterogeneous and homogeneous media. The correlation of recovery factor at gas breakthrough versus the gravity number in heterogeneous media followed a similar trend as that found for homogeneous water-wet porous media. However, at a given gravity number, the recovery factor in heterogeneous media was greater than that in the homogeneous media. This implies that heterogeneous media will be better target reservoirs for applying the GAIGI process compared to the homogeneous reservoirs.

Acknowledgements

I have become indebted to many people throughout this work for their support, advice, encouragement, and patience. There is no way to acknowledge them all or even any of them properly. I owe very special thanks to all of them.

In the first place, I would like to thank my supervisor Professor Ioannis Chatzis for providing feedback, comments, suggestions, and enlightening discussions throughout this research. His diverse experience and knowledge about the subject of this thesis led to many worthwhile discussions that were influential in completing this thesis. I am truly fortunate to have been able to join his research group and work with him.

I would like to gratefully thank Dr. Koichi Takamura for reading and evaluating this thesis as external examiner, and for providing motivating comments and suggestions. The discussions that we had in September 2010 while attending the *11th International Symposium on Evaluation of Wettability and its Effect on Oil Recovery* were helpful in improving this thesis.

I owe thanks to the other members of my dissertation committee, Dr. Anthony L. Endres, Dr. Jim F. Barker, Dr. Marios Ioannidis, and Dr. William Epling for the valuable time they spent reading my proposal and my thesis and for their insightful questions, intriguing ideas and constructive suggestions. Special thanks to Dr. Ioannidis for the practical advice he provided during the NMR tests, and for sharing his lab equipments with me.

My friends in Waterloo, too many to name individually, have been and continue to be a source of encouragement, ideas, and support. However, special thanks are due to Dr. Nima Rezaei and Dr. Lesley James for the many enjoyable and instructive discussions we've had, and for creating a fantastic atmosphere in the lab.

The financial support for my PhD program provided by the National Iranian Gas Company (NIGC) and the research grant provided by the Natural Sciences and Engineering Research Council of Canada (NSERC) are gratefully acknowledged.

My deepest gratitude goes to my parents for their never fading support, unconditional love, and patience. I also owe thanks to my sisters and brothers for their encouragement and continuous source of inspiration. I am eternally grateful to my husband Hossein, for his love, inestimable understanding,

and strength throughout the years. Without him, and his ability to raise my spirits when I was most discouraged, I could never make it this far. Thank you Hossein, you were the wind beneath my wings.

At last but not the least, I have been very grateful to have an angel from the heaven in the last year of my PhD program, my beloved daughter, Sana. She brought enjoyable moments and happiness to my life during the most important phase of my PhD journey.

Rafat Parsaei, Fall 2011

Dedication

This thesis is dedicated to

my parents,

my husband, Hossein,

my daughter, Sana,

and my sisters and brothers

Table of Contents

List of Figures

List of Tables

List of Symbols and Abbreviations

Latin Symbols

A	area [L^2]
g	acceleration due to gravity [LT^{-2}]
H	volume percentage of heterogeneities [-]
K	absolute permeability [L^2]
k	relative permeability [L^2]
L	length of porous medium [L]
N_B	Bond number [-]
N_{Ca}	capillary number [-]
N_{gv}	gravity number [-]
P	pressure [$ML^{-1}T^{-2}$]
PV	pore volume [L^3]
Q_L	liquid withdrawal rate [$L^3\ T^{-1}$]
R	glass bead radius [L]
$RF_{g.bkt}$	oil recovery factor at gas breakthrough [-]
RF^*	normalized oil recovery factor at gas breakthrough [-]
S	spreading coefficient [MT^{-2}]
S_o	average oil saturation [-]
S_{org}	reduced residual oil saturation [-]
S_{or}^*	waterflood residual oil saturation [-]
S_{wc}	connate water saturation [-]
s	surface area [L^2]
T	temperature [Θ]
t	time [T]
t_D	dimensionless time [-]
V_{pg}	pore velocity of the gas–liquid interface [LT^{-1}]
v	displacing fluid velocity [LT^{-1}]
v_c	critical velocity [LT^{-1}]

v	volume of displaced oil/water [L^3]
W_A	work of adhesion [MT^{-2}]
W_C	work of cohesion [MT^{-2}]
x	fraction of packing pore volume contributed by heterogeneities [-]

Greek Symbols

α	constant defined in Eq. (2-5)
θ	contact angle [-]
μ	viscosity [$ML^{-1}T^{-1}$]
ρ	density [ML^{-3}]
σ	surface tension [MT^{-2}]
ϕ	porosity [-]

Subscripts

bkt	breakthrough
g	gas
H	heterogeneity
L	liquid
M	matrix
o	oil
or	residual oil
org	reduced residual oil
S	solid
V	vapor
WR	water removal
w	water
wc	connate water

Superscripts

*	saturation/recovery limit, e.g., S_{or}^*, RF^*
min	minimum

Chapter 1

Introduction

1.1 Background

The growing world energy demand attributable to the rapid industrialization requires the production of increasing quantities of crude oil and at the same time maintaining acceptable cost levels. According to the latest report by the Oil and Gas Journal quoted from the International Energy Agency, the worldwide oil demand would climb to 89.3 million b/d this year (Radler and Bell 2011). To meet the energy demand, many abandoned, matured reservoirs have become the subject of Enhanced Oil Recovery (EOR) field trials in recent years. An important example of those reservoirs is the one which has undergone a secondary waterflood. The oil saturation remaining over the course of waterflooding can occur typically in 15 to 35% of the pore space; however, values as high as 50% pore volume have also been found in sandstones, dolomite rocks and carbonate rocks (Chatzis et al. 1983). The oil resources left-behind after primary and secondary stages have been estimated at the value of approximately 2 trillion barrels worldwide (Rao et al. 2004). Occurrence of a large amount of residual oil upon waterflooding necessitates considering an enhanced oil recovery method to extract oil from these "already discovered" resources.

The laboratory experiments have shown that nearly 100% of the waterflood residual oil can be recovered by tertiary gas injection under the conditions of water-wet porous media and positive oil spreading coefficient (Kantzas et al. 1988a). Several field reviews have also demonstrated oil recoveries of 85% to 95% of the original oil in place (Carlson 1988; Johnston 1988; Fassihi and Gillham 1993; Kulkarni 2004). This tertiary recovery process, known as gravity assisted inert gas injection (GAIGI), involves injecting gas into a relatively high permeability reservoir containing light

oil at the state of waterflood residual oil. Upon gas invasion, a continuous oil phase known as oil bank is formed and grows in size as it propagates between the gas-invaded zone and the water-saturated zone. It was shown by Kantzas et al. (1988a, 1988b) that gravity forces play a very important role in the oil drainage, and hence the recovery factor of this process. Therefore, the potential candidates to apply the GAIGI process are the reservoirs with a reasonable dip angle or the reef type reservoirs where a gravitationally stable injection scheme is often possible. With the emerging technology of drilling horizontal wells, it is feasible to take advantage of the gravity force to assist the downward movement of oil even in a non-dipping reservoir (Rao 2001). The process includes gas injection into the gas cap to drain the oil in a gravitationally stable manner into horizontal producers at the bottom of the pay zone. A schematic of the gravity assisted gas injection process is shown in Figure 1-1 for two configurations of dipping and non-dipping reservoirs where vertical and horizontal production wells are employed, respectively. The gas injection rate and/or the oil production rate need to be controlled to provide the conditions of gravity-dominated flow regime (Jadhawar and Sarma 2010).

Aside from the configuration, heterogeneities of the petroleum reservoirs, in terms of porosity, permeability and wettability, have a profound effect on the flow pattern and production history of the GAIGI process. However, the complete understanding of the reservoir heterogeneity effects is still limited. Therefore, the main objective of this research was to further investigate the impact of reservoir pore structure and wettability heterogeneities on the GAIGI process in producing waterflood residual oil.

There are two modes of the gravity drainage process in porous media: (1) the free-fall gravity drainage, and (2) the controlled (or forced) gravity drainage. The first mode is referred to the case where the oil drains under the sole action of gravity forces. The free-fall gravity drainage occurs in naturally fractured reservoirs after depletion of oil in the fractures or gas injection into the fractured system (Schechter and Guo 1996). At the lab scale, this process is carried out by opening the top and bottom of the porous media to the atmosphere. Thereby, the liquid (oil and water) flows at the maximum possible rate, governed by the gravity forces. The controlled gravity drainage refers to the mode when the liquid content drains at a controlled rate. This could be accomplished either by maintaining the gas cap pressure at a constant level through gas injection, or withdrawing liquid at a constant rate. In the experimental and theoretical study by Ayatollahi (1994), a detailed description of the free-fall and controlled gravity drainage processes is given. Also, in an attempt to find the effect

of production rate on the GAIGI process, he performed several controlled gravity drainage tests at different withdrawal rates in homogeneous glass bead packs. The need to find the impact of production rate on the GAIGI process in heterogeneous porous media was the motivation to undertake investigation on this area as the other objective of this thesis.

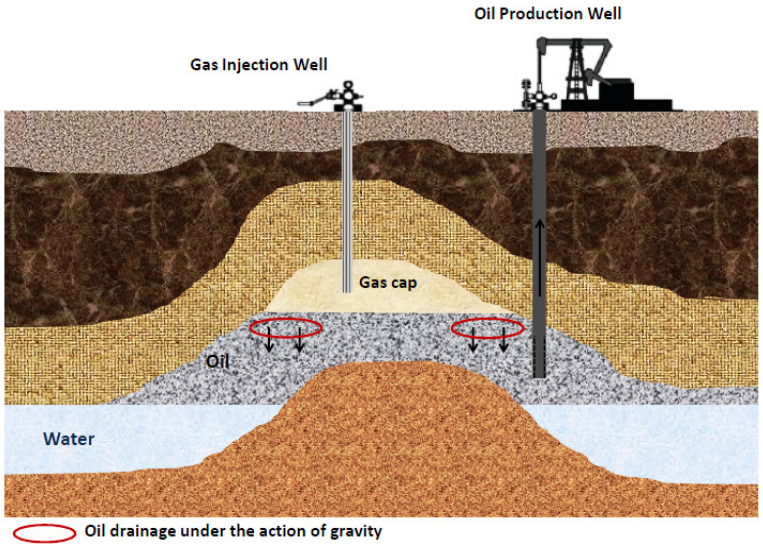

(a)

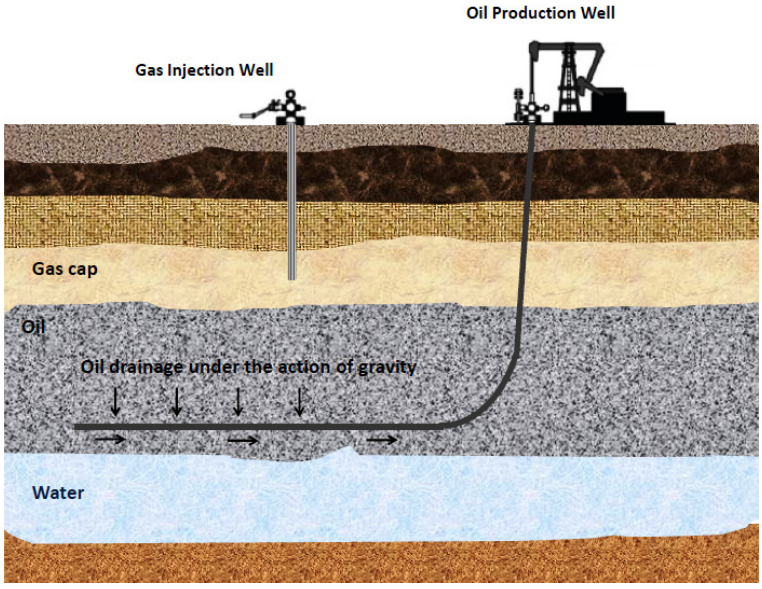

(b)

Figure 1-1: Schematic of gravity drainage process in (a) dipping reservoir (b) non-dipping reservoir

1.2 Objectives and Approach

This thesis concentrates on the experimental investigation of the GAIGI process in glass bead packings exhibiting pore structure or wettability heterogeneities. More specifically, this research is directed towards the study of the impact of heterogeneities in the form of randomly distributed isolated regions having contrasting wettability/permeability compared to that in the continuum. Motivations for this study are: (1) bypassing a significant amount of oil upon waterflooding that necessitates applying an efficient tertiary oil recovery process such as the GAIGI process to sweep the oil left behind in the reservoir after secondary recovery; (2) the heterogeneous nature of petroleum reservoirs that considerably influence the location, flow, and distribution of the fluids. To attain the goal of this thesis, several experiments were run to explore the effects of residual oil saturation, volume% of heterogeneities in the packed models, and liquid withdrawal rate on the production characteristics of the GAIGI process. In addition, by using dimensionless numbers, the operating parameters of gravity drainage were scaled for a typical reservoir.

1.3 Overview of the Thesis

The thesis is organized as follows. Chapter 2 focuses on reviewing the research papers that have addressed the effect of different factors on gravity drainage, among which are: oil spreading coefficient, mobile water and connate water saturation, and injection/withdrawal rates. However, the literature on the impact of permeability and wettability heterogeneities on oil recovery are presented in Chapter 3 and Chapter 4, respectively, with the intention of treating the topics in appropriate depth which is the objective of this thesis.

The main contribution of this thesis begins with Chapter 3, which gives detailed descriptions of the experimental procedures that were followed to examine the impact of pore structure heterogeneities on waterflood residual oil as well as their influence on the oil production mechanism through the GAIGI process. The results are discussed thoroughly and the detail of presenting the main governing variables into the dimensionless forms is described.

In Chapter 4, the steps for creating heterogeneous packed columns exhibiting wettability contrast between the continuum and the imbedded isolated regions are described. The chapter is followed by

the detail of the porous media preparation for the gravity drainage tests. The outcomes are then discussed and are compared to the ones obtained in Chapter 3 by developing a correlation between normalized recovery factor at gas breakthrough and the gravity number.

Finally, Chapter 5 presents conclusions and recommendations for future work to enhance the applicability of the outcomes of this research to the systems with different conditions.

Chapter 2

Literature Review of Experimental Studies on Gravity Drainage Process

2.1 Introduction

The gravity drainage studies were initiated in the 1940's. The focus of early studies was to enhance the understanding of the gravity drainage process. The later experimental works covered a wide range of subjects including the study of the effects of oil spreading coefficient, miscibility, mobile water saturation, connate water saturation, and reservoir heterogeneities on the gravity drainage process. In this chapter, an effort is made to review the literature dealing with the impact of these factors on oil production mechanisms over the course of gravity drainage process. For the systems with pore structure heterogeneities and wettability heterogeneities the literature is reviewed in Chapter 3 and Chapter 4, respectively.

2.2 Pioneers in Gravity Drainage Experiments

Katz (1942) pioneered gravity drainage experimental studies by conducting oil drainage tests in a sand column and measuring the local oil saturation at the end of the experiments. Katz found very low oil saturation in the upper part of the column, confirming Leverett's (1941) hypothesis on the importance of gravitational and capillary forces in immiscible gas injection displacements. Later, Stahl et al. (1943) used air to displace various liquids under free-fall condition in a column containing Wilcox sand. The experiments were stopped periodically to take samples for saturation measurement. Their results showed dependence of liquid saturation on the column height for both equilibrium and

dynamic conditions. Lewis (1944) gave a detailed description of operating conditions under which a gravity-stabilized flood front is attained during the field scale gravity drainage process. Terwilliger et al. (1951) conducted gravity drainage experiments under controlled flow rates in silica sand porous media and used brine and gas as the experimental fluids. They determined in situ wetting phase saturation by measuring the conductivity of brine in the system. Their theoretical study was based on the Buckley and Leverett (1942) approach and the proposed model was compatible with the measured saturation profile. After several similar studies involving gravity drainage process from 1950's to early 1970's (e.g., Nenniger and Storrowll 1958; Essley et al, 1958; Templeton and Nielsen 1962) the experimental work by Dumoré and Schols (1974) was a breakthrough where they developed a drainage capillary pressure function from free-fall gravity drainage of oil. They also posed the concept of "film flow" and its role in achieving low residual oil saturation.

Following these pioneering studies, more complicated systems such as three-phase gravity drainage were considered. Below is a review of the literature that addressed different aspects of three-phase flow during gravity drainage process.

2.3 The Effect of Spreading Coefficient on Gravity Drainage

The spreading characteristics of fluids play an important role on the displacement mechanism of tertiary gravity drainage since three phases co-exist. If a drop of oil is placed on a liquid substrate such as water, its behavior is determined by the final spreading coefficient ($S_{o/w}$), which is defined as (Harkins 1941):

$$S_{o/w} = W_A - W_C \tag{2-1}$$

where W_A is the work of adhesion for the interface of the two liquids, and W_C is the work of cohesion of oil. If the work of adhesion is greater than the work of cohesion, the oil will spread over water and vice versa. The values of W_A and W_C are defined in terms of the interfacial tension values as follows:

$$W_A = \sigma_{wg} + \sigma_{og} - \sigma_{ow} \tag{2-2}$$

$$W_C = 2\sigma_{og} \tag{2-3}$$

Combining Equations 2-1 to 2-3 gives:

$$S_{o/w} = \sigma_{wg} - \sigma_{og} - \sigma_{ow} \qquad (2\text{-}4)$$

in which σ_{wg}, σ_{og} and σ_{ow} are the water-gas, oil-gas and oil-water interfacial tensions, respectively, measured at thermodynamic equilibrium. $S_{o/w}$ is positive if spreading is accompanied by a decrease in free energy, hence the spreading of oil over water in the presence of gas is spontaneous. Figure 2-1a illustrates the spreading condition in which the contact line between the three phases is unstable and the oil spreads and forms a thin film between the gas and water (Adamson 1960). If $S_{o/w}$ is computed to be negative, the equilibrium state reached by placing a drop of oil over water consists of a monolayer of oil plus a lens of oil (Figure 2-1b).

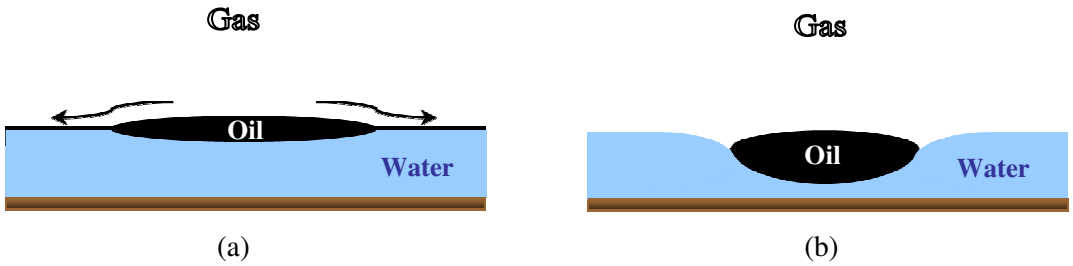

(a) (b)

Figure 2-1: Three-phase fluid configuration under: (a) positive oil spreading coefficient conditions ($S_{o/w} > 0$), oil spreads spontaneously and forms a thin film, (b) negative oil spreading coefficient conditions ($S_{o/w} < 0$), oil remains as a lens and the three phases meet at a point

Dumoré and Schols (1974) used the concept of spreading of oil on water in the presence of gas to explain the very low saturations obtained by gravity drainage in highly permeable sand columns. In the late eighties, the effect of oil spreading coefficient and the role of film flow in gravity drainage were investigated by the porous media research group at the University of Waterloo (Chatzis et al. 1988). They used glass etched micromodels to visualize the effect of wettability and spreading coefficient on the displacement mechanism of tertiary gravity drainage. Four possible combinations of wettability and spreading coefficient were considered: a) water-wet porous medium and positive spreading coefficient, b) water-wet porous medium and negative spreading coefficient, c) oil-wet porous medium and positive spreading coefficient, and d) oil-wet porous medium and negative

spreading coefficient. For these four scenarios of wetting and spreading conditions, the pore scale distribution of oil, water and gas is shown in Figure 2-2.

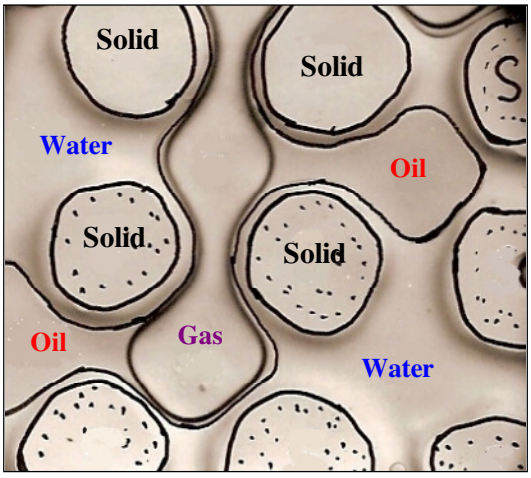

a) water-wet and positive spreading coefficient (modified after Chatzis et al. 1988)

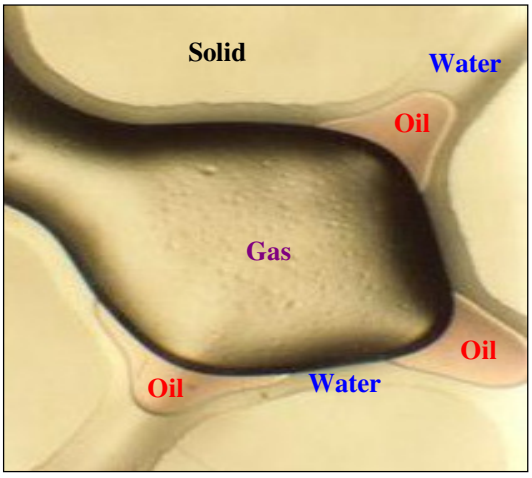

b) water-wet and negative spreading coefficient (modified after Chatzis et al. 1988)

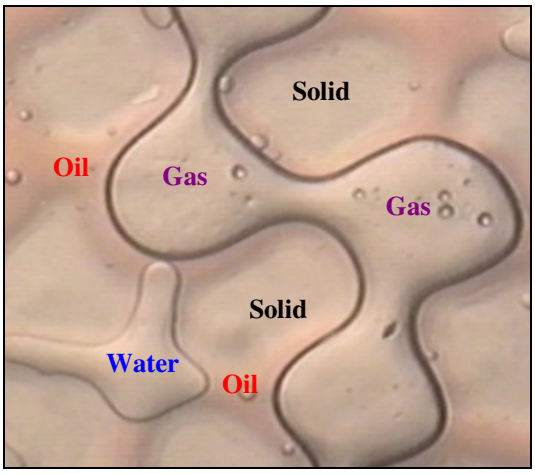

c) oil-wet and positive spreading coefficient

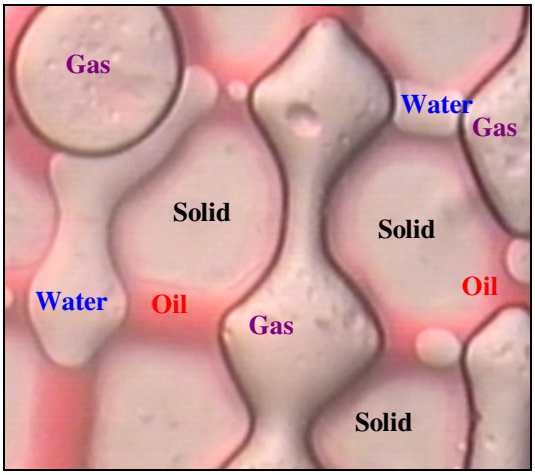

d) oil-wet and negative spreading coefficient

Figure 2-2: Pore scale three-phase fluid distribution for different wettability and spreading coefficient conditions

When the spreading coefficient is positive and the medium is water-wet, gas does not see the water in the presence of oil because oil is the non-wetting phase with respect to water and the wetting phase relative to gas (Figure 2-2a). The spreading oil films maintain continuity of the oil phase throughout

the gas invaded zone, which in turn facilitates the drainage of waterflood residual oil under the action of gravity.

For the conditions of water-wet porous medium and negative spreading coefficients of oil over water, both water and gas are continuous phases in the gas invaded pore spaces while the oil-phase remains discontinuous. Therefore, residual oil in a pore invaded by gas is not efficiently displaced, as can be seen from Figure 2-2b. However, the residual oil blobs in the gas invaded pores which have an oil-gas interface on one end and an oil-water interface at the other end have probability to mobilize over time as the water from the water-filled pores drains by gas invasion. This phenomenon is influenced by the prevailing capillary pressure conditions and the relative permeability of water.

When a porous medium is oil-wet, both gas and water are non-wetting phases while the oil (as the wetting phase) covers the solid surface; therefore, regardless of the value of the spreading coefficient, the oil cannot spread over water in the presence of gas in oil-wet media. Accordingly, only the oil and the gas can maintain continuity throughout the gas-invaded zone, while the residual water ganglia cannot spread over oil (see Figure 2-2c and d). The oil-wetting condition results in oil occupying the small pores and the corners of gas invaded pores. This results in establishing higher residual oil saturation by gas injection and gravity drainage conditions.

Øren et al. (1992), in a visualization study characterized the pore-scale displacement mechanisms of mobilization and production of waterflood residual oil by immiscible gas flooding. The pertinent experiments were conducted in a horizontal, water-wet, two-dimensional glass micromodel, under the conditions of positive and negative spreading coefficients. For both positive and negative spreading systems, a double-drainage mechanism was found responsible for mobilization and reconnection of waterflood residual oil. The two drainage events include the displacement of oil by gas and the displacement of water by oil, as illustrated in Figure 2-3 for a positive spreading system. The oil/water displacement can lead to coalescence of oil in the oil-filled pore throats and bodies, provided that the oil flow paths are short. However, for vertical gas flooding, reconnection of oil blobs can take place because of the larger pressure gradient developed by gravity force.

In spite of the occurrence of a double-drainage mechanism for both spreading and non-spreading cases, the oil recovery at gas breakthrough was significantly lower for the negative spreading system (18% versus 84% recovery for positive spreading system) because of two main reasons. Unlike the positive spreading case in which the movement of a gas/oil interface always results in an oil-water

interface advancement, in a negative spreading system not all gas-displacement events lead to an oil/water interface movement, because no continuous oil films separate the gas and water. Moreover, the absence of continuous oil films hinders the drainage of oil after being isolated by the gas loop.

Øren and Pinczewski (1994) broaden their experimental study and conducted the immiscible gas flooding tests in oil-wet two-dimensional glass micromodels, under both positive and negative spreading conditions. Comparing the oil recovery results with the results of the previous work (Øren et al. 1992), they found that under the conditions of strongly water-wet porous media and negative oil spreading coefficient the waterflood residual oil recovery by gasflooding was lowest, because neither the oil wetting films nor the spreading films contributed in oil continuity.

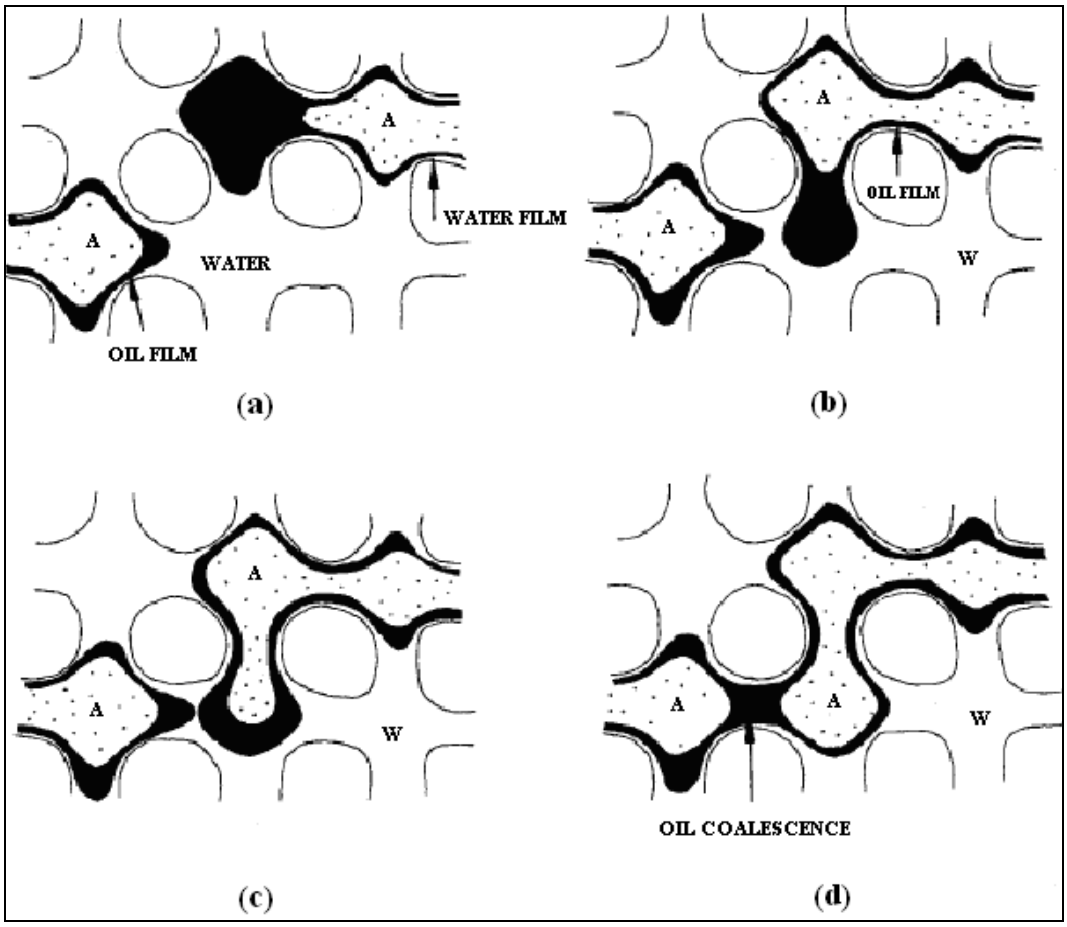

Figure 2-3: Double-drainage mechanism and oil-blob coalescence for positive spreading system (oil shown in black), (modified from Øren et al. 1992)

Catalan (1992) ran several experiments in glass bead packs to test the effects of positive versus negative spreading coefficient of oil over water on gravity drainage to recover the waterflood residual oil. Very little oil was recovered in the water-wet system when the spreading coefficient was negative (17.3% versus 87.5% for positive spreading coefficient system).

Blunt et al. (1995) addressed the fundamental mechanisms of oil recovery through three-phase flow gravity drainage in water-wet porous media both theoretically and experimentally. For the positive oil spreading coefficient condition, they calculated the thickness and stability of the oil layer and found that considerable recovery of oil by drainage only happens when the oil layer occupies crevices or roughness in the pore space. In this study, a parameter (α) was defined, which governs the distribution of oil, water, and gas in vertical equilibrium under the gravity drainage process:

$$\alpha = \sigma_{ow}(\rho_o - \rho_g) / \sigma_{go}(\rho_w - \rho_o) \tag{2-5}$$

where ρ_g, ρ_o and ρ_w are the gas, oil and water densities, respectively. Experiments conducted by Blunt et al. (1995) in sand packs and capillary tubes showed that for $\alpha>1$ there is a finite height above which residual oil saturation approaches zero (i.e., oil only exists as films with molecular thickness) while for $\alpha<1$, a large quantity of oil is trapped in the gas invaded zone. The authors also confirmed that a negative spreading coefficient leaves behind a large magnitude of oil in a water-wet reservoir, and causes poor oil recoveries through gravity drainage.

The spreading coefficient not only affects the residual oil saturation but also changes the drainage capillary pressure curve and oil relative permeability curves for tertiary gas injection (Kalaydjian 1992; Kalaydjian et al. 1993). Absence of hydraulic oil continuity for a non-spreading system necessitates a higher level of capillary pressure to drain an oil blob; therefore, the drainage capillary pressure curve deviates from that of the spreading system (Kalaydjian 1992). In addition, the oil relative permeability was found to be lower for the case of negative spreading coefficient compared to that of the oil spreading systems owing to loss of the hydraulic continuity (Kalaydjian et al. 1993).

In a theoretical study by Mani et al. (1996) a mechanistic model was established at the pore-level to investigate the effects of the spreading coefficient on oil recovery through capillary-dominated, immiscible gas injection in a porous medium initially saturated with water and oil. Three displacement events were found to be involved in three phase flow: direct water drainage, direct oil

drainage, and double drainage. The latter mechanism, which has been previously introduced by Øren et al. (1992), was reported to be responsible for oil recovery, especially for the spreading systems. For the non-spreading cases, the direct water drainage mechanism seemed to be the main contribution event in oil recovery (Mani et al. 1996). In addition, Mani et al. confirmed the experimental results reported by Kalaydjian (1992) and Øren and Pinczewski (1994) which showed that for a spreading oil system the residual oil saturation is much lower than in a non-spreading case. Moreover, for systems with highly negative spreading coefficients, oil recovery by gas injection decreases with the magnitude of the spreading coefficient, while for positive spreading systems it is independent of the spreading coefficient. Therefore, in a non-spreading system the residual oil saturation after gas injection increases with the magnitude of the spreading coefficient (Mani et al. 1996). In other words, two-phase (Araujo et al. 2001) and three-phase (Kalaydjian et al. 1993) oil relative permeabilities are higher for oil-spreading than for non-spreading conditions for gas drainage displacements.

Grattoni and Dawe (2003) emphasized the importance of wettability in conjunction with the spreading characteristics of the oil on waterflood residual oil displacement by solution gas drive. To evaluate the performance of such a depressurization process, they conducted visualization experiments in glass-etched micromodels and quantitatively in sintered-bead micromodels, with different wettability and under different oil spreading coefficient conditions. The experimental results demonstrated that in a water-wet porous medium and for oil spreading condition, the immobile oil ganglia could be displaced by the gas since it forms the spreading oil film. However, for non-spreading conditions, displacement of discontinuous oil ganglia by the gas phase is not that efficient. In contrast, in an oil-wet system, the continuity of oil phase is assured because of the solid surface wettability; therefore, as the solution gas is released, it can effectively expands the oil phase, allowing the oil to be produced through wetting films even at lower gas saturations. The economical eficiency of depressurizing a reservoir was found to depend on parameters like critical gas saturation, the rate of saturation change, and the gas saturation remaining at the end of the process, all of which are affected by the surface and interfacial properties mentioned above (Grattoni and Dawe 2003). In a recent study, Maeda and Okatsu (2008) stressed the importance of the thin oil film drainage mechanism to enhance the waterflood residual oil recovery by immiscible gas in the water-wet oil reservoir.

Overall, it can be concluded from the literature that the spreading characteristic of oil over water is beneficial in providing oil continuity and results in low residual oil saturation through gas injection gravity drainage processes. Considering this conclusion along with the fact that the spreading coefficients of most of the crude light oils are positive (Muskat 1949), we used a spreading type of oil throughout our experimental work. The details of fluid surface tensions and spreading coefficient calculations are presented in the next chapter.

2.4 The Effect of Mobile Water Saturation on Gravity Drainage

The mobile water saturation in the oil reservoir strongly affects the recovery efficiency of the gas-oil displacement process through three main mechanisms: (1) shielding the oil from the injected gas and consequently delaying oil production, (2) decreasing gas injectivity, and (3) lowering the oil relative permeability (Kulkarni and Rao 2005). Moreover, wettability is the key parameter that affects the shielding phenomenon (Rao et al. 1992; Rao 2001). This phenomenon is more pronounced in water-wet media than the oil-wet media and leads to decreased oil recovery in water-wet media in gas miscible cases (Rao et al. 1992; Wylie and Mohanty 1999).

According to another study by Farouq Ali (2003), the need to displace a significant amount of water in the reservoir could cause economical failure of tertiary recovery by gas injection process. This issue will be addressed in section 3.5 of this thesis. Moreover, the injected gas (such as CO_2) is lost into the reservoir brine to a significant extent.

2.5 The Effect of Connate Water Saturation on Gravity Drainage

In the three-phase gravity drainage process, connate water is usually considered as immobile; however, micromodel investigations have shown that the connate water does not remain immobile during gravity drainage (Catalan et al. 1994; Sajadian and Tehrani 1998). The mobilization and redistribution of the connate water is because the balance between capillary and gravity forces changes in a three-phase system.

Literature review on the effects of connate water on the performance of gas assisted gravity drainage has provided conflicting conclusions. The role of connate water in gravity drainage has been stressed for the first time in the early seventies by Dumoré and Schols (1974). Their gravity drainage experiments in Bentheim sandstones and sand columns with the presence of immobile connate water

resulted in extremely low oil saturations, for both low and high gas-oil interfacial tensions. Later, relative permeability studies showed that gravity drainage can be very efficient in water-wet, connate-water-bearing reservoirs (Hagoort 1980). However, based on centrifugal gas-oil displacements, Nahara et al. (1990) concluded that if the water remains immobile, the gas-oil relative permeabilities are not affected by the presence of water. Pavone et al. (1989) performed free fall gravity drainage experiments in fractured reservoir cores under the conditions of low interfacial tension and found that the presence of immobile water reduces the oil relative permeability, thereby reducing the oil production. This conclusion was inconsistent with Hagoort's observation in which the relative permeability of the oil improved under the condition of the existence of connate water. Skauge et al. (1994) conducted gravity drainage experiments at various connate water saturations using radioactive brine, Marcol 172 and *n*-Decane. They reported that the presence of connate water increases oil production. Maximum oil recovery by gravity drainage process was attained when connate water saturation was about 30% PV. In another study by this author, in which centrifuge gas drainage experiments were performed in "Oseberg formation" cores, an increase in connate water led to higher oil recovery (Skauge 1999). A recently-published simulation study has addressed the effect of connate water saturation on the overall performance of immiscible gravity drainage (Jadhawar and Sarma 2010). By lowering the fraction of water initially present in the pore spaces, the more effective oil drainage occurs under gravity.

2.6 Effect of the Gas Injection Rate on Gravity Drainage

During a gravitationally stable gas flood, an uncontrolled gas injection rate may lead to premature gas breakthrough and hence poor sweep efficiency of the process. Therefore, a critical rate is often defined below which a relatively stable flood front is established. For miscible gravitationally stable gas flood several theoretical expressions for critical velocity have been proposed and modified throughout the years (Hill 1952; Dumore 1964; Brigham 1974; Piper and Morse 1982; Skauge and Poulsen 2000; Pedrera et al. 2002; Muggeridge et al. 2005).

For immiscible tertiary gravity drainage process, Chatzis and Ayatollahi (1993) investigated the effect of production rate on oil recovery by controlled gravity drainage. Tertiary mode of gravity drainage was employed to recover the waterflood residual oil from the water-wet glass bead packed columns. The experimentally measured macroscopic velocity of the gas–liquid interface was

incorporated in the gravity number and the results were expressed in a dimensionless form rather than the macroscopic velocity itself. They found a strong dependence of oil recovery factor at gas breakthrough on the value of the gravity number. Moreover, they studied the relation between the oil bank size and the gravity number. Their results revealed that under the conditions of low production rates, corresponding to the conditions of gravity numbers larger than 150, the oil bank increased in size linearly and for values of gravity number less than 150, the size of the oil bank increased non-linearly with time.

Riazi et al. (2006) studied the effect of gas injection rate on gravity drainage performance under the secondary condition. Their porous medium was a very low permeability and fractured limestone core. They found a critical rate for injected gas at which the oil recovery factor was at a maximum value. For the gas injection rates lower or higher than the critical rate, the oil recovery was less than the recovery at the critical rate. Although the experimental data showed this trend very clearly, the underlying theoretical concepts for critical rate calculation have not been clarified completely. Besides, their experimental methodology involved constant rate gas injection which could only be carried out at the laboratory scale and is not feasible in an oil reservoir. Instead, the condition of constant production rate is practically attainable at both the lab and field scale to investigate the impact of fluid dynamics on gravity drainage process performance.

In a recent study by Jadhawar and Sarma (2010) reservoir simulation was conducted to check the reservoir sensitivity at different gas injection and oil production rates. At a given gas injection rate, a higher oil production rate yielded a larger gas to oil ratio.

2.7 Summary

Film flow of oil in the GAIGI experiments is the main mechanism to attain very low oil saturation under the conditions of positive spreading coefficient of the oil over water in the presence of gas.

The effect of connate water saturation on gravity drainage has two roles. On one hand, in water-wet porous media where connate water covers the solid surface of the pore space, the spreading films of oil on water surface contribute in oil production to reach very low residual oil saturation. On the other hand, the relative permeability to oil decreases as a result of the presence of connate water saturation in the pore space. This will cause reduction in the pathway for oil permeability to be produced through the gravity drainage process.

To enhance the sweep efficiency of the gas injection gravity drainage process, it is essential to establish a gravitationally stable flood front. For this purpose, the gas injection rate and/or oil production rate should be controlled to minimize viscous instabilities associated with high gas or oil production rates. This conclusion is aside from the possible impact of reservoir heterogeneities on stability of the displacement which is described in the following two chapters for systems with permeability and wettability heterogeneities.

Chapter 3

The Effect of Macroscopic Pore Structure Heterogeneities on the GAIGI Process

3.1 Introduction

Traditionally, all oil reservoirs were treated as homogeneous, an assumption which is now considered to be simplistic. The oil reservoirs are heterogeneous in terms of their porosity, permeability and wettability. Therefore, it is necessary to incorporate these heterogeneities into studies related to the oil reservoirs. Tertiary gas injection processes, when assisted by gravity forces, have been shown to be very efficient in sweeping the residual oil from homogeneous porous media. However, a better understanding of the physics associated with flow behavior in heterogeneous porous media over the course of tertiary gravity drainage necessitates further study of this problem. The focus of this chapter is to explore the impact of permeability heterogeneities on the GAIGI process in terms of flow behavior, oil bank formation and evolution, oil recovery factor, and residual oil saturation. The first part of this chapter reviews several works that have addressed the permeability heterogeneity of porous media in their experimental studies on gravity drainage. The chapter then presents the experimental methodology that we followed to examine the effects of permeability heterogeneity in the form of isolated large-pore-size regions embedded in a small-pore-size continuum on the GAIGI process. Following that, the experimental results are discussed in detail. Finally, the applicability of the GAIGI process at the field scale is evaluated using dimensionless numbers.

3.2 Literature

The gravity-assisted inert gas injection (GAIGI) process has been extensively studied in our laboratory in homogeneous media and the results demonstrated very high oil recovery efficiency (Kantzas 1988; Chatzis et al. 1988; Kantzas et al. 1988 (a & b); Dullien. et al. 1991; Catalan 1992; Ayatollahi 1994). This success stems from the favorable water-wetness and homogeneity of the porous media tested and the positive spreading coefficient of oil over water in the presence of gas. These factors result in continuity of the oil phase in the form of oil films in the pore space invaded by gas and the development of an oil bank under the action of gravity. However, the assumption of a homogeneous reservoir is very simplistic. All natural hydrocarbon reservoirs are heterogeneous in their pore structure and wettability characteristics. Permeability and wettability vary both laterally and vertically at different scales and cause variations in fluid distribution within the reservoir rock (Levorsen 1967).

Considering the non-homogeneous nature of reservoir rocks, the effects of a few features of heterogeneity on gravity drainage have been further explored. Kantzas et al. (1993) focused on the role of pore structure heterogeneity in the forms of vugs and fractures on GAIGI performance. Their results demonstrated that the effect of vugs on oil recovery is minimal, whereas the presence of fractures could reduce the oil recovery efficiency.

The effect of vertical and parallel-type permeability heterogeneity on the oil recovery efficiency of the GAIGI process was investigated by Catalan et al. (1994) in our laboratory. Two-dimensional glass bead models were employed to visually study the movement of different phases during gravity drainage. The model consisted of three zones extending from the bottom to the top of the column, each one occupying one-third of the model width. The central zone contained beads of smaller size, and thereby lower permeability than the other two adjacent zones. The positions of both water-oil and oil-gas interfaces were higher in the central zone, caused by smaller pore sizes and therefore, larger capillary pressures. Although the thickness of the oil bank kept increasing, the difference in height for the oil-gas interface was constant over time. Since the gas pressure was the same in all three zones and all times, the position of interfaces must compensate for differences in capillary pressure caused by dissimilarities in pore sizes. Therefore, a non-uniform saturation distribution along the column horizontal cross-section was established (Figure 3-1). However, they found a relatively small effect of such type of heterogeneity on oil recovery. The reason could be explained in the following way:

gas breakthrough occurs first in the larger permeability zones while the oil bank in the central zone has not been produced completely. The oil present in the lower permeability zone where capillary pressure is high has a tendency to flow towards the adjacent zones where capillary pressures are lower. Therefore, the amount of oil retained by capillary forces at the end of gravity drainage in the central zone is smaller than in the low capillary pressure zones (Catalan et al. 1994).

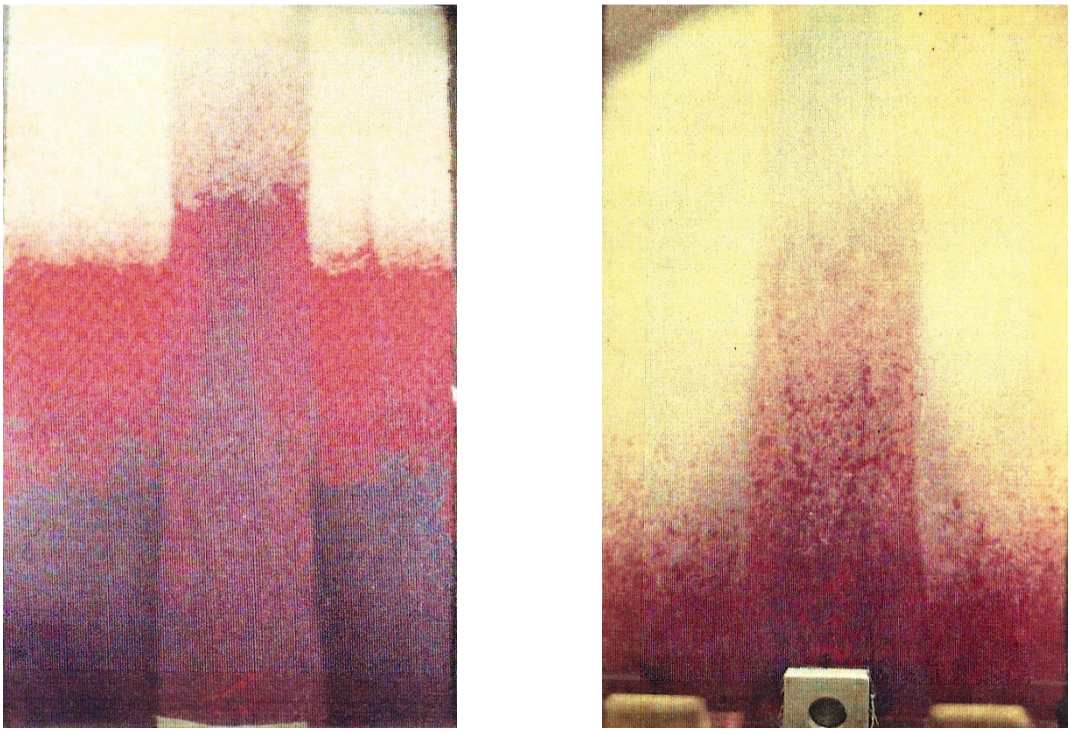

(a) (b)

Figure 3-1: Tertiary gravity drainage in a model with macroscopic, parallel-type heterogeneity: (a) Oil banks in different permeability zones, (b) Residual oil (red) and water (blue) at the end of a gravity drainage experiment (from Catalan et al. 1994)

In another study by Catalan et al. (1994), flow visualization experiments in glass micromodels exhibiting microscopic heterogeneities were carried out to show the role played by pore level heterogeneities on secondary and tertiary gravity drainage. The two types of heterogeneities considered in this study are shown in Figure 3-2 and Figure 3-3. In model I (Figure 3-2), the heterogeneity consisted of randomly distributed relatively large pore bodies connected by relatively large pore throats, imbedded in a square network of narrow throats. Model II (Figure 3-3) consisted of randomly distributed pore bodies connected by large pore throats imbedded in a network of smaller pore throats and pore bodies.

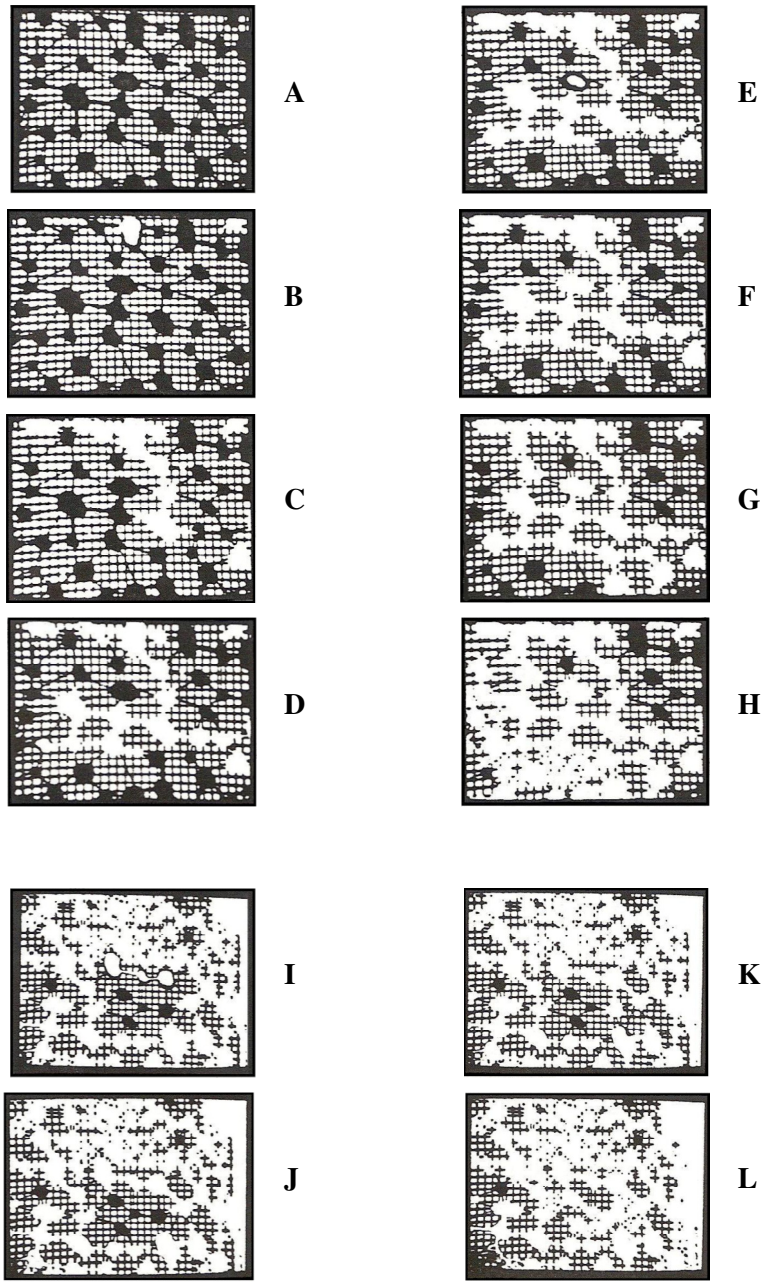

Figure 3-2: Secondary gravity drainage of oil from glass capillary micromodel I (from Catalan et al. 1994)

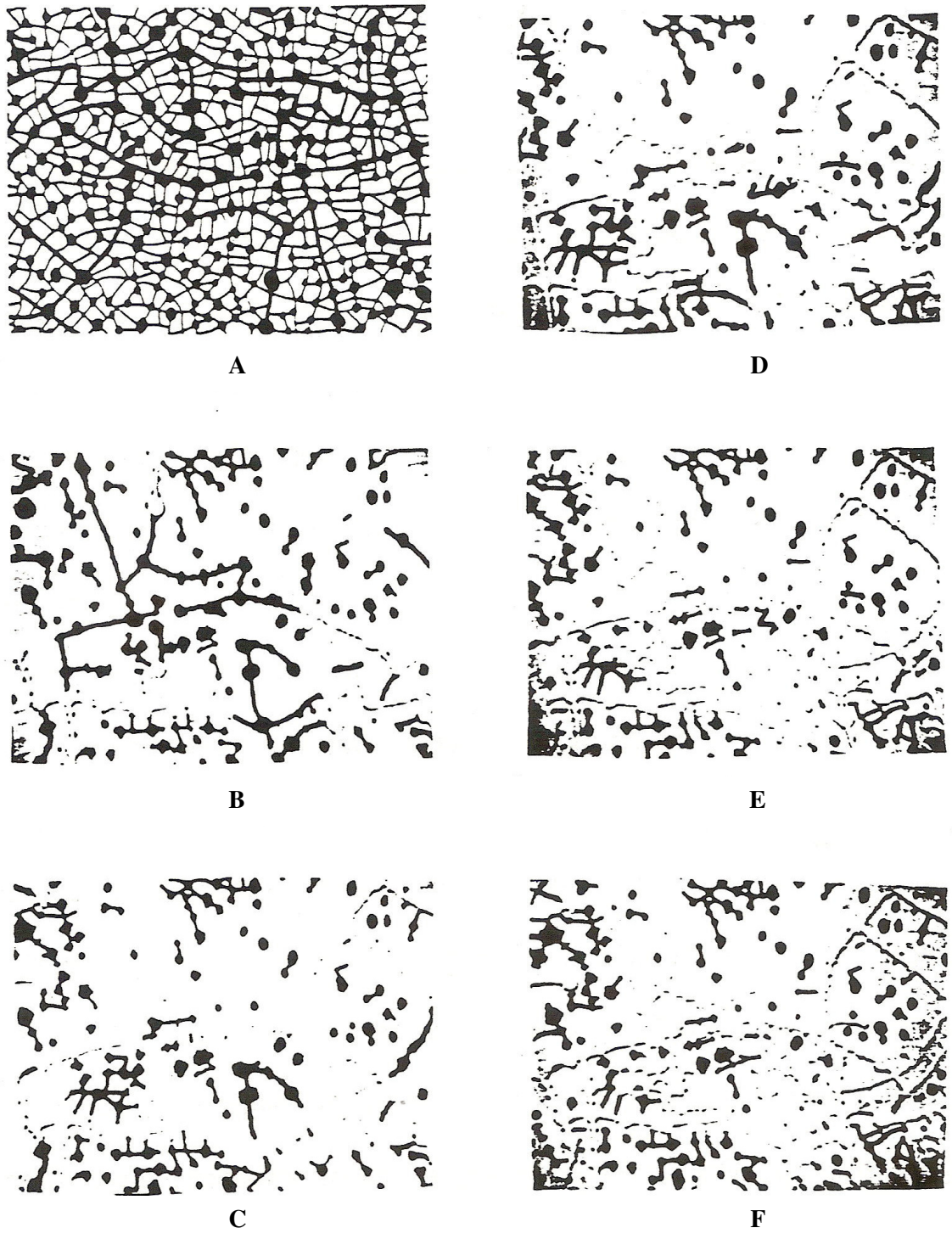

Figure 3-3: Tertiary gravity drainage of oil from glass capillary micromodel II (from Catalan et al. 1994)

Figure 3-2 shows the time-lapse photographs of the gas pathways during free fall gravity drainage of the pore space filled with Soltrol oil (stages A-H). The pathway of least resistant to the fluid flow, which consisted of the continuum of large pore bodies, drained first. Some of the oil, as wetting phase compared to air, was bypassed in several large pores as shown in photograph H. However, the drainage of the bypassed large pores occurred as the process continued, which is shown in photographs I to L. Also, the hydraulic continuity of the wetting phase in the corners of the pores invaded by gas resulted in further drainage of oil.

The time-sequence photographs of gravity drainage of waterflood residual oil in the micromodel II is shown in Figure 3-3. Comparing stages D and B showed the drainage of some of the bypassed oil in large pores. Maintaining the gas-oil position constant allowed for further reconnection, drainage, and redistribution of residual oil (Catalan et al. 1994).

Catalan et al. (1994) also conducted a tertiary free fall gravity drainage experiment in model I. A snapshot of the micromodel at the state of waterflood residual oil saturation is shown in Figure 3-4A. Over the course of gravity drainage, the residual oil was partially displaced and redistributed in smaller pores, as shown in Figure 3-4B.

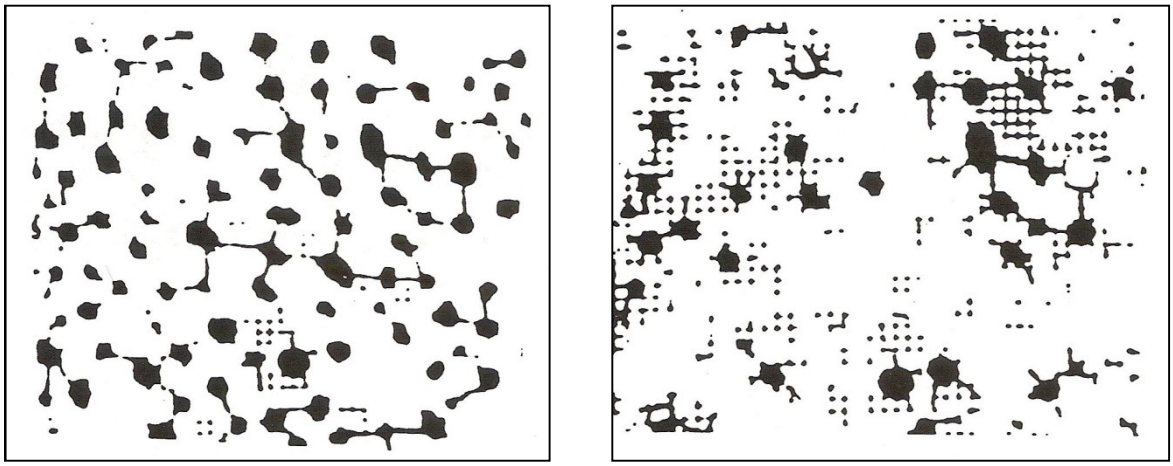

At waterflood residual oil
(A)

Gravity drainage at gas breakthrough
(B)

Figure 3-4: Tertiary gravity drainage of oil from glass capillary micromodel I (from Catalan et al. 1994)

In another experimental study in our laboratory, Ayatollahi (1994) performed gravity assisted inert gas injection in layered porous media, including unconsolidated glass bead and sand columns, and consolidated glass bead micromodels. The production history diagram of the tertiary gravity drainage in the stratified glass bead column is shown in Figure 3-5. The formation of an oil bank started in the first high permeability zone. The gas-liquid interface then passed from the high to low permeability zone without any instability. However, near the boundary of the low to the high permeability zone, the oil in the oil bank lost its continuity and oil started to infiltrate through the water zone on the top of the boundary. As the drainage continued from the bottom of the column, the oil in the oil bank drained to the high permeability zone by means of fingering.

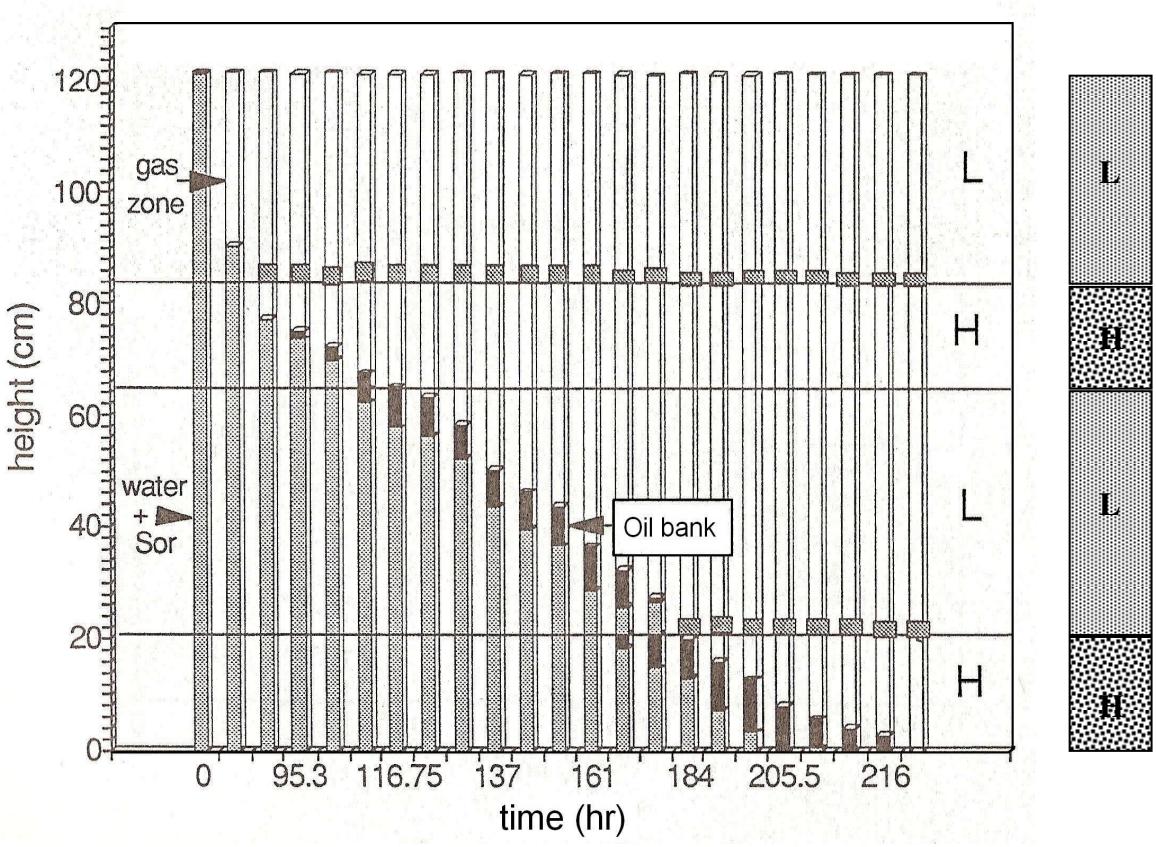

Figure 3-5: Production history showing the gas-oil, oil-water and the size of oil bank with time for layered glass bead column, H: High permeability layer, L: Low permeability layer (modified from Ayatollahi 1994)

Figure 3-5 also illustrates that while some water was retained at the boundary of low to high permeability layers because of the capillarity and wettability conditions, no significant amount of oil was held-up when the oil bank passed through the low permeability region. Therefore, the oil recovery efficiency by GAIGI process in the stratified porous media was analogous to that in homogeneous porous media.

In order to develop a better understanding of the oil bank propagation in a layered permeability system, a two-dimensional sintered glass bead model was used by Ayatollahi (1994). Figure 3-6a–c demonstrates the mechanism of oil fingering and shows how these fingers propagate to assist oil drainage from the low to high permeability layer. The gas invasion occurred in the same pathways followed by the oil up until the time of breakthrough and some of the oil left behind in the gas invaded part of the porous medium (Figure 3-6d). Therefore, the very low permeability zone reduced the rate of oil production by film flow although the oil recovery for tertiary gravity drainage in stratified porous media was found to be analogous to that in homogeneous porous media (Ayatollahi 1994).

Ayatollahi also performed free-fall secondary and tertiary gravity drainage in a stratified glass bead column with four layers having permeability contrast. The results for total oil recovery under secondary conditions showed that the performance of secondary gravity drainage in stratified porous media was lower than that in homogenous porous media because of the oil retention at the boundary of the low permeability to high permeability layers. By injecting gas at a high pressure, it was possible to provide gas-phase continuity, and thereby improve the oil recovery by gravity drainage due to the film flow mechanism and maintaining a high capillary pressure value. During the tertiary gravity drainage, no oil was held-up in the vicinity of the low to high permeability layers, and the oil recovery was comparable to that in homogeneous porous media (Ayatollahi 1994).

To the knowledge of the author of this thesis, no further work has been carried out to study other aspects of the permeability heterogeneity effects on tertiary GAIGI. However, there are a few published papers considering the impact of permeability heterogeneity on other EOR displacement processes including two-phase miscible and immiscible displacements. In a theoretical study by Correâ and Firoozabadi (1996), the predicted oil saturation profile from a mathematical model for a layered medium showed that the residual oil tends to accumulate in the low permeability zone in two-phase gas-oil gravity drainage.

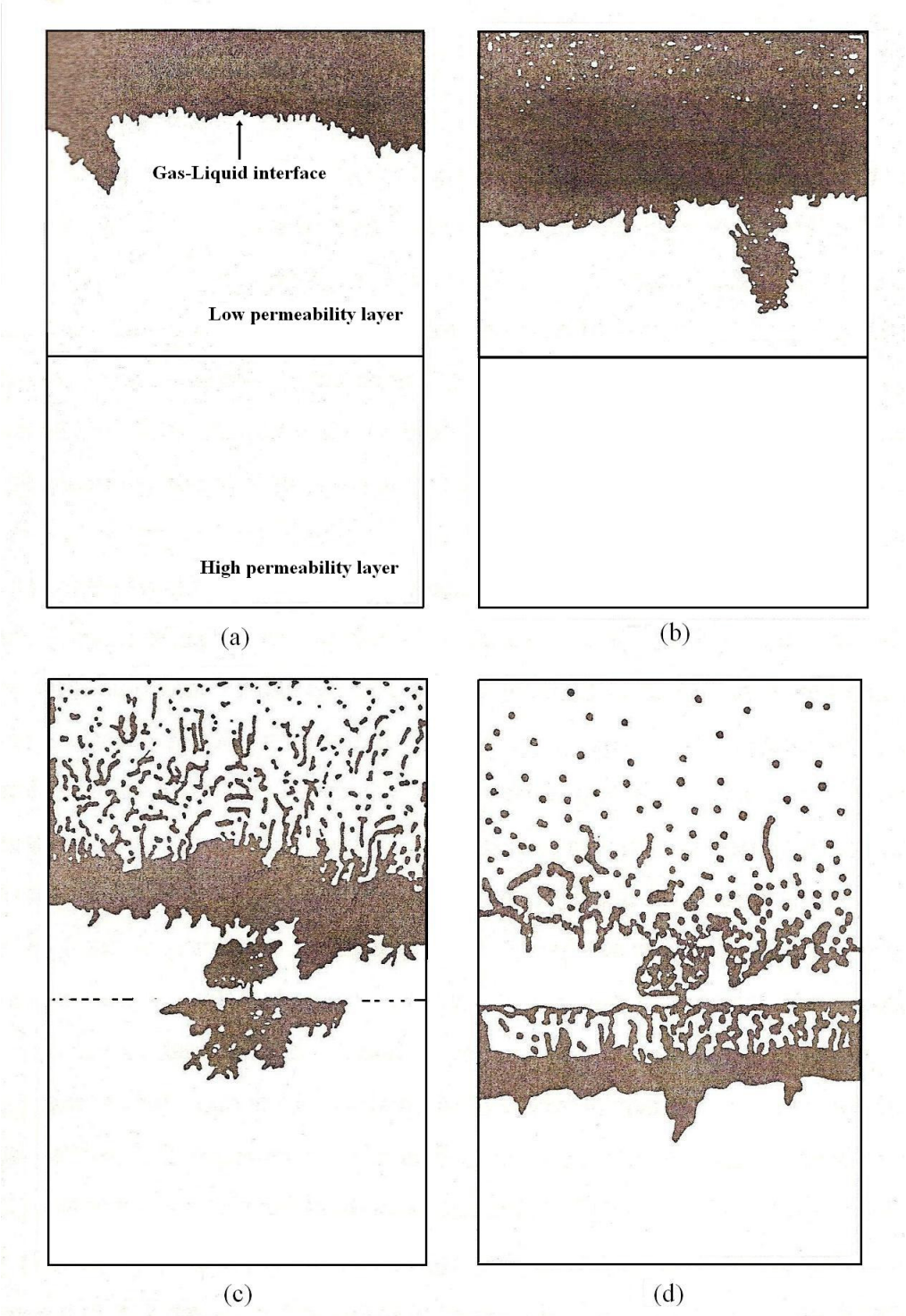

Figure 3-6: Oil bank propagation in two-dimensional sintered glass bead model during tertiary controlled gravity drainage (modified from Ayatollahi 1994)

A group of researchers investigated the effect of permeability and wettability heterogeneities in the form of lenses, stripes, layers and quadrants in the porous media on the performance of miscible (McKean and Dawe 1990) and immiscible displacement processes (Dawe et al. 1992; Marcelle-De Silva and Dawe 2003; Dawe and Grattoni 2008). The two-dimensional design of the glass bead models facilitated the visualization of drainage and imbibition displacements. They have reported that the fluid displacement patterns were significantly affected by heterogeneities, especially at lower displacement rates under which the capillary forces are more dominant. When oilflooding a heterogeneous medium containing zones with different permeabilities, oil displaced water mainly from the high permeability regions where the oil pressure was lower. Similarly, during waterflooding the porous media with permeability heterogeneity, water flowed through the low permeability zone because water pressure was less. As a result, some oil was bypassed in the high permeability zone.

This chapter explores the performance of the gravity-assisted inert gas injection process for tertiary oil recovery from heterogeneous packed columns. Specifically, the objective is to consider the randomly distributed type of heterogeneity configuration in the form of isolated large-pore-size regions in a smaller pore-size continuum at the macroscopic scale that have been not been addressed in previous studies. We also investigated the effect of residual oil saturation on the GAIGI process, a parameter which has been overlooked to date.

3.3 Experimental Aspect

3.3.1 Porous Media Models

Waterflooding and tertiary oil recovery using controlled gravity-assisted drainage experiments were conducted in glass bead packed-columns having a length of 43 cm and diameter of 2.7 cm. The use of transparent glass models, with dyed oil, enabled monitoring fluid movement during different tests. Columns were packed using small glass beads as unconsolidated continuum, with an average particle size of 507 μm, and pieces of consolidated large glass beads, with an average particle size of 1125 μm, that were randomly placed within the packed column. The heterogeneities in the pore structure were created by sintering glass beads of larger size at 720 °C and then cutting the sintered core samples into smaller pieces. These pieces were subsequently placed in a column at random during packing where they form the isolated high permeability regions in a packing with the unconsolidated

lower permeability continuum, known as the matrix. The bulk volume of these sintered pieces was measured to be on the order of 3–12 cm^3 using the volume displacement test of Archimedes. Three levels of heterogeneity volume fraction in the packed column were considered in this work including 0%, 17% and 38%. The absolute permeability of these packings was measured by the steady-state method at 179.6 ± 3.0, 190.9 ± 2.9 and 206.1 ± 1.0 Darcy, respectively.

In preparing the heterogeneities, the sintered glass beads were used because of two reasons: first, to be consistent in the volume of heterogeneities throughout the experiments, and second, to keep the glass beads having contrasting properties in a bulk form. To diminish the effect of consolidation on permeability of the inclusions, the temperature and duration of sintering in a muffle furnace were controlled in a manner whereby the glass beads fused slightly without significant change in permeability. This is depicted in the microscopic photo of sintered glass beads shown in Figure 3-7.

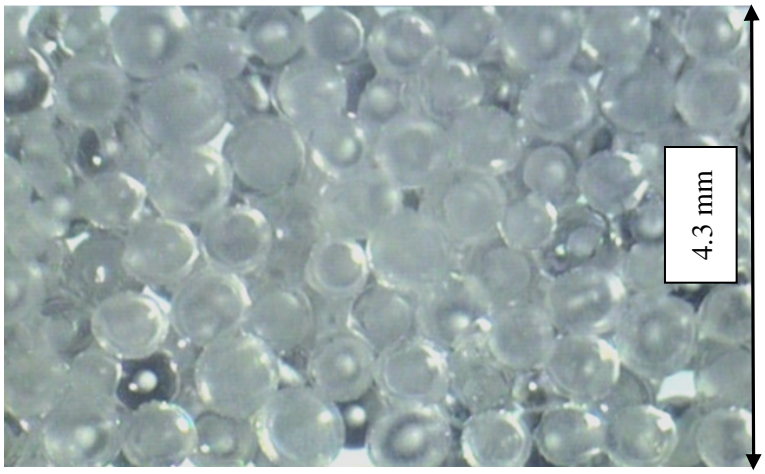

Figure 3-7: A snapshot of glass beads sintered together at 720 °C

3.3.2 Fluids Used in the Experiments

The laboratory fluids used in the experiments were deionized/degassed water, kerosene (dyed with oil-red) and air. The fluid properties and the methods by which the corresponding properties were measured are shown in Table 3-1. Having the tension values, the spreading coefficient of dyed kerosene over water, which is defined in Equation 2-4, is estimated at 16 mN/m, showing strong spreading conditions. The interfacial properties of dyed kerosene seem to be very close to the tension

values of crude oil, and hence give a similar spreading coefficient as the crude oil which is a privileged condition (Koichi et al. 2012).

Table 3-1: Physicochemical properties of fluids used at room conditions

fluid	density* (kg/m^3)	viscosity† (mPa.s)	interfacial tension‡ (mN/m)	
			$\sigma_{fluid/air}$	$\sigma_{oil/water}$
dyed kerosene	779	0.899	24.0	32.0
water	997	0.891	72.0	

∗ measured by a pycnometer
† measured by a Cannon-Ubbelohde viscometer
‡ measured by the pendant drop method

3.3.3 Experimental Methodology

The experimental procedure for waterflooding and controlled gravity drainage tests was as follows:

1. A 1.5cm layer of fine glass beads (average size of 210 μm) was placed at the bottom of the cylindrical physical model to act as capillary barrier and delay gas breakthrough. The column was packed by randomly placing the consolidated large-glass-bead pieces in the small glass beads continuum. Then, carbon dioxide gas was passed through the media from the bottom to displace the air out while the column was positioned vertically. Afterward, several pore volumes of degassed water was injected to fully saturate the packed column by forcing the trapped CO_2 to go into water and continuing until the resident water become free of the dissolved CO_2.

2. The oil was injected from the top of the column to displace water from the exit at the bottom. About 1.5 pore volume of the oil was injected to establish initial oil conditions.

3. To create the so-called normal waterflood residual oil saturation condition, water was introduced from the bottom of the column to displace the oil upwards. The water-oil interface velocity was set such that the corresponding capillary number was 2.97×10^{-6}. This condition is favorable for establishing the maximum residual oil saturation (Morrow and Songkran 1981).

4. The controlled GAIGI experiment was started by withdrawing the liquid from the bottom of the column at a constant rate using a syringe pump. This withdrawal causes the air to invade the medium at the top of the column at constant atmospheric pressure. A water-oil separator, which was connected

to the packed column at one end and the syringe pump at the other end, facilitated the separation of produced oil and water as well as monitoring the volume of oil produced versus time. The gas-liquid interface was also recorded using a digital camera. A schematic of the experimental setup is shown in Figure 3-8.

3.4 Experimental Results and Discussion

3.4.1 Magnitude of Residual Oil Saturation

To establish the condition of residual oil saturation, the heterogeneous packed column saturated with oil was subjected to waterflooding (stage 3 of the experimental methodology). The amount of residual oil saturation is affected by the interplay of capillary, buoyancy and viscous forces. Over the course of waterflooding, capillary forces cause oil trapping while viscous pressure gradient and the buoyancy forces can overcome the capillary forces and mobilize the trapped oil. The dimensionless ratios of viscous to capillary forces and gravity to capillary forces are identified as the capillary number (N_{Ca}) and Bond number (N_B), respectively:

$$N_{Ca} = \frac{v_w \mu_w}{\sigma_{ow}} \tag{3-1}$$

$$N_B = \frac{\Delta\rho_{ow}\, g\, R^2}{\sigma_{ow}} \tag{3-2}$$

where v_w is the displacing fluid velocity (here water), $\mu_w$is the displacing fluid viscosity, σ_{ow} is the oil-water interfacial tension, $\Delta\rho_{ow}$ is the oil-water density difference, and R is the average glass beads radius. Considering the effects of viscous, capillary and buoyancy forces on the trapping mechanism, waterflood residual oil saturation could be maximized provided that the displacements are carried out at sufficiently low capillary number and bond number (Morrow and Songkran 1981). Since the type of fluids as well as the glass beads size remained the same throughout the experiments, the Bond number was identical for all of the tests ($N_B = 4.29\times10^{-3}$). Therefore, waterflooding was carried out at a flow rate corresponding to a very low capillary number ($N_{Ca} = 2.97\times10^{-6}$) to attain the maximum waterflood residual oil saturation. Maintaining a capillary dominated displacement, residual oil saturations as high as 16% pore volume were obtained, which is in agreement with the literature values (Chatzis et al. 1983). For the heterogeneous porous media subjected to the same conditions of

waterflooding as the homogeneous packed column, the amount of trapped oil was much higher depending upon the extent of heterogeneity. Figure 3-9 depicts the magnitude of waterflood residual oil versus the volume fraction of heterogeneity at three levels for 19 performed experiments in total. This figure illustrates that there is a linear relationship between the magnitude of trapped oil after waterflooding and the volume fraction of large-pore-size isolated regions in the packings. The average measured values for the residual oil saturations are 16.0% ± 0.5%, 23.0% ± 0.6% and 29.5% ± 1.1% of the total pore volume for 0%, 17% and 38% volume fraction of heterogeneity, respectively. The results can be interpreted based on the pore scale trapping mechanisms. During an immiscible displacement, the displacing phase tends to flow in the pathway with least resistance to the flow, i.e., where the displacing fluid pressure is lower. Therefore, upon waterflooding, water which is the wetting phase imbibes the smaller pores of the matrix and displaces the oil. Such displacement results in a residual non-wetting phase saturation of about 16% in the matrix. However, the larger pores in the heterogeneities become bypassed and cannot be invaded by water. Consequently, the regions of large pores retain the oil in place because of the bypassing mechanism, thus a residual oil saturation of about 85% is established in the large pore-size regions. Therefore, about 16% of the matrix pore volume and approximately 85% of the pore volume in the sintered regions contribute in attaining the overall waterflood residual oil saturation. A time-sequence schematic of waterflooding a heterogeneous porous medium and oil trapping mechanism is shown in Figure 3-10.

A comparison of experimental data for the magnitude of the waterflood residual oil at the macroscopic scale and the predicted values based on Chatzis et al. (1983) experimental results for heterogeneous glass bead micromodels is also shown in Figure 3-9. This figure demonstrates prediction errors of 1.2% for the heterogeneous media containing 17 volume % heterogeneities. The close match of the macroscopic scale experimental data and the predicted values supports the fact that the pore scale trapping mechanism explains the magnitude of residual oil very well for the case of 17% heterogeneity level. For the case of 38% heterogeneity, on average there is a discrepancy of about 3.8 % PV (11.5% error) between the experimental and anticipated magnitude of waterflood residual oil. This difference could be explained by looking closer at the oil-water imbibition curves for the large and small beads used as heterogeneity and matrix, respectively. Figure 3-11 shows the imbibition curves for the packings of two different sizes of glass beads which were obtained using the porous plate method for water-oil fluid pairs. When water imbibes the heterogeneous packed column during waterflooding, it displaces oil to the residual saturation of about 16% in the matrix. Under the

same capillary pressure, about 85% of oil will be trapped in the large-bead pieces. This state of residual oil saturation occurs if the water front bypasses the heterogeneity and invades the matrix before water can invade the heterogeneity. Such a condition arises if the length of heterogeneities is short enough so that the water pressure plus the hydraulic pressure equivalent to the length of the heterogeneity is less than the entry pressure to the large-pore-size region. Unlike the large-bead-size sintered pieces used for the 17% volume fraction of heterogeneity, some of the pieces used for the 38% level of heterogeneity had a length of more than about 4 cm. Therefore, water partially imbibed into the long pieces under a lower capillary pressure before the waterfront in the surrounding matrix bypassed the long pieces. This lower capillary pressure resulted in smaller residual oil saturation than the expected value of 85% in the long patches. For example, a piece that has a length of about 5 cm would experience a residual oil saturation of about 75%, as can be seen from Figure 3-11. Consequently, the presence of long sintered pieces in the porous media for the case of 38% heterogeneity caused the magnitude of waterflood residual oil to be lower than the expected value if complete bypassing was possible.

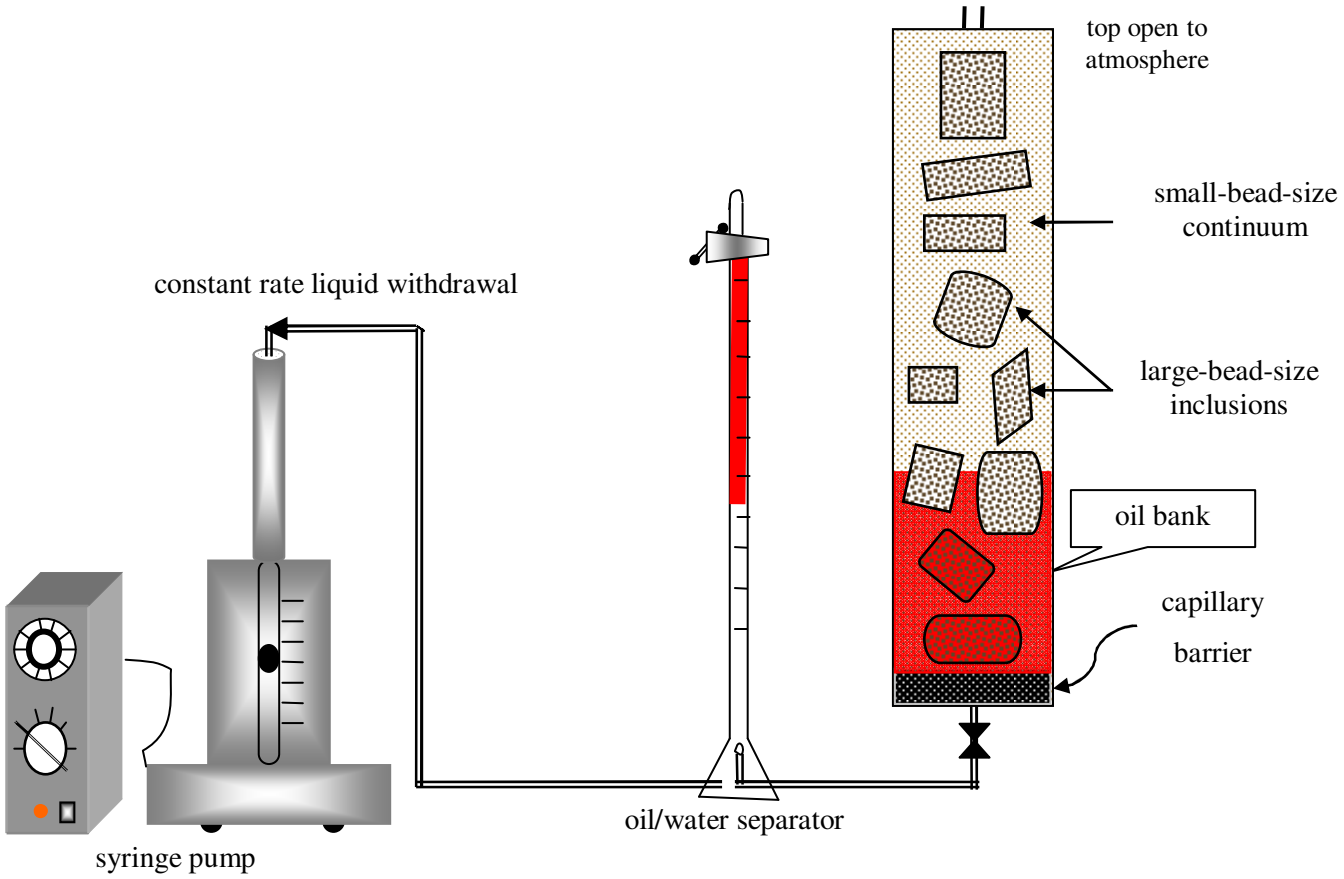

Figure 3-8: Schematic of the experimental setup for the tertiary gas injection gravity drainage

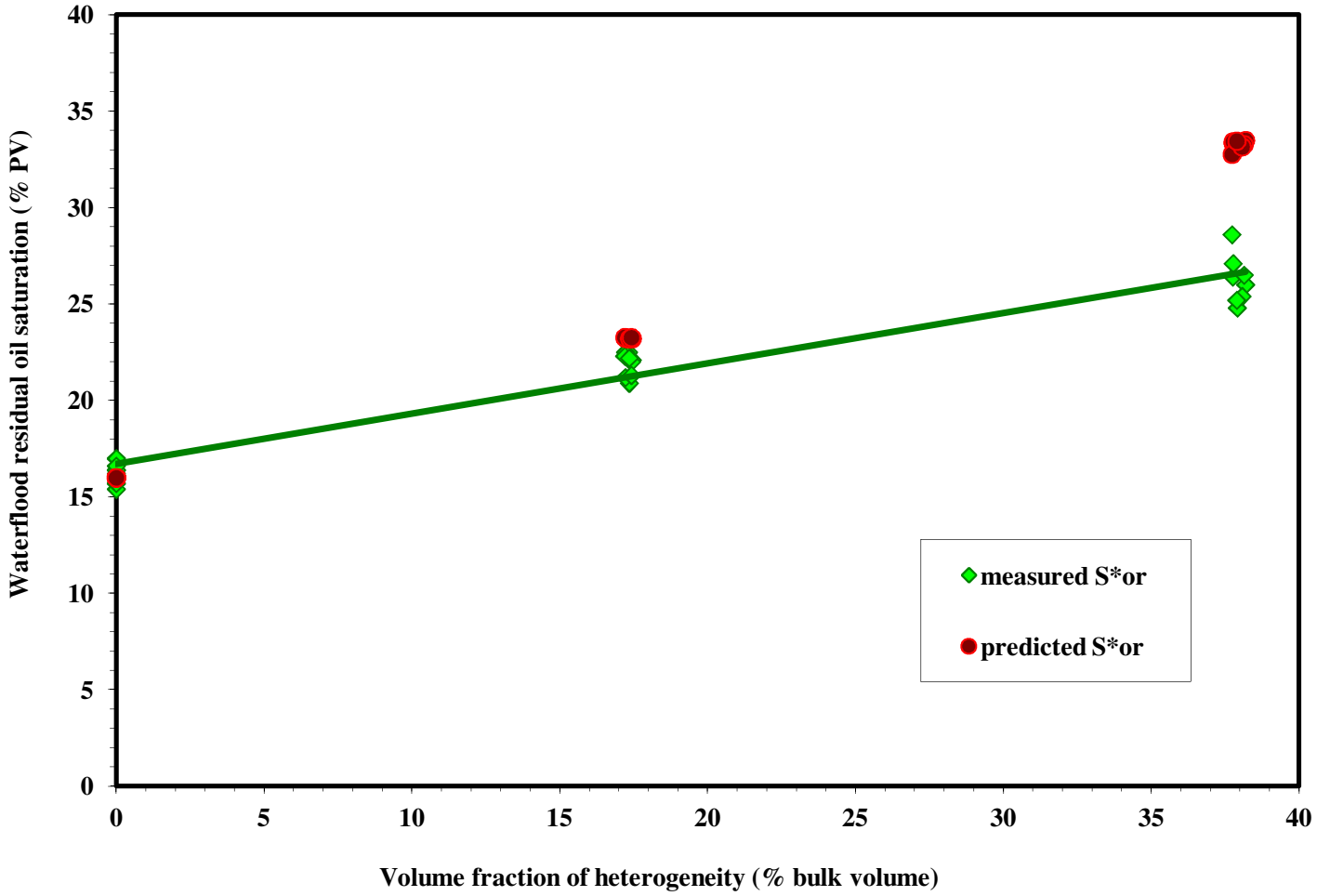

Figure 3-9: Waterflood residual oil saturation at different heterogeneity levels

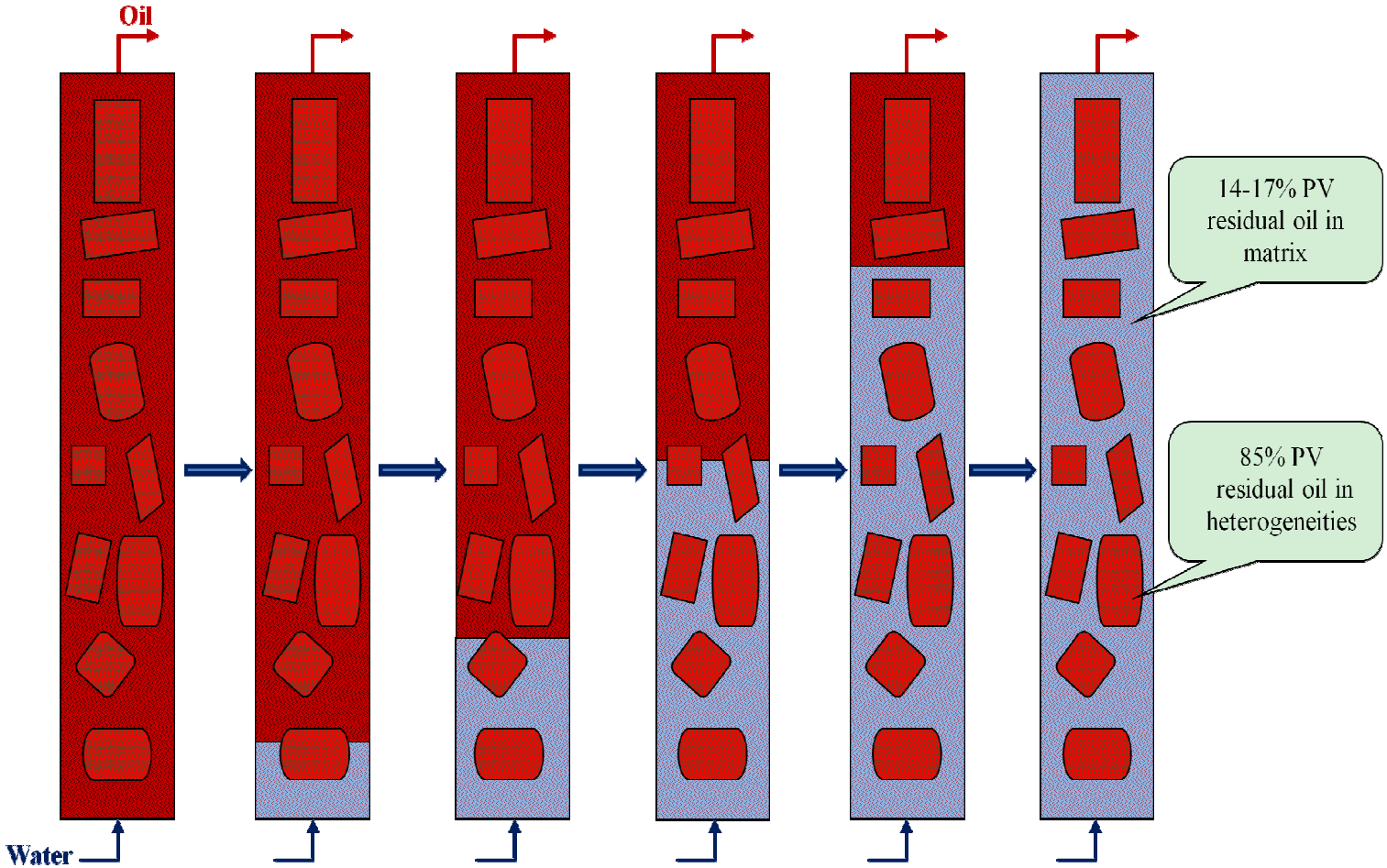

Figure 3-10: Schematic of time-sequence of oil trapping mechanism upon waterflooding in packed column exhibiting pore structure heterogeneities (large-bead-size inclusions embedded in small-bead-size matrix)

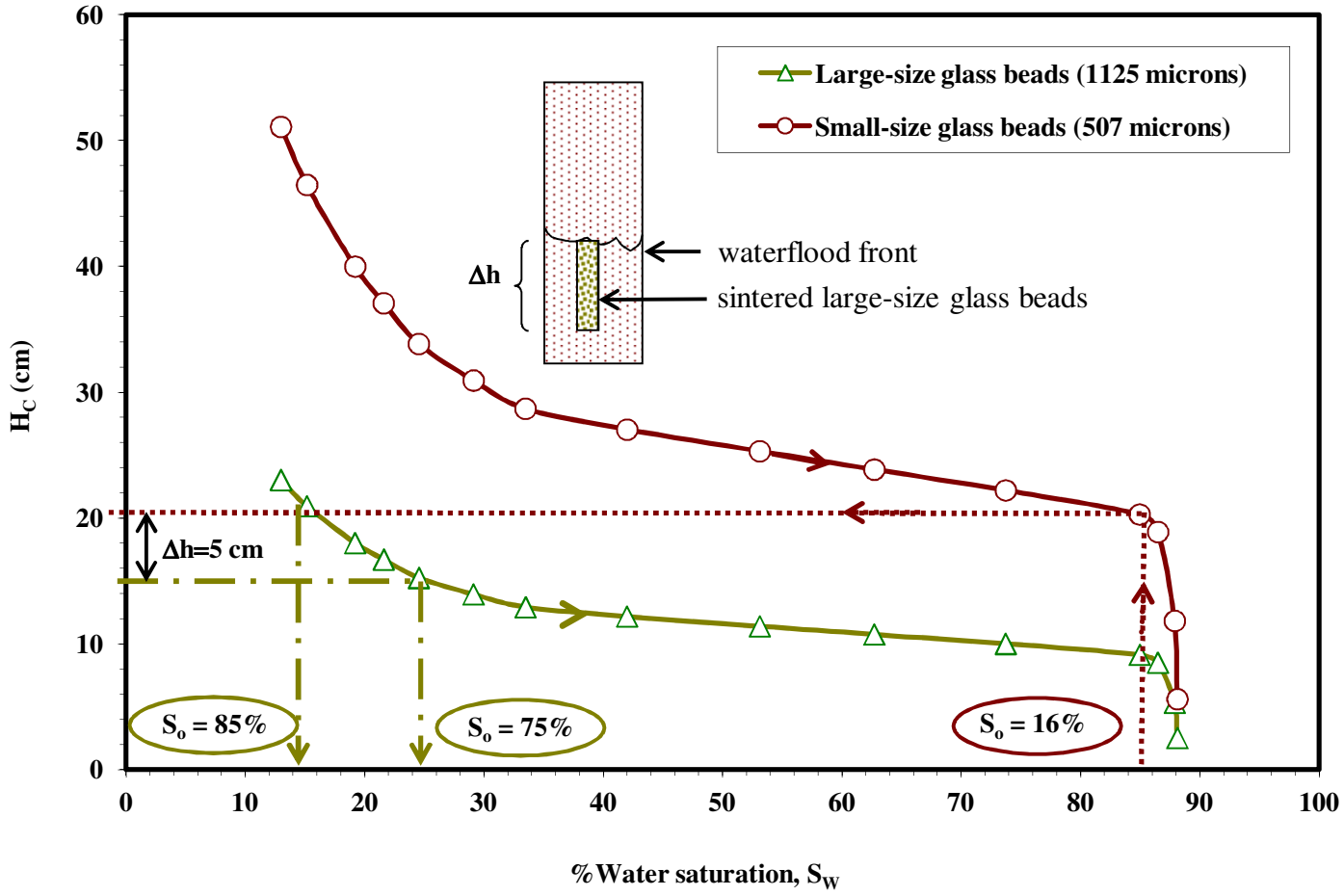

Figure 3-11: Water-oil imbibition curves for small size glass bead used as continuum and large size sintered glass beads used as heterogeneity

3.4.2 Recovery of Waterflood Residual Oil using the GAIGI Process

After performing waterflooding tests, the oil trapped in the matrix is about 16% PV and the rest of residual oil trapped in the heterogeneities is proportional to the volume fraction of heterogeneity. The packed column was then drained at a constant liquid withdrawal rate from the bottom in order to produce the trapped oil blobs in the form of an oil bank created due to the gravitational segregation. As the withdrawal was carried out from the bottom (see Figure 3-8), air invaded the porous medium from the top at constant atmospheric pressure. The GAIGI experiments were randomly conducted at three levels of volume fraction of heterogeneity and eight levels of withdrawal rate. Randomization is necessary to reduce the effects of unknown bias such as instrumentation drift. The experimental conditions and results are summarized in Table 3-2.

During the early stage of withdrawing liquid from the bottom of the packed columns, only water is produced while an oil bank is forming ahead of the gas–liquid macroscopic interface. The oil bank grows in size as the gas-liquid interface advances towards the bottom of system. The oil production starts at the time when the oil bank arrives at the production end. The pore-scale mechanism of oil bank formation during the GAIGI process is described as follows: consider the waterflood residual oil trapped within the reservoir where oil is trapped in relatively large pore bodies of a water-wet reservoir, as illustrated in Figure 3-12. Introducing an inert gas with low volumetric flow rate could effectively mobilize the trapped oil under the conditions of water-wet media and positive spreading coefficient of oil over water. When the gas phase invades the pores filled with waterflood residual oil, the trapped oil spreads spontaneously over the water phase (Chatzis et al. 1988). Therefore, a thin film of oil is formed between water, which occupies the corners of pores, and the invading gas. As the gas invasion continues, more residual oil will spread over water. Thereby, continuous films of oil could be formed that can effectively contribute to the flow of oil towards the production end by gravity forces. As a result of this oil-spreading phenomenon, oil accumulates at the advancing tips of the gas–liquid interfaces and over time an oil bank forms. As the oil bank propagates downwards, the trapped oil blobs are accessed by the oil bank and become reconnected with the continuous oil phase. The oil bank depletion begins when it arrives at the production end. The oil production continues until the air breaks-through the fine layer of beads, used as a capillary barrier at the bottom of the column for attaining more residual oil recovery and minimizing capillary-end effect.

Table 3-2: Summary of the experimental results for the GAIGI experiments in packed columns at different levels of permeability heterogeneity fraction and withdrawal rate[†]

exp. no.	H	ϕ	PV_T	PV_M	PV_H	VS_{or}	Q_L	$RF_{g.bkt}$	V_{pg}	N_{gv}	S_{org}	S_{wc}
17	0.00	38.93	101.4	101.4	0.0	15.4	2.0	69.48	0.207	643.6	4.63	10.32
1	0.00	38.78	100.9	100.9	0.0	16.4	3.2	58.54	0.345	386.5	6.74	8.33
20	0.00	39.46	102.2	102.2	0.0	16.4	6.4	53.66	0.681	195.6	7.44	8.28
6	0.00	38.63	101.2	101.2	0.0	17.0	8.0	44.12	0.919	145.0	9.39	9.43
10	0.00	39.16	102.0	102.0	0.0	16.2	12.0	33.33	1.487	89.6	10.59	8.24
13	0.00	39.15	101.6	101.6	0.0	16.6	20.0	13.86	2.618	50.9	14.07	9.55
19	0.00	39.00	101.5	101.5	0.0	15.7	30.0	0.00	3.943	33.8	15.47	9.76
15	17.35	35.55	95.3	85.3	10.0	20.9	2.0	75.12	0.240	590.0	5.46	10.65
23	17.32	35.64	95.7	85.7	10.0	22.5	2.0	76.00	0.233	606.7	5.64	9.71
24	17.22	35.37	95.5	85.5	10.0	21.2	3.2	71.70	0.380	372.6	6.28	8.66
2	17.22	35.29	95.3	85.3	10.0	22.5	6.4	61.78	0.799	177.3	9.03	8.49
4	17.19	35.08	94.9	84.9	10.0	22.3	8.0	59.64	0.932	152.1	9.49	9.32
8	17.45	35.91	95.7	85.7	10.0	22.1	12.0	52.49	1.471	96.3	10.97	10.65
11	17.42	35.66	95.2	85.2	10.0	22.0	20.0	19.91	3.052	46.4	18.49	9.65
16	17.35	35.70	95.7	85.7	10.0	22.2	50.0	10.36	7.897	17.9	20.80	11.27
18	17.42	35.57	95.0	85.0	10.0	21.3	50.0	0.00	8.077	17.5	22.42	11.25
21	37.76	32.28	88.6	66.3	22.3	26.4	2.0	83.33	0.258	592.4	4.97	9.29
7	37.77	32.31	88.3	66.0	22.3	27.1	3.2	77.86	0.420	363.9	6.80	8.48
3	38.19	32.56	88.0	65.7	22.3	26.0	6.4	73.46	0.835	183.2	7.84	9.75
5	37.91	32.52	88.9	66.6	22.3	24.8	8.0	69.35	1.049	145.8	8.55	10.25
9	37.73	33.42	91.8	69.5	22.3	28.6	12.0	58.04	1.599	95.6	13.08	9.39
12	38.14	32.79	89.1	66.8	22.3	26.5	20.0	52.83	2.774	55.1	14.03	10.29
14	38.07	32.95	89.7	67.4	22.3	25.4	40.0	34.65	6.371	24.0	18.51	15.02
22	37.89	32.25	88.2	65.9	22.3	25.2	80.0	17.06	14.377	10.6	23.71	14.59

[†]H: heterogeneity fraction (Vol. %)
ϕ: porosity (%)
PV_T: total pore volume (mL)
PV_M: pore volume of matrix (mL)
PV_H: pore volume of heterogeneity (mL)
VS_{or}: volume of waterflood residual oil (mL)
Q_L: liquid withdrawal rate (mL /h)
$RF_{g.bkt}$: oil recovery factor at gas breakthrough (%S_{or}^*)
V_{pg}: average gas–liquid interface pore velocity (m/day)
N_{gv}: gravity number, $N_{gv}=K\Delta\rho_{og}g/\mu_o V_{pg}$
S_{org}: reduced residual oil saturation (% PV)
S_{wc}: connate water saturation (% PV)

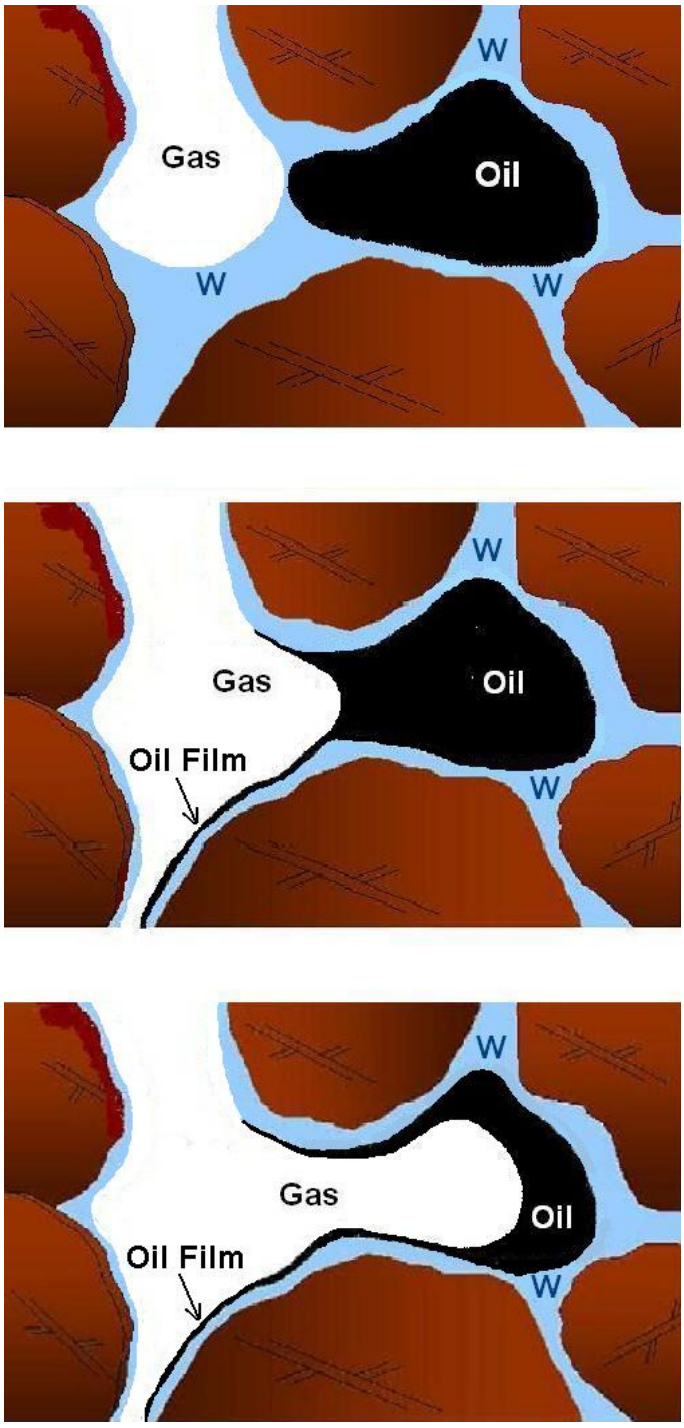

Figure 3-12: Pore-scale fluid distribution during gravity-assisted oil mobilization with gas injection for water-wet and positive spreading coefficient conditions

A schematic of the GAIGI process in water-wet porous media is shown in Figure 3-13. Depending upon the state of the three phases, four distinct zones can be distinguished. The gas zone is the area that has been depleted from oil and water by gas injection with the assistance of gravity forces and film flow. However, some water remains as the wetting film covering the solid surfaces. Also, a small amount of oil exists in this zone in the form of spreading films covering the water surface. The transition zone is where oil, water and gas maintain hydraulic continuity and flow together. The continuous oil films assist in drainage and reconnection of the residual oil to form the oil bank where oil is in the form of continuous bulk phase. The density difference between oil, water, and gas helps in maintaining the oil bank ahead of the gas zone and oil accumulates at the top of the water zone. Finally, the water zone is where water is in the form of a continuous phase with waterflood residual oil present in it. The residual oil ganglia get reconnected as the oil bank propagates towards the water zone.

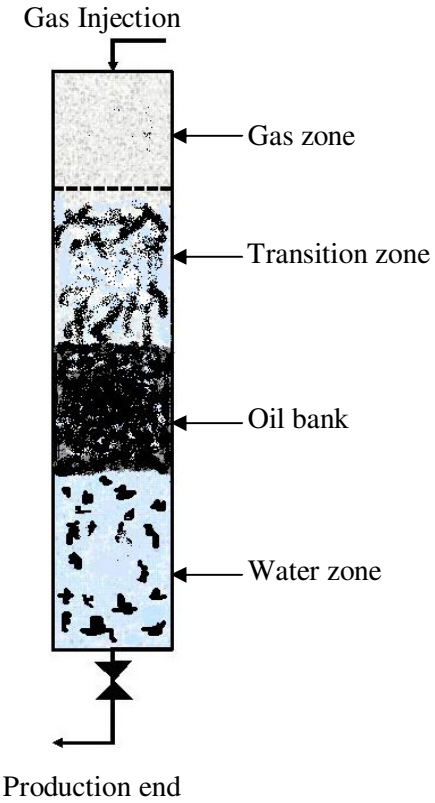

Figure 3-13: Schematic of the gravity drainage process in water-wet porous media (modified from Chatzis and Ayatollahi 1993)

The performance of the GAIGI process for heterogeneous porous media in terms of oil recovery factor up to the time of gas breakthrough as a function of time is shown in Figure 3-14 for a sample of nine of the tests at three arbitrary levels of withdrawal rate (the pertinent data are given in Table A.1 to Table A.3). The same trend was observed for the other levels of withdrawal rates, not shown in the figure for clarity. This figure shows that, for the same level of heterogeneity fractions, the recovery factor at gas breakthrough changes inversely with the withdrawal rate. When the liquid is pumped out of the reservoir at sufficiently low rates, more residual oil blobs will be touched by the invading gas and spread over water. Therefore, there is enough time for the spreading oil films to reconnect and assist in draining of the isolated oil blobs, and hence results in formation of the oil bank. At high withdrawal rates, the unfavorable condition of larger viscous forces compared to the gravity forces causes viscous instability, and hence early gas breakthrough and poor sweep efficiency.

It is also evident from Figure 3-14 that the recovery efficiency for heterogeneous media containing a higher volume fraction of heterogeneity is higher compared to the counterpart homogeneous case. This performance is better compared to waterflooding, which showed relatively low sweep efficiency for heterogeneous porous media. When performing GAIGI in heterogeneous media, the gas invasion occurs primarily in the large-pore regions, because gas is the non-wetting phase with respect to both water and oil, and spreading of oil over water in the presence of gas starts in the high permeability regions. The spreading oil films are in contact with regions that contain a high amount of by-passed oil. Consequently, more oil can be connected through the continuity of the oil films in the large-pore size regions and formation of the oil bank occurs earlier than for the case of homogeneous media, as observed visually during the experiments. Early formation of the oil bank in the packed columns with heterogeneities results in accessing more residual oil blobs and a higher recovery factor is attained in comparison to the homogeneous media. This effect is more pronounced at lower withdrawal rates because the gravity force is higher compared to the viscous force associated with the smaller withdrawal rates.

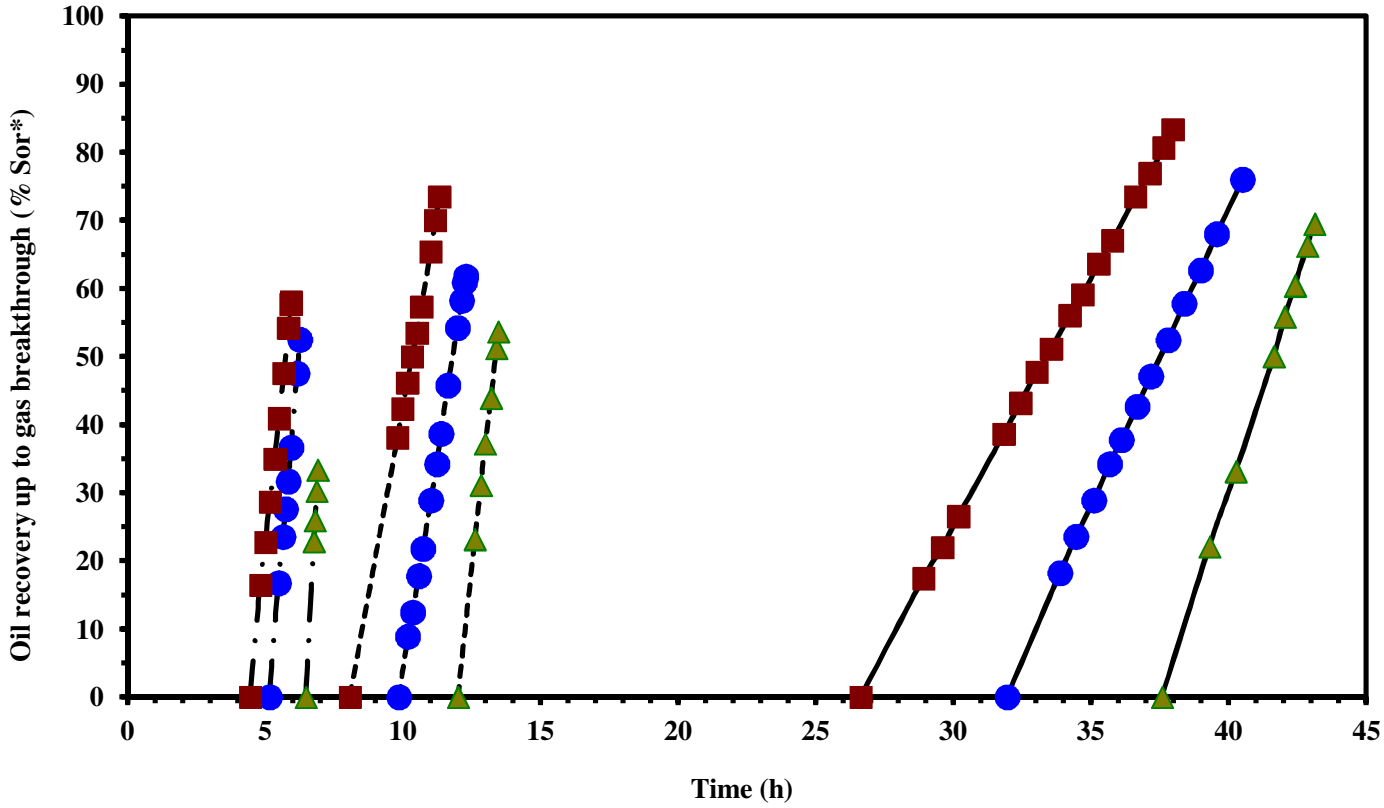

Figure 3-14: Cumulative oil recovery up to gas breakthrough for various permeability heterogeneity levels and withdrawal flow rates. Heterogeneity levels: (▲) 0%, (●) 17%, (■) 38%, Withdrawal rates: (—) 2.0 mL/h, (---) 6.4 mL/h, (- · -) 12.0 mL/h (the data are given in Table A.1 to Table A.3)

The differences in the time of oil and gas breakthrough as well as the slope of the production curves (shown in Figure 3-14) for various sets of experiments are because of the differences in withdrawal rates. For each set of three experiments carried out at the same withdrawal rate, but at various heterogeneity levels, the time to reach oil and gas breakthrough changes inversely with the magnitude of heterogeneity. The differences in the time of oil and gas breakthrough were caused by the variation in total pore volume and also the magnitude of waterflood residual oil saturation at different heterogeneity levels. The variation in the total pore volume at different heterogeneity levels was due to the lower porosity in the heterogeneities as a result of the sintering process (about 32% porosity for sintered beads compared to 38% porosity for unconsolidated glass beads). Accordingly, the permeability of sintered media changed slightly, from 1125 Darcy for unconsolidated glass beads to about 806 Darcy for the sintered case with the same glass bead size.

Figure 3-15 shows the gas–liquid interface position against time for six of the experiments as an example. The macroscopic velocity of the gas–liquid interface for the packed columns having variable magnitude of heterogeneity was determined from the slope of the fitted lines shown in Figure 3-15. We refer to this velocity as pore velocity (V_{pg}). Despite the variation in the average pore velocity of the gas–liquid interface in packed columns containing different fractions of heterogeneity, the plots are all linear showing a gravitationally stable interface movement in homogeneous as well as heterogeneous porous media. In addition, it was shown by Deng (1996) that there exist a critical velocity beyond which fingering will develop during the downward displacement of the oil bank by the gas phase. This velocity is defined by:

$$v_c = \frac{g\,\Delta\rho_{og}}{(\mu_o / k_o) - (\mu_g / k_g)} \tag{3-3}$$

where k_o and k_g are the oil and gas relative permeabilities, respectively. For the system of fluids and porous media we used in this study, the critical velocity is estimated at about 170 m/day. Comparing this value with the V_{pg} data shown in Table 3-2, it is clear that the macroscopic velocity of the gas–liquid interface for all of the performed experiments is much less than the critical velocity, confirming a stable gravity drainage displacement.

The relatively higher oil recovery efficiency of the GAIGI process in the high permeability isolated regions compared to the matrix was further verified by determining the local residual oil saturation.

At the end of a successful gravity drainage test, the glass beads were removed carefully from the column at different cross sections and the oil content of each sample was measured. Analysis of the residual oil was carried out by means of a gas chromatography (Agilent 6890A), using a capillary GC column (HP-1 Crosslinked Methyl Siloxane) and a flame ionization detector (FID). At first, external standard samples of known concentrations of kerosene in ethanol were prepared, followed by diluting the solutions with dichloromethane as a recommended solvent for the GC test. The standard samples were then injected into the GC column and the characteristic peaks of ethanol and kerosene components were taken. Calibration curves were obtained by plotting the characteristic peak heights versus the corresponding concentrations of kerosene and ethanol, separately. Kerosene is a complex mixture of hundreds of components; therefore, the GC analyzer yielded a spectrum of characteristic peaks corresponding to each component. To be consistent in all tests and assuming that the kerosene composition remained the same throughout the analysis, a peak at the retention time of 6.18 minutes was chosen as the representative peak for kerosene. This peak was relatively high and hence easy to read. The test samples were prepared through washing the kerosene content of glass bead samples (taken from the packed column) by known amounts of ethanol, then diluting the solution with dichloromethane. Next, the solutions were analyzed by GC. By comparing the characteristic peak heights of the test samples with the calibration curve, the concentrations of kerosene in the samples were determined. The kerosene concentrations were then converted to saturation (% PV) having the amount of added ethanol and dichloromethane, along with the porosity and bulk volume of glass bead samples.

The residual oil saturation remaining in the matrix and heterogeneities after gravity drainage test was plotted versus the height of the packed column, and is shown in Figure 3-16. This figure demonstrates the position dependence of the residual oil remaining in the column for both media. It is clear that drainage of oil from the high permeability isolated regions was more efficient than that in the continuum at any location. However, for the upper 75% of the column height the recovery of oil is nearly completed in heterogeneities as well as in the continuum. The relatively high oil content of the lower portion of the matrix is because of the capillary-end effects. We made an effort to diminish the end effect by using the capillary barrier, which delayed the gas breakthrough, but a much longer column should be used to minimize the end effect. In a long column it is expected to have a similar saturation distribution for the upper part of the column ($\approx 2\%$) and the same amount of oil would be

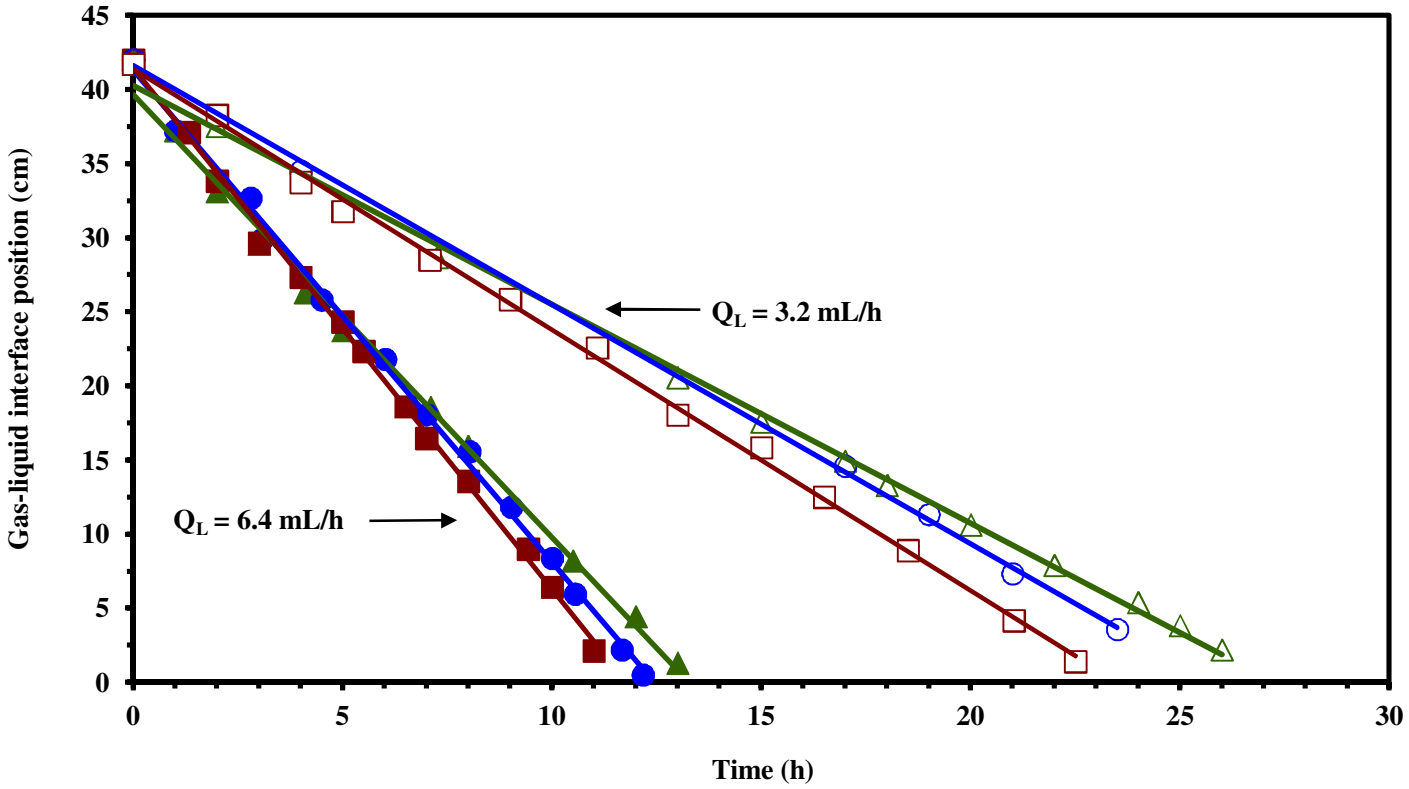

Figure 3-15: Comparison of the gas–liquid interface position during the gravity drainage tests at various levels of permeability heterogeneity and withdrawal rates (the data are given in Table A.4 and A.5)

(Δ) 0% Heterogeneity, 3.2 mL/h withdrawal rate (○) 17% Heterogeneity, 3.2 mL/h withdrawal rate (□) 38% Heterogeneity, 3.2 mL/h withdrawal rate (▲) 0% Heterogeneity, 6.4 mL/h withdrawal rate. (●) 17% Heterogeneity, 6.4 mL/h withdrawal rate. (■) 38% Heterogeneity, 6.4 mL/h withdrawal rate

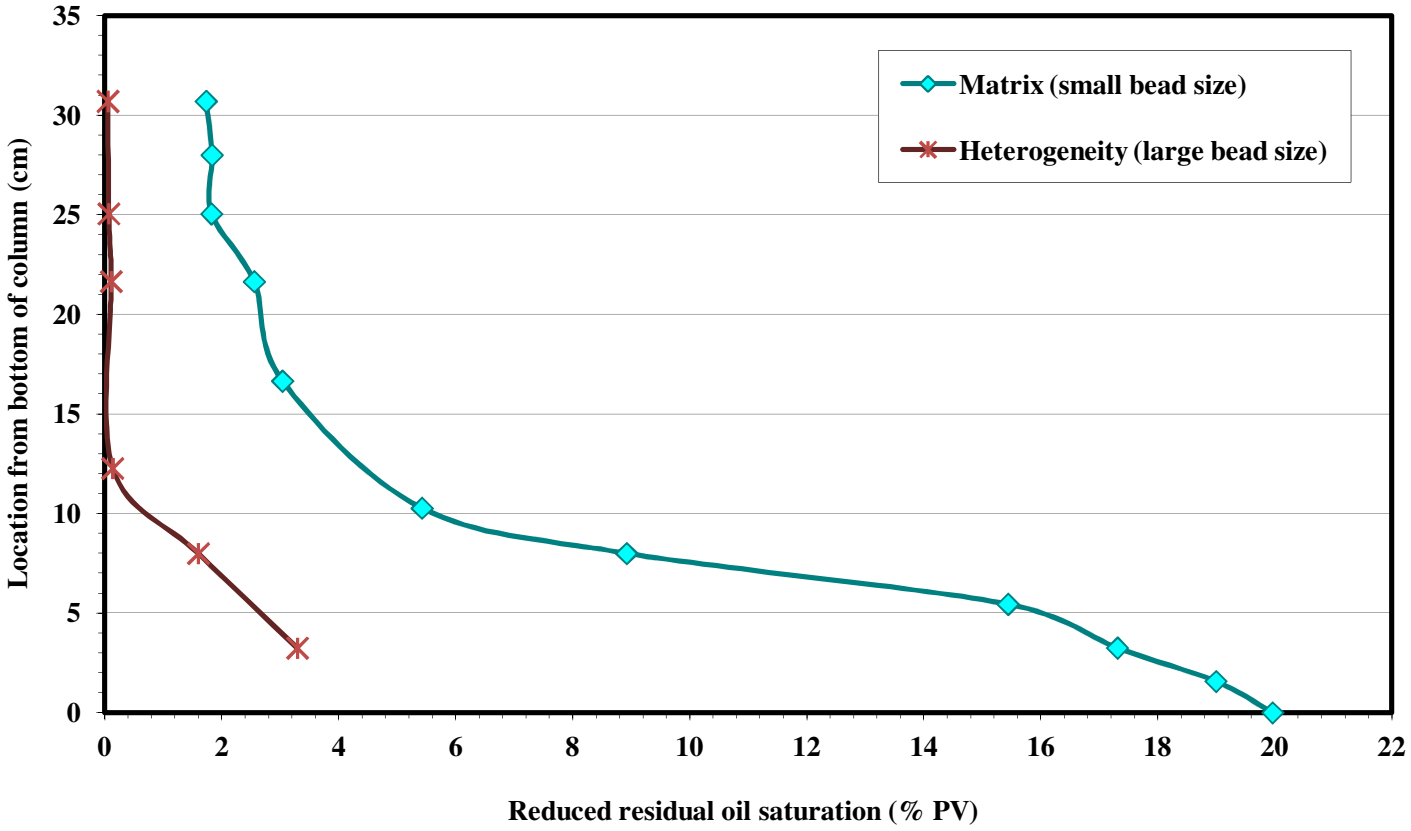

Figure 3-16: Saturation distribution of reduced residual oil at the end of a gravity drainage test corresponding to N_{gv} = 18

retained due to capillarity at the bottom of the column. However, compared to the total height of the column, this retained oil occupies a smaller portion of the column. Therefore, the overall oil recovery is predicted to be higher in a long column compared to the size of column used in this study.

3.4.3 Correlation of the Oil Recovery Factor with the Gravity Number

In order for the experimental results to be applicable for different scales and operating conditions, they need to be presented in the form of dimensionless scaling groups. The significant parameters for the GAIGI process include the average permeability of the porous media, fluid densities and viscosities, and the operating conditions such as oil production rate. These parameters were combined by Hagoort (1980) to obtain a dimensionless number known as the gravity number (N_{gv}), which represents the relative magnitude of the average oil velocity in the gas invaded zone ($K\Delta\rho_{og}g/\mu_o$) to the macroscopic velocity of the oil bank (V_{pg}):

$$N_{gv} = \frac{K\,\Delta\rho_{og}\,g}{\mu_o\,V_{pg}} \tag{3-4}$$

where K is the absolute permeability of the porous medium (see section 3.3.1), and V_{pg} is the average velocity of the macroscopic gas–liquid interface calculated from experimental data of the gas–liquid interface position measured during the course of experiments. The macroscopic velocity could also be calculated using the following equation when experimental data are not available:

$$V_{pg} = \frac{Q_L}{\phi A(1 - S_{wc} - S_{org})} \tag{3-5}$$

in which Q_L is the liquid withdrawal rate, ϕ is the porosity, and A is the cross sectional area of the porous medium.

Using Equation 3-4, the data of production characteristics shown in Figure 3-14 were presented in the dimensionless form, as illustrated in Figure 3-17. This figure shows that the gravity number describes quite well the combined effects of operating and physicochemical parameters on the oil recovery through the GAIGI process for all three levels of heterogeneity. The correlation trends reveal the strong dependence of recovery factor at gas breakthrough on N_{gv} at the values of gravity number less than about 150 for all three levels of heterogeneity. In addition, the higher the reservoir

average permeability and also the difference between the injected gas and the reservoir oil densities, the more effective is the segregation of the fluids under the gravity assisted conditions; therefore, the oil recovery is more efficient. At low enough withdrawal rates, the spreading films of oil in the depleted zone flow faster than the macroscopic gas–liquid interface; therefore, it is more likely for the oil films to drain and create an oil bank. In contrast, the faster the liquid is pumped out, corresponding to a high downward velocity of the gas–oil interface, the lower is the sweep efficiency of the process since a smaller amount of residual oil is reconnected through the continuous oil films.

Plotting the experimental data of the percentage of un-recovered oil versus N_{gv} in log-log scale gives straight lines with similar slopes for different levels of heterogeneity. This means that the oil production through the GAIGI process is is mainly governed by the matrix permeability. Nevertheless, Figure 3-18 shows that the minimum required gravity number to attain oil production is different for each heterogeneity level. The minimum gravity number, N_{gv}^{min}, was obtained at 34, 18 and 8 for 0, 17, and 38% heterogeneity fractions, respectively. The smaller amount of N_{gv}^{min} in heterogeneous porous media shows that the maximum pumping rate below which the oil bank formation occurs is higher compared to that in the homogeneous media. In fact, the large magnitude of gravity force in the high permeability regions can overcome the viscous forces, corresponding to a higher withdrawal rate, and assists in the formation of the oil bank and consequently oil recovery. The larger magnitude of waterflood residual oil in the high permeability isolated regions is another factor that promotes oil bank growth in heterogeneous media even at low gravity numbers. This analysis of the minimum (critical) gravity number could be applied in other length scales since it is presented in the dimensionless form. An application of this analysis is described in section3.5.

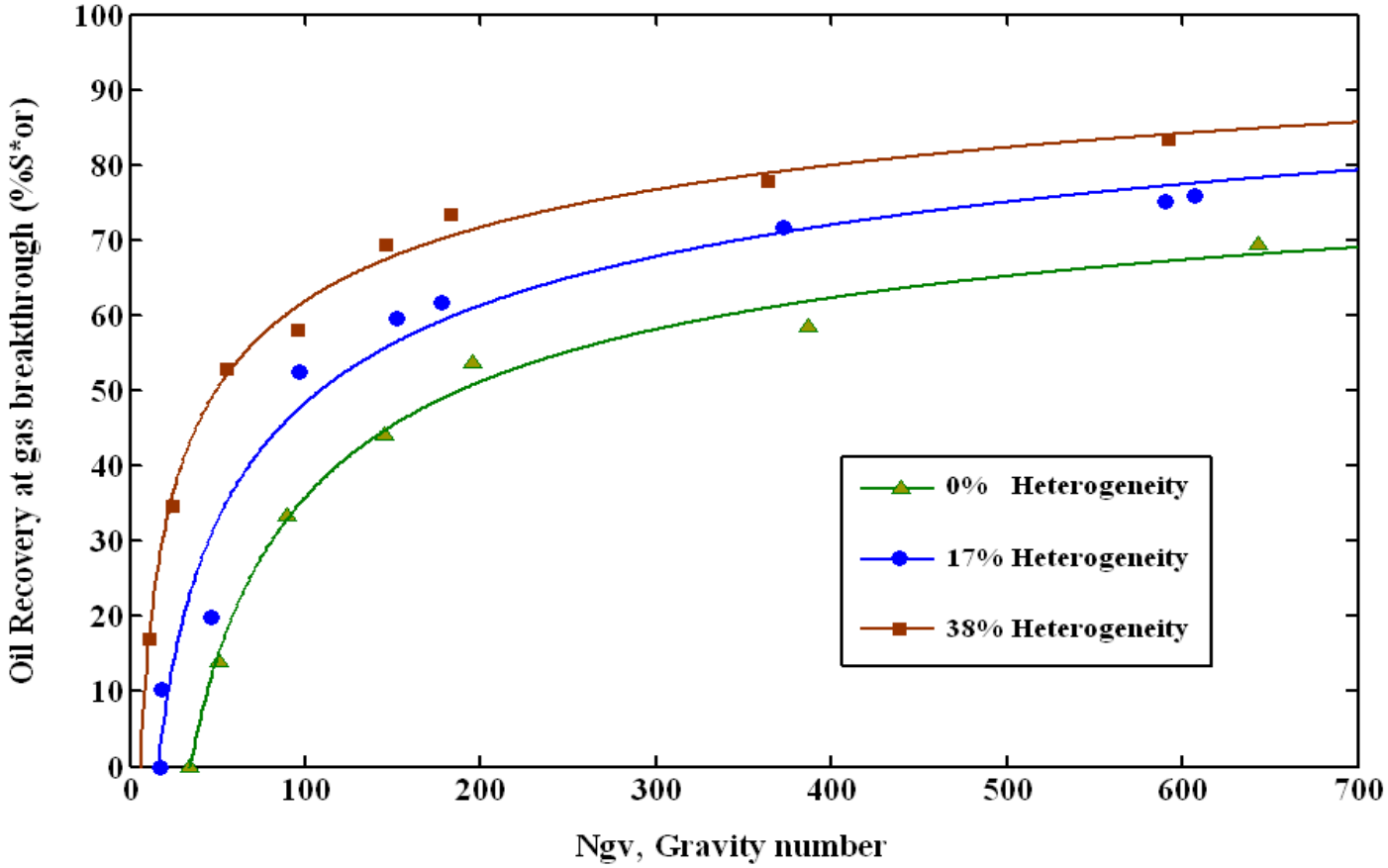

Figure 3-17: Correlation of the oil recovery factor at gas breakthrough with the gravity number at different levels of pore structure heterogeneity

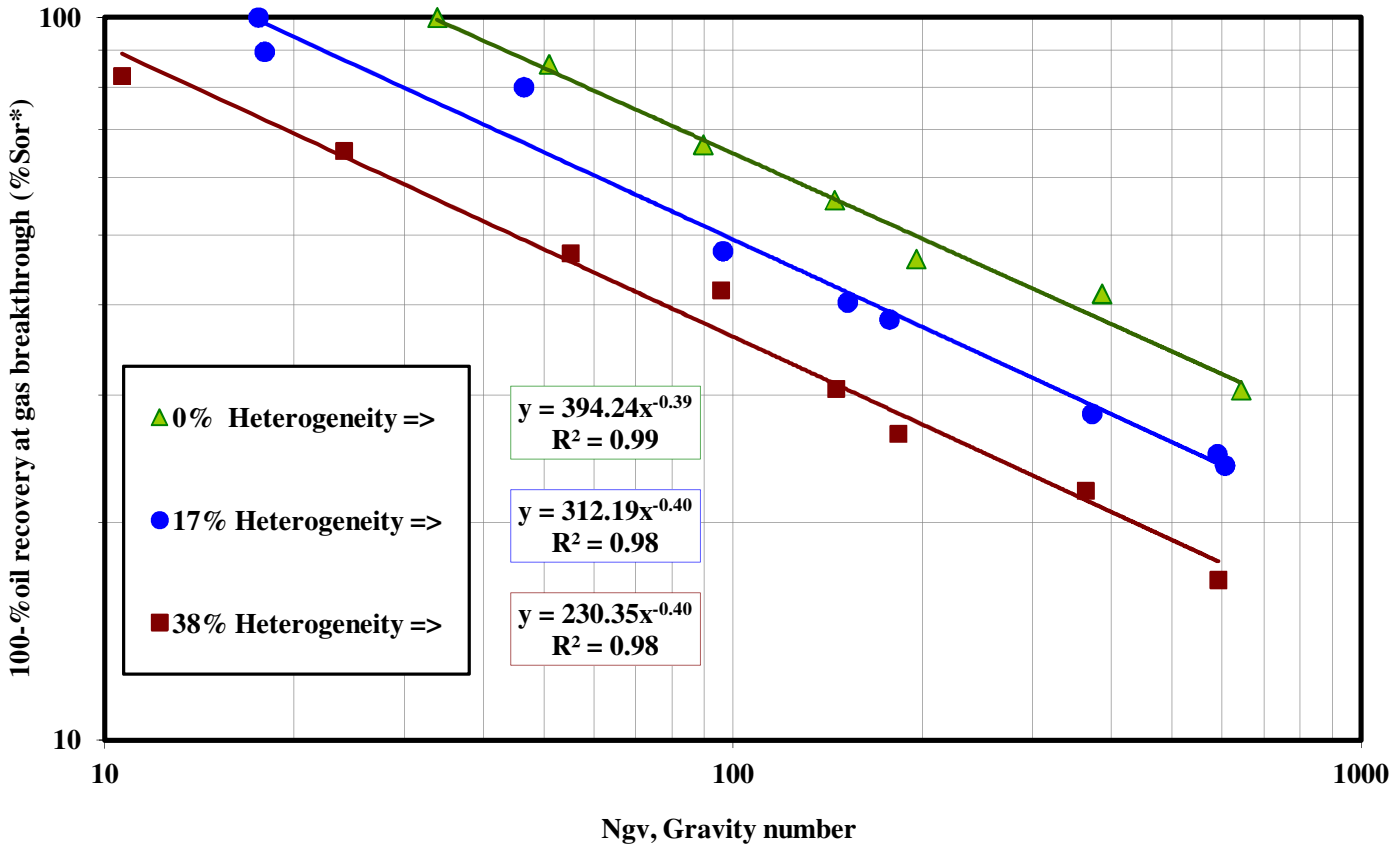

Figure 3-18: Logarithmic-scale correlation of the percentage of un-recovered oil at gas breakthrough with the gravity number for different levels of pore structure heterogeneity

3.4.4 Prediction of the Oil Recovery Factor for Heterogeneous Media

The total oil recovery from a heterogeneous porous media up to the gas breakthrough could be considered as the sum of the recoveries from the heterogeneity and matrix, respectively:

$$\%\ Total\ oil\ recovery = \frac{[\,PV \times S_{or}^{*} \times RF_{g.bkt}\,]_{Het} + [\,PV \times S_{or}^{*} \times RF_{g.bkt}\,]_{Matrix}}{total\ volume\ of\ \ waterflood\ \ residual\ oil} \qquad (3\text{-}6)$$

where PV is the pore volume, $RF_{g.bkt}$ is the recovery factor at gas breakthrough, and S_{or}^{*} is the waterflood residual oil saturation. The recovery factor in the matrix is considered to be the percentage of oil recovered from the corresponding homogeneous packed column through the GAIGI process performed at the same withdrawal rate. For the sintered and higher permeability regions, the recovery factor was unknown experimentally; therefore, we computed this value from the data of homogeneous small-bead-size porous media. The procedure was such that the gravity number corresponding to the permeability of the sintered media was calculated, then the recovery factor was computed from the correlation of the recovery factor with the gravity number for homogeneous media (Figure 3-17 or Figure 3-18). In fact, we considered each large-bead-size region by itself as a small homogeneous medium. The gas–liquid interface velocity of the sintered regions was also unknown experimentally and was computed from the data of production rate and porosity of the sintered medium.

Following the above procedure, Equation 3-6 was applied to predict the oil recovery factor at gas breakthrough in heterogeneous media, given the information of the production characteristics of the counterpart homogeneous media (consisting of the glass beads of the same size as the matrix in heterogeneous packed columns), and the petrophysical properties of the matrix and heterogeneity. The predicted results of the oil recovery factor are shown in Figure 3-19 and Figure 3-20 for the packed columns containing 17%, and 38% heterogeneity, respectively. The comparison of the measured and calculated recovery factors for both cases of heterogeneity levels demonstrates satisfactory agreement. In addition, quantitative evaluation of the match of the calculated values and experimental data illustrates the goodness of fit for both cases, with better agreement for the case of 17% heterogeneity as the R^2 were estimated at 95% for the case of 17%, and 83% for the case of 38% heterogeneities. In spite of the relatively high values of R^2 (especially for the 17% heterogeneity

case), the model computation seems to underestimate the magnitude of the recoverable oil. Apparently, the large-pore-size heterogeneity regions not only contribute in attaining a high recovery factor because of the relatively high effective permeability and the large residual oil content, but also improve the overall oil recovery efficiency of the matrix through GAIGI due to the early formation of an oil bank. This effect is more pronounced in the low gravity number range. Figure 3-19 and Figure 3-20 show that the suggested computation model predicts the production data adequately as the gravity number increases, but fails to predict the recovery data well at low values of the gravity number (high withdrawal rates). As the production rate increases, the model predicts a very low recovery factor for the matrix, but in reality the formation of an oil bank in the heterogeneities facilitates the reconnection of the oil blobs trapped in the matrix, and hence more oil than expected is produced from the matrix zone. For the case of 38% heterogeneity, such an effect is more intensified as the waterflood residual oil content is higher; consequently, the oil bank develops at a much earlier stage of the withdrawal period and improves the oil recovery efficiency in the continuum. Therefore, as shown in Figure 3-21, the magnitude of error in predicting the recovery factor versus the gravity number increases with an increase in the withdrawal rate (decrease in N_{gv}).

3.4.5 Distribution of the Residual Oil Saturation at the End of a GAIGI Test

Over the course of the gravity-assisted inert gas injection process, the flow of the three phases is such that waterflood residual oil blobs are joined through continuous spreading oil films over water in the presence of gas. This produces an oil bank which eventually arrives at the production side. However, not all of the trapped oil blobs have the chance to connect with the continuous oil films and depending on the gravity number conditions some of the residual oil remains in the gas invaded zone. Figure 3-22 demonstrates the magnitude of the remaining oil after the GAIGI process (known as the reduced residual oil saturation, S_{org}) as a function of gravity number for three levels of heterogeneity. While the magnitude of waterflood residual oil is highly sensitive to the presence of heterogeneity (Figure 3-9), the reduced residual oil saturation after the GAIGI process seems to be similar for each set of experiments carried out at the same withdrawal rate, regardless of the presence of heterogeneity. Considering the results shown in the Figure 3-16 and Figure 3-22, it is concluded that the matrix permeability is the controlling parameter for the GAIGI process in heterogeneous porous media and hence remaining of residual oil occurs mainly in the continuum.

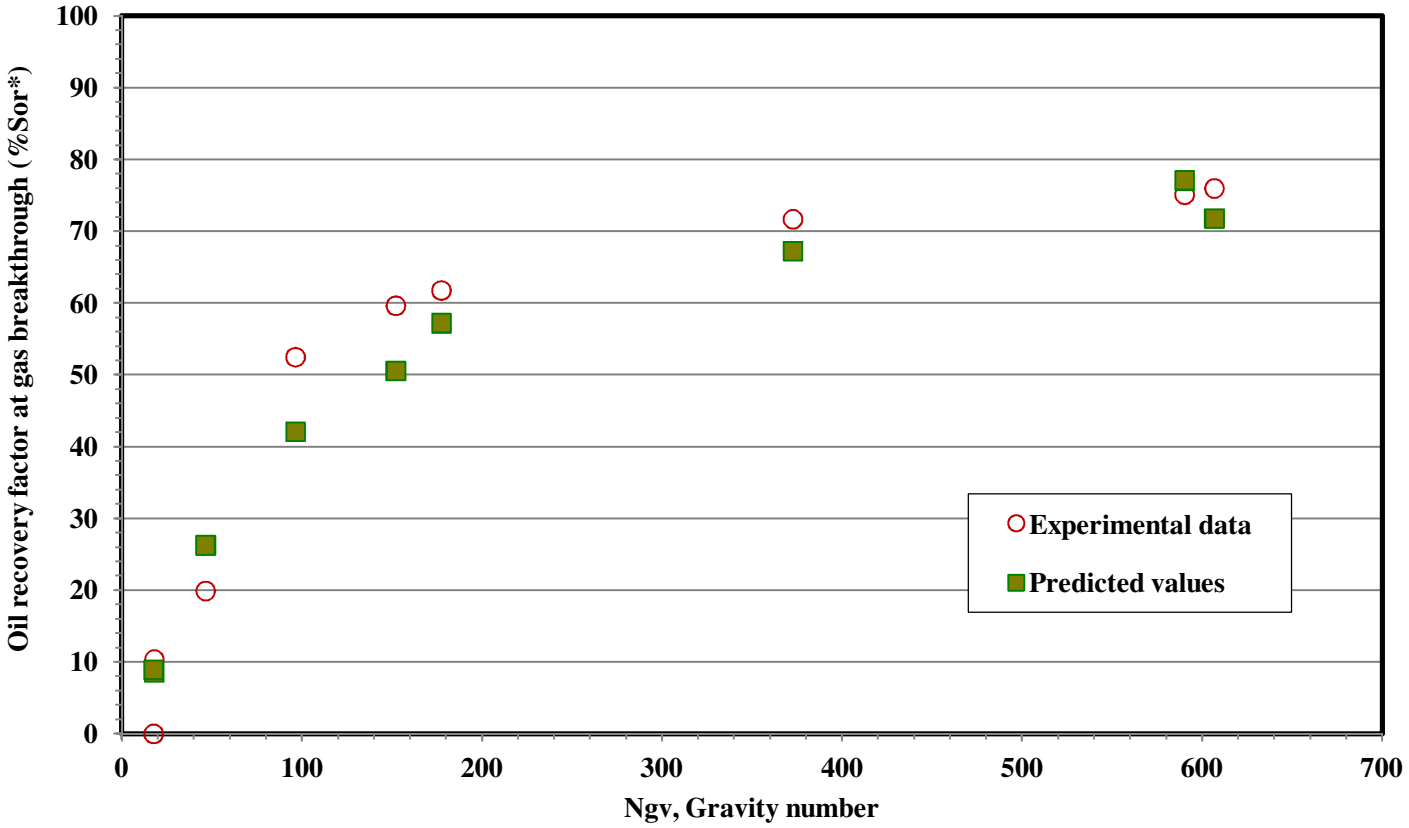

Figure 3-19: Comparison of the experimental and predicted values of the oil recovery factor at gas breakthrough for the packed columns containing 17% permeability heterogeneity

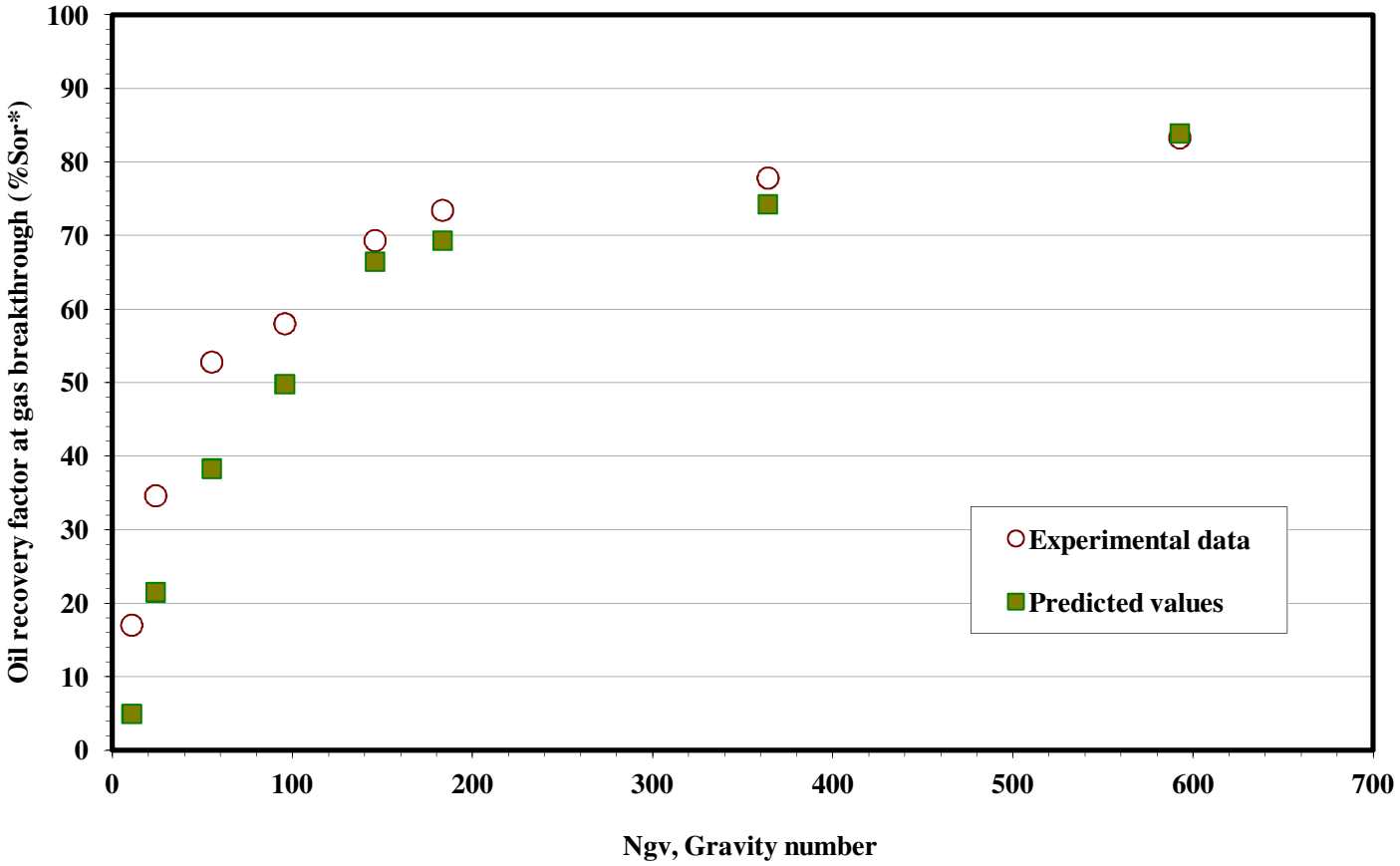

Figure 3-20: Comparison of the experimental and predicted values of the oil recovery factor at gas breakthrough for the packed columns containing 38% permeability heterogeneity

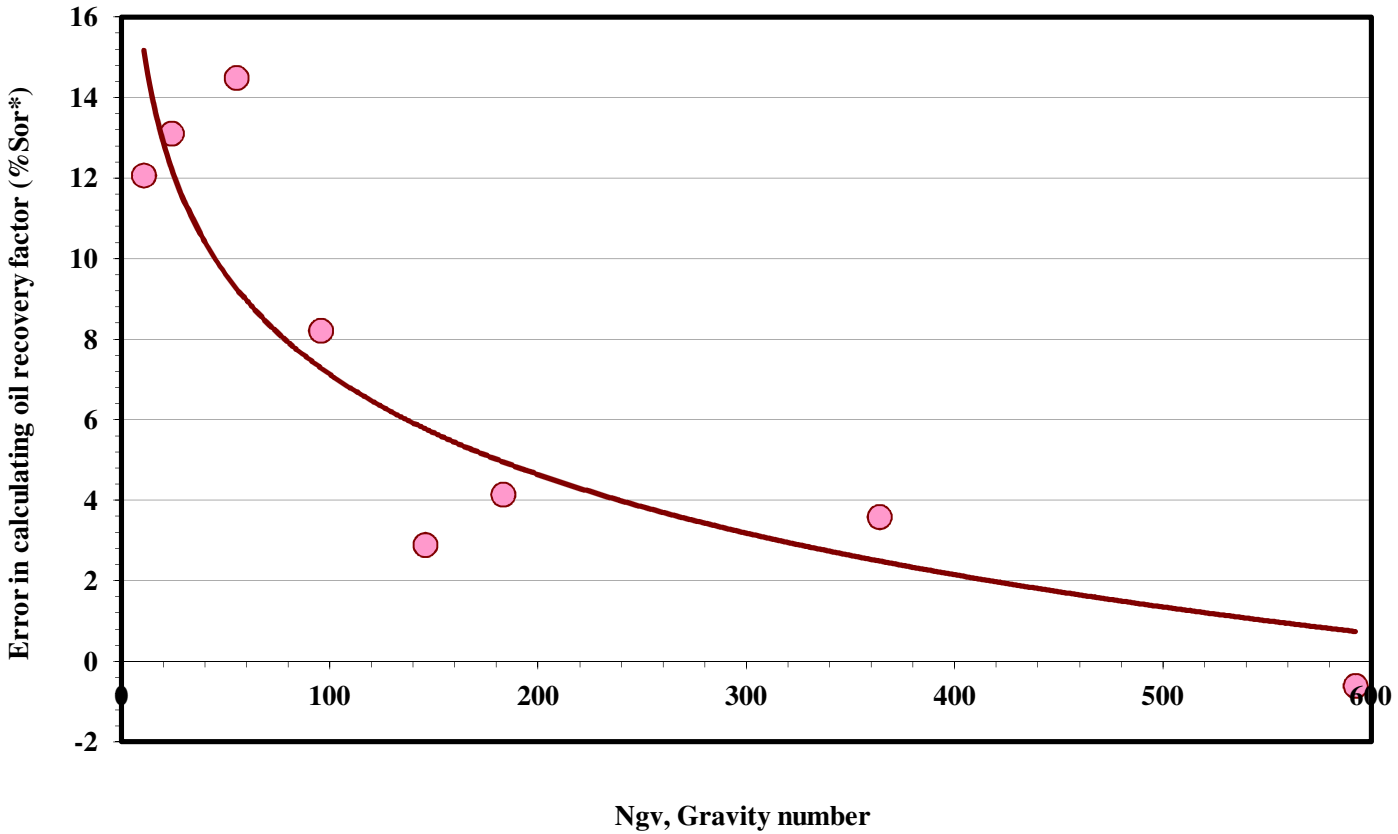

Figure 3-21: Prediction error in calculation of the oil recovery factor at gas breakthrough for the packed columns containing 38% pore structure heterogeneity

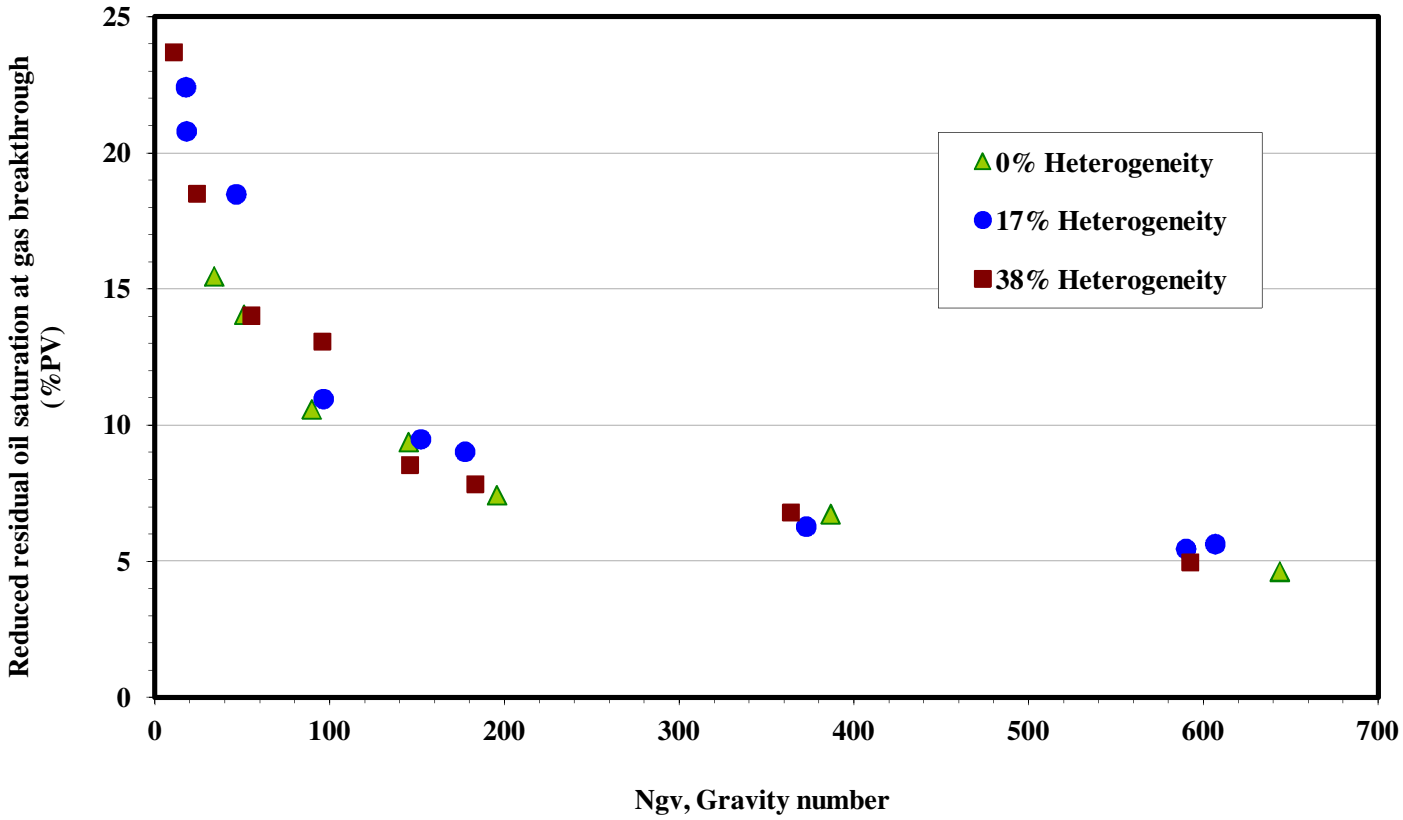

Figure 3-22: Average reduced residual oil saturation at gas breakthrough for packed columns at different heterogeneity levels

3.5 Application of the GAIGI Process in the Field Scale

The experimental results presented in this chapter could be used to examine the applicability of the GAIGI process in an oil reservoir. The upscaling was performed using dimensionless groups. The main variables governing the performance of the reservoir were combined into the dimensionless group known as gravity number, N_{gv}. A detailed description of the relation between the oil recovery factor and the gravity number as well as the residual oil saturation and the gravity number was presented in the previous sections. To account for the reservoir thickness and hence the time for oil and gas breakthrough during the GAIGI process in the reservoir, the dimensionless time for controlled gravity drainage is used:

$$t_D = \frac{t V_{pg}}{L} \tag{3-7}$$

where t_D is the dimensionless time, t is the actual time, and L is the length of the porous medium. Applying the two dimensionless numbers, namely N_{gv} and t_D, and using the experimental results, calculations were conducted for a hypothetical reservoir to study the effects of withdrawal rate and reservoir effective permeability on the required time to achieve an arbitrary recovery factor of 60% of S_{or}^* through the GAIGI process. Table 3-3 describes the characteristics of the reservoir under study taken from the literature (Jadhawar and Sarma 2010) with some modifications. The reservoir fluids were considered to be crude oil with an API gravity of 35º, and a solution gas with a specific gravity of 0.7. The oil and gas density and oil viscosity at reservoir conditions were estimated by applying the pertinent correlations given by Ahmed (1989) and Burcik (1979).

Assuming that the experimental model results are representative of a small section of the reservoir undergoing tertiary GAIGI type recovery, the ratio of dimensionless groups in one scale over the dimensionless groups in another scale should be equal to one to have similar flow behavior in both systems (Rapoport 1955). Considering this concept, the calculation was initiated by first selecting the experimental conditions under which the oil recovery factor of about 60% of S_{or}^* was obtained (see Table 3-4). By setting the gravity number in the lab scale (shown in Table 3-4 for three levels of heterogeneity fraction) equal to the gravity number in the field scale, the pore velocity of gas–liquid interface in the reservoir was calculated using Equation 3-4 for the given oil viscosity and gas–oil density difference at the reservoir condition. The calculation was repeated for an average reservoir

permeability ranging from 0.5–1.0 Darcy. The liquid withdrawal rate at the reservoir conditions was then estimated using Equation 3-5.

Figure 3-23 shows the estimated liquid withdrawal rate versus the reservoir average permeability for recovering 60% of the residual oil at gas breakthrough at three levels of heterogeneity fraction. This figure illustrates that to attain the specific recovery factor mentioned above through GAIGI, a higher pumping rate could be applied in an oil reservoir with higher permeability and with a larger fraction of heterogeneity. This means that the higher the reservoir permeability and heterogeneity are, the better economical profitability is achieved because in a shorter length of time we can reach the desired level of cumulative oil production.

Table 3-3: Description of a typical reservoir (modified from Jadhawar and Sarma 2010)

pay zone thickness	40 m
horizontal well spacing	160 Acre
temperature	82 ºC
permeability	0.5-1.0 D
oil API gravity	35º
bubble point pressure	3580 psi
solution gas-oil ratio	778
oil-gas density difference at reservoir condition	511 kg/m^3
oil viscosity at reservoir condition	0.55 cp

Table 3-4: The experimental conditions corresponding to the oil recovery factor of about 60% of S_{or}^*

heterogeneity fraction (% bulk volume)	experiment number	N_{gv}	S_{wc} (%PV)	S_{org} (%PV)	t_D at oil breakthrough	t_D at gas breakthrough
0%	1	386.5	8.33	6.74	0.807	0.916
17%	4	177.3	8.49	9.03	0.781	0.973
38%	9	95.6	9.39	13.08	0.713	0.950

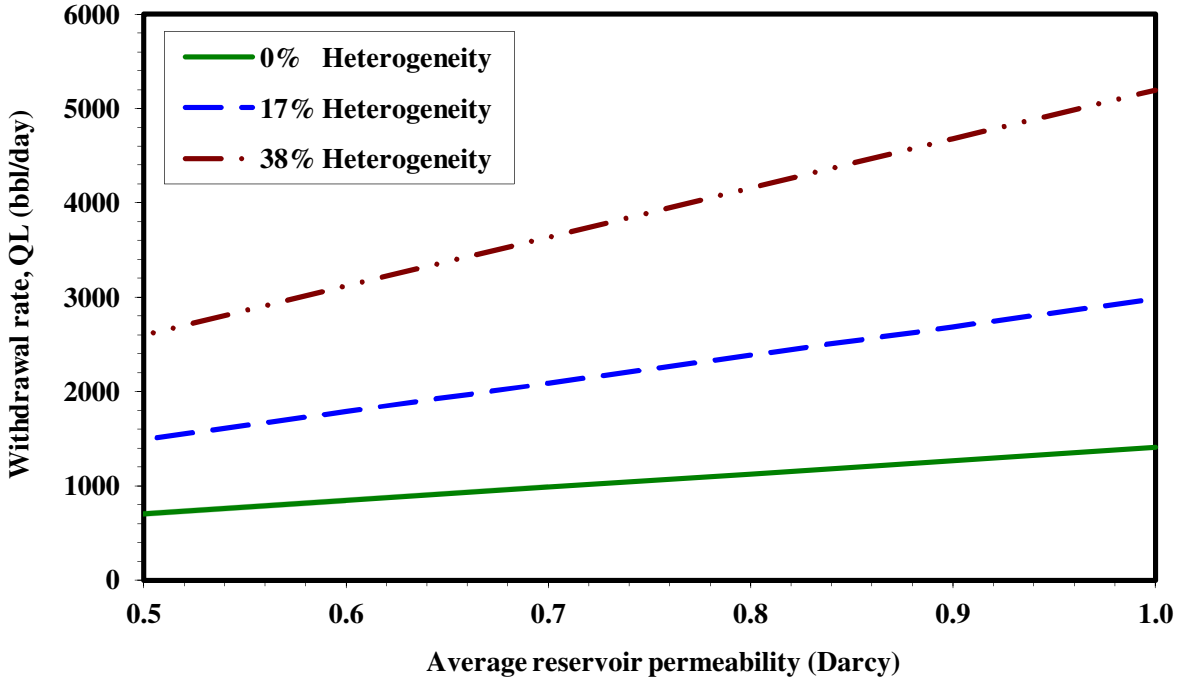

Figure 3-23: Liquid withdrawal rate for the GAIGI process to recover 60% of waterflood residual oil at gas breakthrough for a 40 m thick reservoir with 160 acres well spacing area for different average reservoir permeability and heterogeneity levels

In the same way, the dimensionless time at the lab scale was set equal to that in the reservoir scale to find the time of oil and gas breakthrough in the reservoir using the data shown in Table 3-4 and applying Equation 3-7. Figure 3-24a and b show the time when the oil bank and the gas phase arrive at the production well, respectively. Panels a and b of Figure 3-24 illustrate that the conditions of high average reservoir permeability and high heterogeneity fraction make the GAIGI process more economical since a shorter time is required to produce a certain amount of oil. Even though the favorable conditions of high permeability and heterogeneity level are beneficial to cut down the cost of the GAIGI process by reducing the time for oil bank formation and consequently shortening the withdrawal period, more consideration should be taken to improve the profitability of the process.

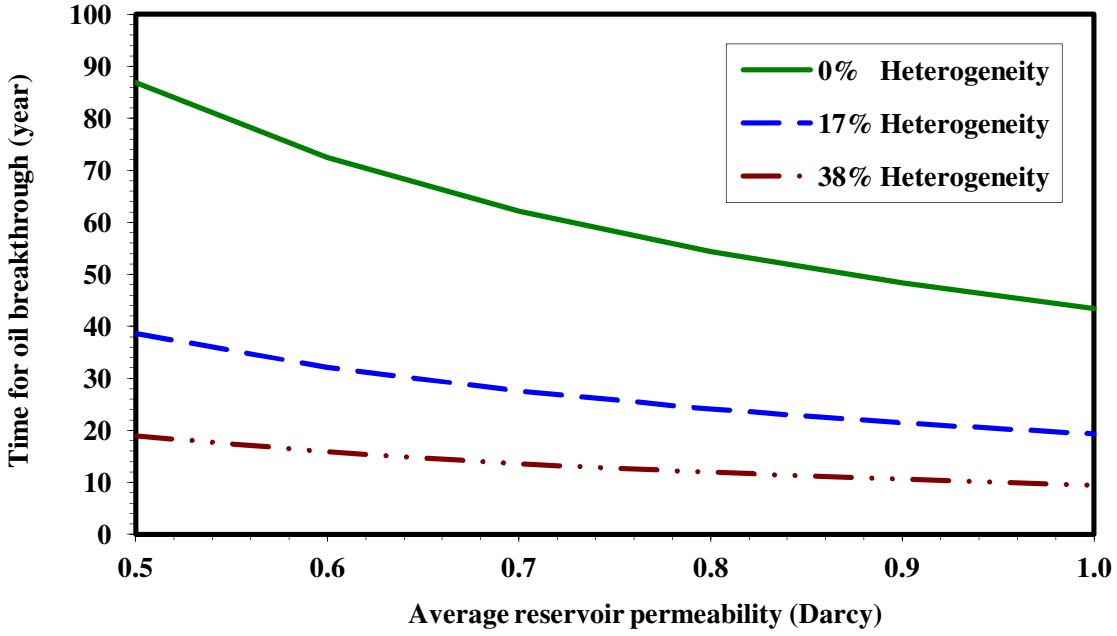

(a)

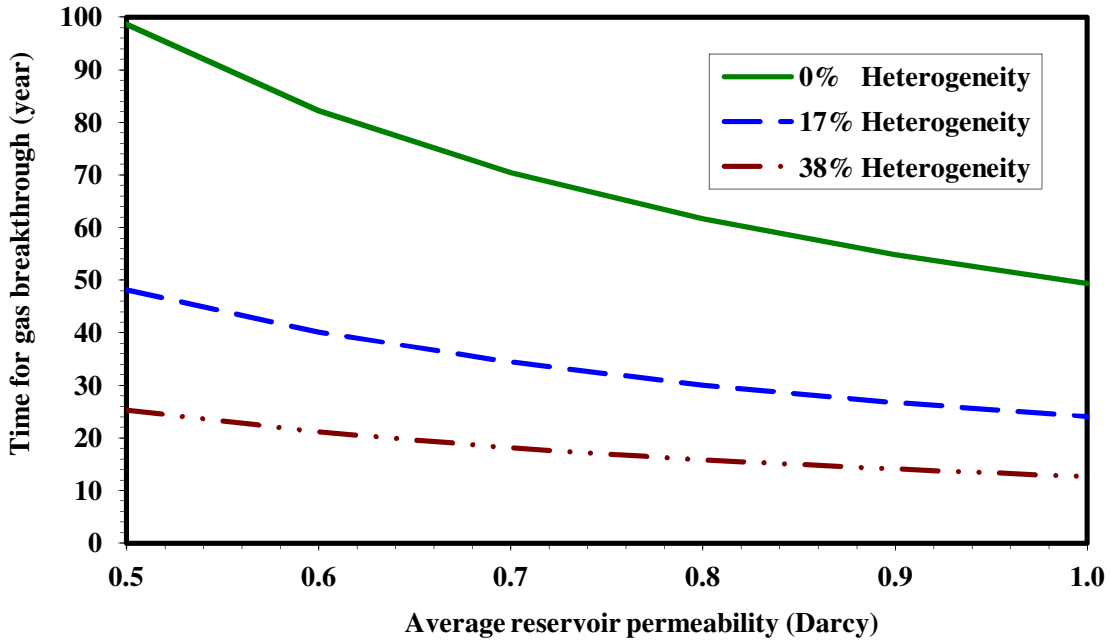

(b)

Figure 3-24: Operating parameters (a) time to oil breakthrough (b) time to gas breakthrough for the controlled GAIGI process corresponding to achieving 60% oil recovery at gas breakthrough for a 40 m thick reservoir with 160 acres well spacing area for different average reservoir permeability and heterogeneity levels

Comparison of panels a and b of Figure 3-24 shows that a long period of the withdrawal time is allocated to water removal from the waterflooded reservoir, i.e., time up to oil breakthrough. This length of time varies from 75% of the total pumping period in the case of homogeneous media up to about 88% in the case of 38% heterogeneity. This means that the focus should be mainly to shorten the time frame of liquid withdrawal during which only water is produced.

To overcome the lengthy time required to carry out the GAIGI process at controlled and low pumping rate conditions, we suggest an alternative process for recovering the waterflood residual oil that will involve two stages: in the first stage, the water presents in the waterflooded reservoir is pumped out at a sufficiently high rate (e.g. at a velocity corresponding to the minimum gravity number) up to the point of gas breakthrough. There is no intent to produce oil at this stage while water is pumping-out; therefore, the water removal could be carried out at the highest possible rate, corresponding to the minimum gravity number, at which no oil is produced through a controlled GAIGI process. The detailed description of the minimum gravity number estimation is given in section 3.4.3. From the values of N_{gv}^{min} for different levels of heterogeneity, the pore velocity of the gas–liquid interface was calculated. The required time for the stage of water removal (t_{WR}) was then estimated considering the following equation:

$$t_{WR} = \frac{L}{V_{pg}} \tag{3-8}$$

where L is the length of the reservoir given in Table 3-3.

In the second stage, the reservoir is shut down until the time an oil bank develops under the action of gravity force and film flow of the spread-out residual oil in the gas invaded pores of the system. For this stage, we used the data of Chatzis and Ayatollahi (1993) in a dimensionless form for the residual oil recovery under free fall gravity drainage. To calculate the time required for the second stage, the dimensionless time equation for free fall gravity drainage of residual oil was applied:

$$t_D = \frac{K \Delta\rho_{og}\, g\, t}{\mu_o \phi (1 - S_{wc} - S_{org}) L} \tag{3-9}$$

Figure 3-25 shows the results of the time necessary for the two stages of the recommended process for the reservoir under consideration to attain 60% oil recovery at different levels of heterogeneity. The total time of controlled and free fall gravity drainage is also shown in Figure 3-26 for comparison. For the whole range of average reservoir permeability and all cases of heterogeneity levels studied, the total time for the controlled and free fall gravity drainage seems to be more reasonable compared to the controlled gravity drainage alone shown in Figure 3-24. Figure 3-26 illustrates that the time required for both controlled gravity drainage (water removal stage) and free-fall gravity drainage is longer for the homogeneous system in comparison to the other two heterogeneous reservoir cases. However, the stage of controlled gravity drainage appears to be more affected by the heterogeneities. In fact, the controlled gravity drainage in the heterogeneous reservoir could be carried out at a higher flow rate (corresponding to a smaller N_{gv}^{min}) without producing the residual oil. For the reservoir with 38% heterogeneity, the controlled gravity drainage withdrawal rate is approximately two times that of the reservoir with 17% heterogeneity, and about four times the withdrawal rate of the homogeneous reservoir. Therefore, the curve showing the time for controlled gravity drainage is situated below the free-fall curve for heterogeneous reservoir cases, as shown in Figure 3-26. In addition, at higher heterogeneity levels, the duration of water removal decreases because the volume of heterogeneities is primarily full of residual oil; therefore, the pumping cost of water is less compared to the time it takes to pump out the water from a homogeneous reservoir having lower residual oil volume present.

Figure 3-26 shows that in a heterogeneous reservoir, the length of oil production is not much affected by the reservoir permeability for the range studied here. This means that the effect of the relatively high waterflood residual oil volume in heterogeneous media on the profitability of the process is more significant in comparison to the permeability of the reservoir. This implies that the heterogeneous reservoirs are more attractive candidates to apply the GAIGI process compared to applying GAIGI in homogeneous reservoir cases.

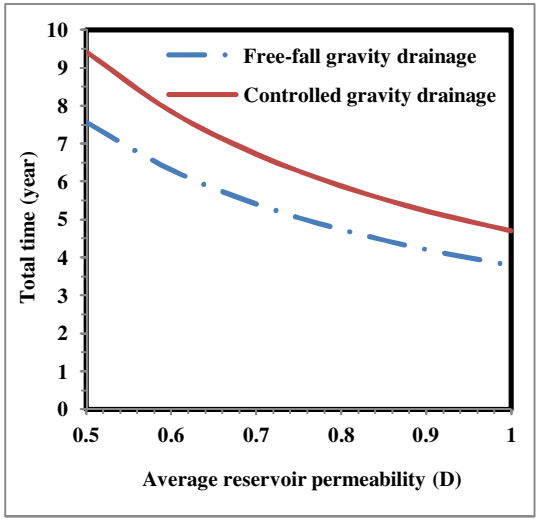

0% Heterogeneity

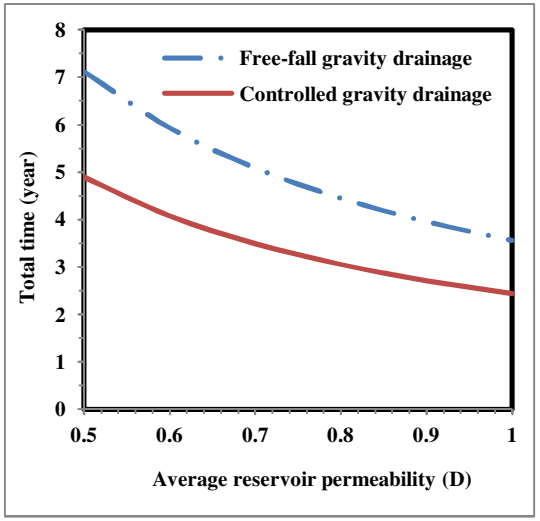

17% Heterogeneity

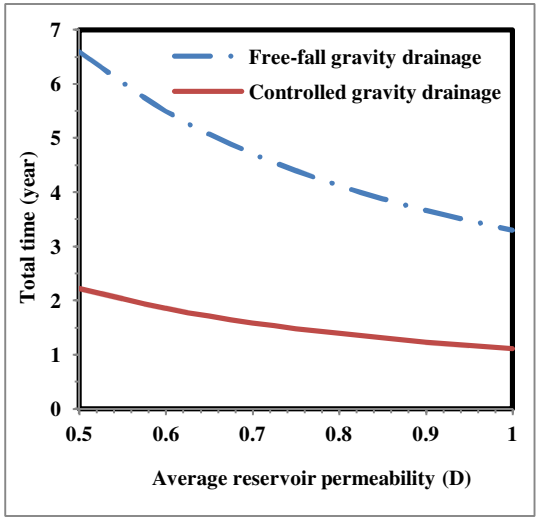

38% Heterogeneity

Figure 3-25: Time of the controlled and free fall gravity drainage to attain 60% oil recovery factor for a 40 m thick reservoir with 160 acres area well spacing

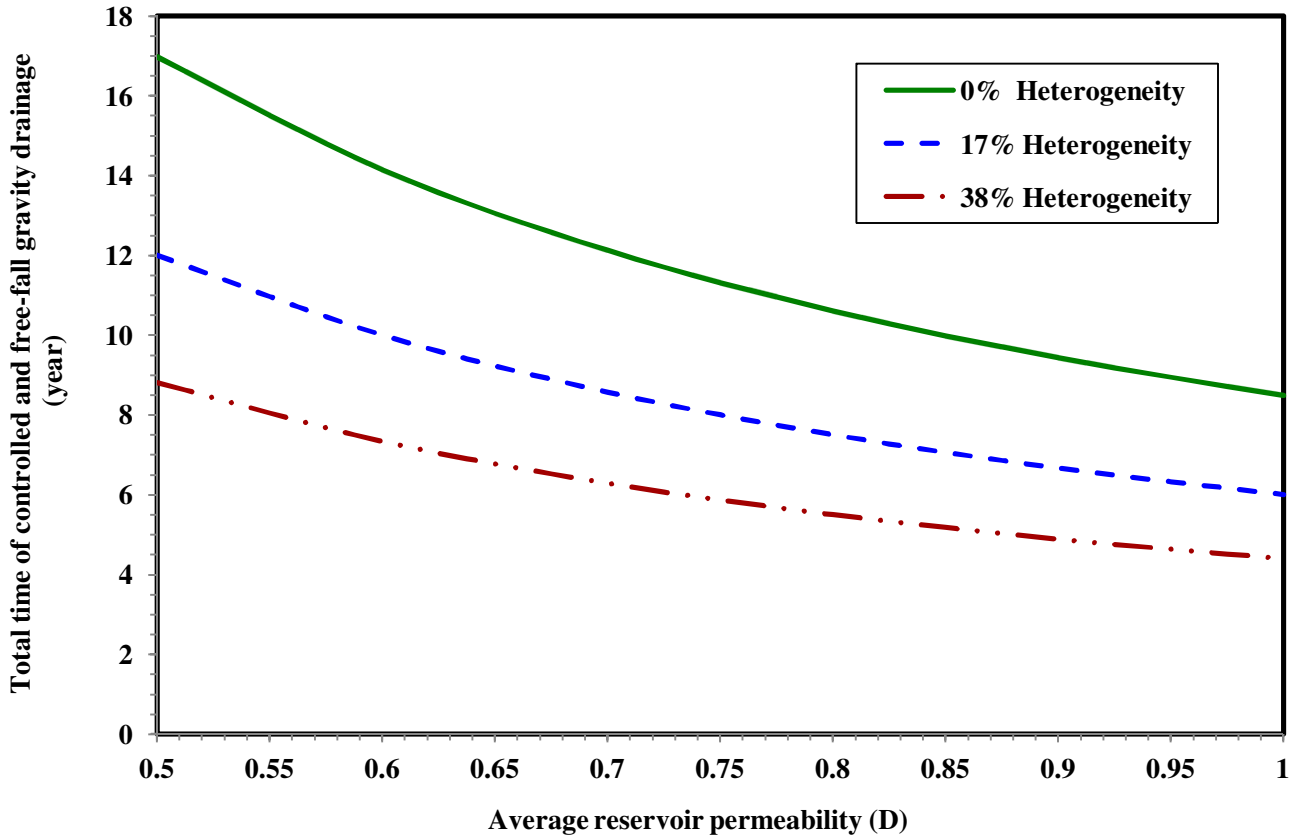

Figure 3-26: Total time of the controlled and free fall gravity drainage to attain 60% oil recovery factor for a reservoir of 40 m thick and 160 acres well spacing area

3.6 Conclusions

Upon waterflooding water-wet porous media exhibiting pore structure heterogeneities, a significant volume of oil is bypassed in the large-pore-size regions. The GAIGI process improves performance of waterflooding since the gas invasion occurs both in the low permeability continuum as well as in the high permeability isolated regions. In addition, the previously established correlation of oil recovery factor at gas breakthrough for homogeneous media could be applied for the type of heterogeneous media used in this study. Also, the oil recovery factor for heterogeneous media up to gas breakthrough could be predicted through the mathematical model developed in this chapter. It was also concluded from the reduced residual oil saturation data that the permeability heterogeneity is not much detrimental to oil recovery by gravity drainage as long as the wettability of the porous medium is uniformly water-wet. The applicability of the GAIGI process at the field scale was examined using the dimensionless groups. High reservoir permeability and heterogeneity fraction are favorable to improve the efficiency of the GAIGI process. However, more encouraging results were obtained when a combination of free-fall and controlled gravity drainage was employed to recover waterflood residual oil.

Chapter 4

The Effects of Wettability Heterogeneity on the GAIGI Process

4.1 Introduction

The gravitationally stable mode of gas injection is recognized as a promising tertiary oil recovery process to recover the oil remaining in petroleum reservoirs after waterflooding. Therefore, it is important to understand the phenomena occurring during the gravity-assisted inert gas injection (GAIGI) process. Owing to the occurrence of three-phase flow of oil, water, and gas over the course of the GAIGI process, wettability of the porous medium has a profound effect on the reservoir production performance. Wettability determines the relative affinity of the solid surface for oil, water, or gas. As such, it defines the development of the wetting films whose formations and thicknesses (along with the spreading films) play important roles in the GAIGI process displacement mechanism. For a long time and for simplicity, oil reservoirs were considered uniformly water-wet. Nowadays, it is admitted that the pore space in reservoir rocks are not uniform in terms of mineral composition and surface roughness, thereby, exhibiting heterogeneous wettability characteristics. The studies carried out to date on the tertiary gravity drainage process have overlooked the heterogeneous wettability characteristics of reservoir. This chapter presents the concepts of wettability and rock surface wettability alteration, the history of studies on the effects of wettability heterogeneities on oil recovery, followed by the methodology and a detailed discussion of results of this experimental work, highlighting the effects of wettability heterogeneity on the oil production characteristics of the GAIGI process.

4.2 Fundamentals of Wettability

4.2.1 Definition and Evaluation Methods

In dealing with any immiscible displacement for oil recovery one needs to consider all active forces that exist between the gas and liquid phases, at the interfaces between two immiscible liquids and between the liquids and solids (Amyx et al. 1960). Wettability is a property of a porous rock which is determined by the combination of all active surface forces. It is defined as "the relative preference of a surface to be covered by one of the fluids under consideration" (Amott 1959). In a rock/oil/brine system and when a reservoir rock is water-wet, there is a tendency for water to occupy the small pores and to contact the majority of the rock surface. In an oil-wet rock, the location of the two fluids is reversed and the tendency of oil is to occupy the small pores and cover the solid surface (Anderson 1986a).

Several methods have been proposed to evaluate the wettability of a solid surface with respect to a fluid system. These methods were developed based on various solid-fluid interactions such as:

a) contact angle measurement,
b) thermodynamics,
c) the interfacial-tension and displacement-pressure measurements,
d) the shape of relative-permeability curves,
e) the shape of the recovery curve,
f) permeability and saturation measurements,
g) spontaneous imbibition experiments,
h) nuclear magnetic relaxation measurements,
i) dye adsorption,
j) the use of well logs,
k) the use of a capillary pressure curve, and
l) imbibition and displacement experiments (e.g. USBM and Amott tests).

Cuiec (1991) has provided a comprehensive discussion of these techniques. The two methods that are based on thermodynamics and contact angle measurement are among the most important and widely-used techniques for solid surfaces and the USBM and Amott tests are the mostly-employed ones by the oil companies for porous media. Given below is a detailed description of these three methods.

In the method based on the thermodynamics, wettability (σ_m) is defined as the energy lost by the system during the wetting of a solid by a liquid:

$$\sigma_m = -\left(\frac{\partial G}{\partial s}\right)_{T,P} \tag{4-1}$$

where G is the free Gibbs energy, T is the temperature, P is the pressure, and s the surface area of the solid. If $(\partial G/\partial s)_{T,P} < 0$, the spreading is spontaneous, and wettability is positive. Wettability can also be written in the following form:

$$\sigma_m = \sigma_{SV} - \sigma_{SL} \tag{4-2}$$

in which σ_{SV} and σ_{SL} are the free surface energy of the solid/vapor and solid/liquid interfaces, respectively. Young's equation is as follows for the case where there is a contact angle (Figure 4-1):

$$\sigma_{SV} - \sigma_{SL} = \sigma_{LV} \cos\theta \tag{4-3}$$

where σ_{LV} is the surface tension of the liquid. Then, the combination of the two Equations 4-2 and 4-3 gives, $\sigma_m = \sigma_{LV} \cos\theta$. Therefore, it is possible to either evaluate σ_{LV} and $\cos\theta$ separately, or the product of $\sigma_{LV} \times \cos\theta$ to estimate σ_m.

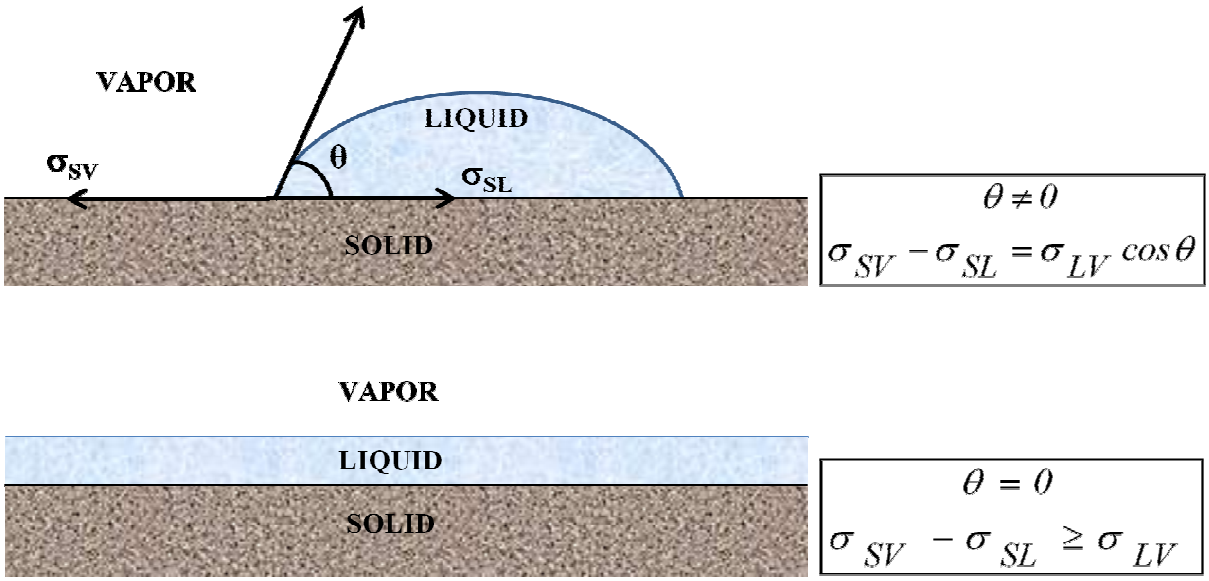

Figure 4-1: Examples of behavior of solid/liquid system (modified from Cuiec 1991)

Another method for characterizing the reservoir wetting state is based on contact angle measurement which is the most universal measure of the wettability of surfaces (Morrow 1990). The procedure consists of placing a drop of one liquid on a flat surface of a solid, with the same mineralogy as the reservoir under study, and bringing the soil/drop in contact with the other fluid. The angle measurement, which is by convention through the denser liquid phase, can be under static or dynamic conditions (Cuiec 1991). If the magnitude of the contact angle is small, the solid is called water-wet; when it is large, the solid is considered as oil-wet, and for angles around 90˚, the surface is said to have neutral or intermediate wettability. Some authors have proposed exact boundaries to determine the type of wettability. However, there is uncertainty associated with choosing a concise boundary owing to the heterogeneities of rock caused by surface roughness, dissimilar mineralogy and complexity of the pore structure. In addition, the required length of time to reach equilibrium in this method cannot be reproduced in the lab (Agbalaka et al. 2008); however, dynamic contact angles are more reproducible and less dependent on measurement method (Buckley and Morrow 1992). Another problem in contact angle measurement is hysteresis; that is when a liquid drop on a surface exhibits different stable contact angles. Despite all these disadvantages, this method is the best technique when pure fluids and artificial cores are used (Anderson 1986b).

For a quantitative evaluation of wettability, Amott (1959) proposed a technique based on the magnitude of water and oil displacement in a porous medium through spontaneous imbibition and forced displacement. The test starts by first bringing the porous medium to the state of residual oil saturation. Then, four measurements are made: (1) water spontaneously displaced by oil from the sample over a period of 20h, v_1, (2) water displaced by oil using a centrifuge, v_2, (3) oil spontaneously displaced by water over a period of 20h, v_3, (4) oil displaced by water using centrifuge, v_4. Amott defined two wettability indices, "the displacement-by-oil ratio", $v_1/(v_1 + v_2)$ and "displacement by water ratio", $v_3/(v_3 + v_4)$. Preferentially water-wet cores have a positive displacement-by-water ratio and a zero value for the displacement-by-oil ratio. In the same way, oil-wet porous media have a positive displacement-by-oil ratio and a zero displacement-by-water ratio. When both ratios are zero, the cores have an intermediate wettability.

The United States Bureau of Mines (USBM) wettability test was developed by Donaldson et al. (1969). In this technique, the work necessary for one fluid to displace the other is compared. For a wetting fluid, the work required to displace a nonwetting fluid from a porous sample is less than the

work required for the opposite displacement because the free energy decreases in the former case (see Equation 4-1). This required work is proportional to the area under the capillary pressure curve; therefore, the USBM index is defined as the logarithm of the ratio of the areas under the capillary pressure curves for oil- and water-drive, respectively. When this index is greater than zero, the core is water-wet, and when it is less than zero, the core sample is oil-wet. The wettability index near zero shows a neutral wettability condition. The main advantage of the USBM wettability test over the Amott test is its sensitivity near neutral wettability (Anderson 1986b).

4.2.2 Influence of Wettability on Oil Recovery

The importance of wettability in controlling the location, flow, and distribution of fluids in a reservoir led to numerous investigations on the effects of wettability on multiphase flow problems ranging from oil migration from source rocks through primary production mechanisms to enhanced oil recovery processes. Most of the early studies of the effect of wettability on oil recovery were based on the assumption that the reservoir-rock surface always maintains a strong affinity for water in the presence of oil (Morrow 1990). The rationale for such a hypothesis was based on two major facts. First, almost all sedimentary rocks are strongly water-wet. Second, water originally occupied the reservoir trap where oil later migrated. It was believed that the connate water (in the form of films on pore surfaces overlain by oil) prevented the oil from touching the rock surfaces (Anderson 1986a). In 1934, Nutting discovered that the wettability characteristics of oil-bearing pore surfaces could be altered to oil-wet. This wettability alteration may occur through physical or chemical adsorption of heavier and more polar fractions of a crude oil on the rock surface. Some of these components are soluble in water; therefore, they can even pass through the water layer on the originally water-wet surface and adsorb onto the rock surface, altering the wettability to oil-wet conditions (Anderson 1986a). Hirasaki (1991) discussed that in crude oil/brine/rock systems the stable and thick films of water show water-wetness of the rock. The existence of stable water films has been shown to depend on the presence of an electrical double-layer repulsion that results from the similarity in the sign of surface charges at the solid/water and water/oil interfaces (Takamura and Chow 1983; Buckley et al. 1989). Also, it was found that water film stability is influenced by brine pH, and the concentration of monovalent cations in solutions (Takamura and Chow 1988; Buckley and Morrow 1992). On the other hand, unstable films are more likely to rupture and may lead to the exposure of the rock surface to the polar components of oil (Hirasaki 1991).

The non-uniform wettability condition in natural reservoirs may also originate from faulting, contrast in lithology, digenesis, and sedimentology complexities (Marcelle-De Silva and Daw 2003), which extends from the kilometer scale down to the pore scale (Levorsen 1967; Link 1982).

Aside from the cause of heterogeneity in wettability of the reservoir rock, several wetting states have been defined based on the distribution of oil-wet and water-wet surfaces. These wetting states include: (1) fractional wettability— also called spotted or Dalmstion wettability— and (2) mixed wettability. Fractional wettability was first proposed by Brown and Fatt (1956). It is referred to as a type of wettability heterogeneity in which some portions of the rock are strongly oil-wet, while the other parts are strongly water-wet. Mixed-wettability was introduced by Salathiel (1973) and describes a special type of fractional wettability where the oil-wet surfaces form continuous paths through the large pores.

The discovery of possible non-uniform wetting conditions in the oil reservoirs opened up new vistas of research on investigating the effects of heterogeneous wettability conditions (of the porous medium) on various rock-flow properties, among which are capillary pressure (e.g., Brandford and Leij 1995; Masalmeh 2002 & 2003; Helland and Skjæveland 2004; Motealleh 2009; Mirzaei 2010), relative permeability (e.g., Dixit et al. 1998; DiCarlo et al. 2000; Masalmeh 2003), and electrical properties (e.g., Sweeney and Jennings 1960; Morgan and Pirson 1964; Donaldson and Siddiqui 1989; Tsakiroglou and Fleury 1999; Moss and Jing 1999) as well as the displacement mechanisms and sweep efficiency of different oil recovery processes (e.g., Dawe et al. 1992; Kiriakidis et al. 1993; McDougall and Sorbie 1995; Caruana and Dawe 1996; Vizika and Lombard 1996; Blunt 1997; Vizika and Duquerroix, 1997; Bertin et al. 1998; Laroche et al. 1999; Marcelle-De Silva and Dawe 2003; Dawe and Grattoni 2008; Szymkiewicz et al. 2010). Capillary pressure, relative permeability, electrical properties, oil recovery efficiency, and displacement mechanisms are all parameters that are strongly affected by the state under which different fluids are distributed (i.e., whether they spread over the solid surfaces as the wetting films or occupy the pore bodies of the reservoir rock in the form of blobs); consequently, the effect of local wettability characteristics of solid surfaces was found to be very substantial. Hence, the obtained behaviors for the aforementioned properties deviate from those of the homogeneous water-wet porous media.

The focus of studies involving wettability heterogeneities effects have been mainly on oil recovery processes in the horizontal direction, some of which are briefly described here.

The effects of carefully-controlled wettability heterogeneities on flow patterns, residual saturation and oil recovery of immiscible displacement processes were examined by Dawe et al. (1992) and later on by Caruana and Dawe (1996), Marcelle-De Silva and Dawe (2003) and Dawe and Grattoni (2008). A two-dimensional transparent model, which allowed visualization of the displacements, was packed with glass beads at four different heterogeneity patterns (i.e., layered, lens (an oil-wet lens embedded in water-wet matrix), quadrant and striped (an oil-wet stripe embedded in water-wet matrix)). Three displacements were followed visually which included: (1) water displacing CO_2, which had been injected earlier to flush the air out of the packed model, (2) oilflooding the porous medium after being saturated with water, and (3) waterflooding the packed model at the state of initial oil saturation. The fluid displacement patterns in systems exhibiting different heterogeneity configurations were interpreted using the capillary pressure equation. During waterflooding, the water phase pressure is lower in the water-wet regions; as a result, these regions provide pathways of least resistance to flow of the water phase for all scenarios of heterogeneity patterns. Further increase in water pressure up to the threshold pressure of the oil-wet zone caused water penetration into the oil-wet zone for the case of the stripe model (see Figure 4-2); however, in the lens model, water did not enter the oil-wet lens even after a large amount of water was injected (see Figure 4-3). For the quadrant model, Figure 4-4 shows that water entered the water-wet quadrant, but no flow occurred in the oil-wet zone. The imbibition front moved stably in the water-wet region as shown in part (a) of Figure 4-5. The oil-wet quadrant in front of this region acted like a filter, i.e., oil was produced via the outlet oil-wet zone, whereas water flowed towards the outlet water-wet quadrant and the displacement advanced with a stable front up until the time of water breakthrough as illustrated in Figure 4-5. Similar to the lens model, further water injection could not sweep oil from the oil wet regions.

During an oilflood, the oil phase pressure is lower in the oil-wet regions, providing more driving force for oil to penetrate into those regions. At low oil flow rates, the capillary forces dominated the flow; consequently, the entrapment increased, whose extent strongly depends upon the configurations of heterogeneities, as can be seen from Figure 4-2 through Figure 4-4. In the stripe model, the water-wet matrix was swept by oil somewhat efficiently, whereas in the lens and quadrant models an extensive area of the water-wet matrix remained unswept.

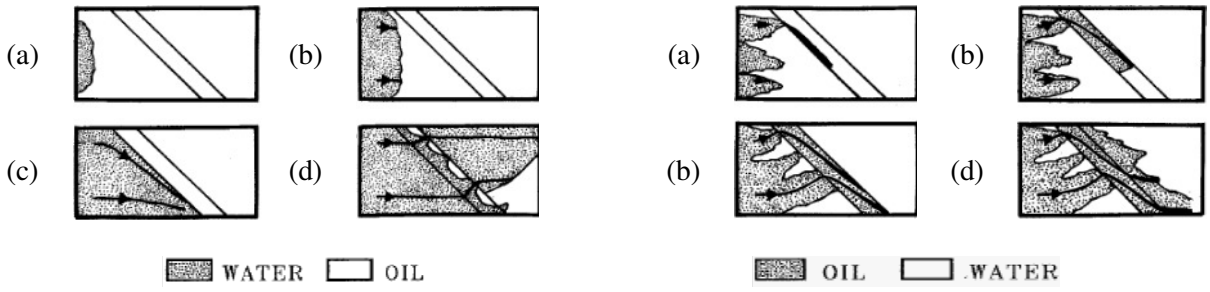

Waterflooding Oilflooding

Figure 4-2: Immiscible displacement front behavior in the stripe model; flow is from left to right (from Caruana and Dawe (1996))

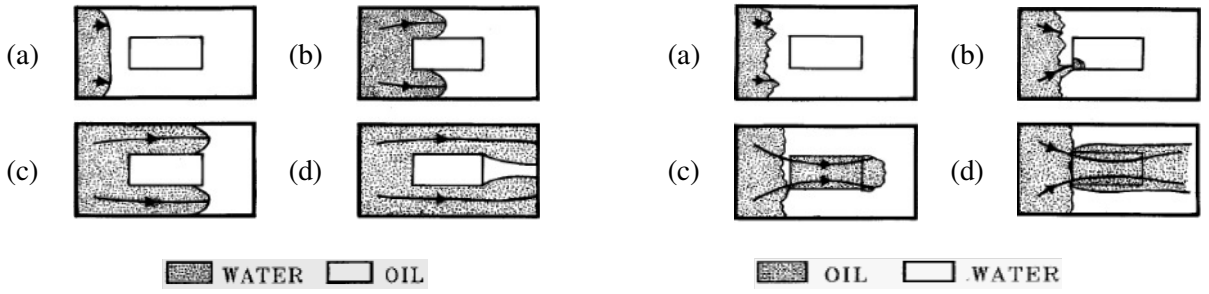

Waterflooding Oilflooding

Figure 4-3: Immiscible displacement front behavior in the lens model; flow is from left to right (from Caruana and Dawe (1996))

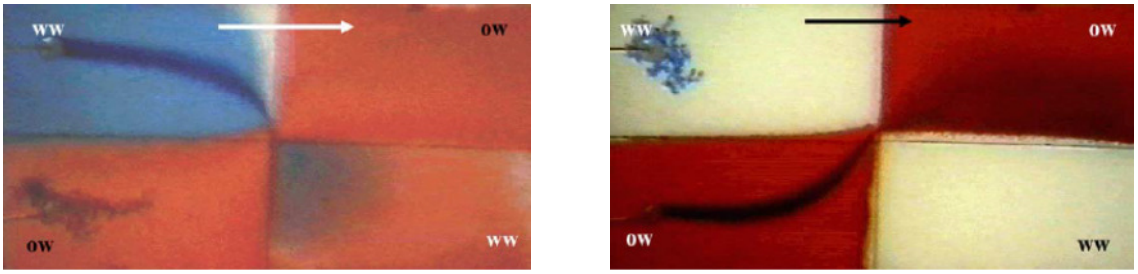

Waterflooding Oilflooding

Figure 4-4: Immiscible displacement front behavior in the quadrant model; flow is from left to right (from Dawe and Grattoni (2008))

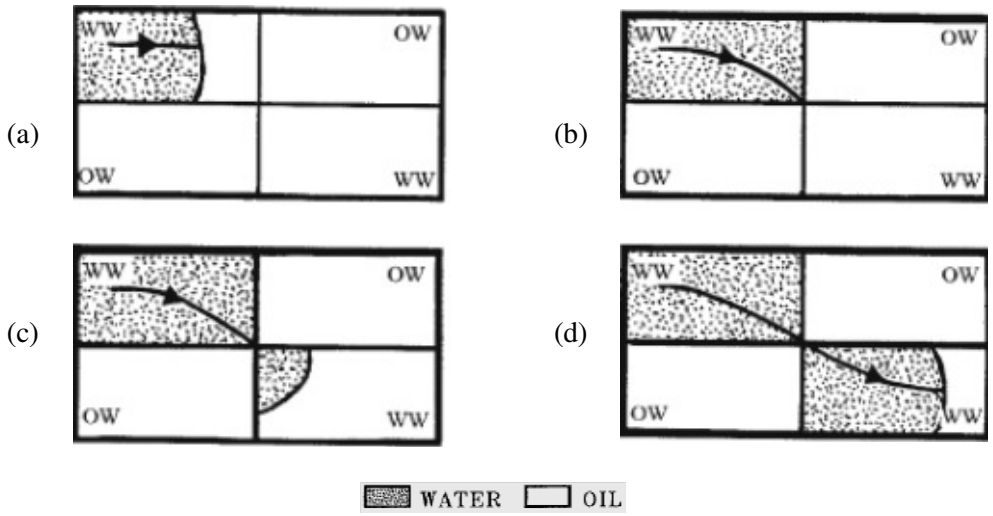

Figure 4-5: Waterflooding the quadrant model; flow is from left to right (from Caruana and Dawe (1996))

Kiriakidis et al. (1993) proposed a deterministic model based on a microscopic approach to find out the flow pattern of the displacing fluid in two-phase immiscible displacement through a porous medium containing a zone of different wettability. A two-dimensional square network of interconnected channels was used for the computer simulations. Three distinct cases of wettability patterns were studied: (a) an oil-wet porous medium, (b) an oil-wet porous medium containing a zone of neutral wettability, and (c) an oil-wet porous medium containing a water-wet zone. The results of this simulation showed that the behavior of the displacing fluid is strongly dependent upon the magnitude of the wettability contrast between the different zones of the porous medium. Also, the injection rate of the invading fluid, and hence the capillary number affected the displacement pattern drastically.

Laroche (1998) focused on the experimental investigation of secondary and tertiary gas injection in micromodels exhibiting wettability heterogeneity. The type of heterogeneity considered was in the form of Dalmatian in which the continuous water-wet surface enclosed regions of discontinuous oil-wet surfaces. The porous medium used in this study was a network of the pore-and-throat type, constructed from glass plates using a lithographic method. Oil-wet patches in a water-wet matrix were obtained by selective silane grafting on the glass surface. Since the silane film is not stable at a high temperature, instead of the conventional procedure to fuse the glass plates at 700 ˚C, the glass plates were jointed face-to-face and were placed into a pressure bath. For the same oil-wet over water-wet

surface ratio different heterogeneity patterns were considered: oil-wet stripes parallel or perpendicular to flow, and oil-wet squares in the water-wet matrix. The fluid system used in the experiments consisted of n-dodecane, deionized water and nitrogen. The experimental results for secondary and tertiary gas injection showed that the amount of trapped oil depends on the type of heterogeneity for any level of applied pressure. Also, gas invasion occurred mainly in the oil-wet regions which exhibit the pathways of least resistance, while in the water-wet regions water bridges drastically increased the resistance to flow. As a result, the best gas injection efficiency was obtained in the uniformly oil-wet medium. It was also concluded that distribution of the irreducible water saturation depends on the type of heterogeneity and affects the displacement patterns of secondary gas injection. The effect of heterogeneity on the sweep efficiency of the tertiary gas injection was even more detrimental compared to the secondary gas injection because the distribution of waterflood residual oil was highly affected by heterogeneity.

Later on, Laroche in collaboration with two other co-workers developed a theoretical model to describe three-phase flow in heterogeneous porous media. The wettability heterogeneity was incorporated into the model by assigning different contact angles to different wettability regions. An electrical analog was used in the network model to calculate immiscible displacements, i.e., for each unit cell the hydraulic conductivity was expressed as a function of the hydraulic conductivity of each phase present in the considered cell. The phase distribution computed for two of the wettability patterns was reported, which seemed to be compatible with the experimental results qualitatively, yet more work needs to be done to improve the quantitative agreement with the experiments (Laroche et al. 1999).

Although the literature reviewed here have considered a variety of immiscible displacements, a few conclusions can be made. The displacement patterns were all affected by the presence of wettability heterogeneities in the porous media tested. Therefore, the oil recovery efficiencies were poor as a result of dominant capillary forces near the regions with contrasting wettability which led to a significant entrapment of oil.

4.2.3 Influence of Wettability on Gravity Drainage

In a homogeneous water-wet porous medium, gravity drainage was found to be very efficient in the pioneering experimental study by Dumoré and Schols (1974). Numerous studies undertaken since that

time have confirmed that high oil recovery factors are attainable in water-wet sandstone cores, bead packs and sand columns through both secondary and tertiary modes of oil recovery gravity drainage (Chatzis et al. 1988; Kantzas et al. 1988a; Dullien et al. 1991; Chatzis and Ayatollahi 1993; Catalan et al. 1994; Blunt et al. 1995; Vizika and Lombard 1996). Moreover, Jerauld has reported the success of the gravity drainage process in the Prudhoe Bay field, as a residual oil saturation of about 5% was achieved in the gas cap zone, which was initially saturated with oil (Jerauld 1997). The drainage of oil through the spreading oil films on the water layer in the presence of invaded gas was found to be the main mechanism contributing to oil recovery in the gravity drainage process. Kantzas et al. (1988b) were the first ones who visually investigated the role of spreading films in two-dimensional glass-etched micromodels. It was concluded that the formation and extent of the spreading oil films are highly affected by the local wetting characteristics and also the spreading coefficient of the system.

Despite the promising results of the GAIGI process in recovering waterflood residual oil from a uniformly water-wet media, it is not realistic to anticipate similar flow mechanisms and recovery results in all types of reservoirs. The effect of wettability heterogeneity on secondary and tertiary gravity drainage has not been well explored. Until now, two experimental studies on the performance of secondary gravity in porous media exhibiting wettability heterogeneities have been published by Vizika and her research group (Vizika and Lombard 1996; Vizika and Duquerroix 1997). Below is a summary of these studies.

Vizika and Lombard (1996) implemented a gas-oil free-fall gravity drainage process in uniformly water-wet, uniformly oil-wet and fractionally-wet sand-packs. Fractionally-wet conditions were obtained by uniformly mixing 50% water-wet and 50% oil-wet sand. The water and oil saturation profiles were determined by the gamma-ray technique and CT-scanner. In situ saturations and the oil production curves demonstrated the highest recovery efficiency when the porous medium was water-wet and the oil exhibited spreading condition. The drainage of oil primarily occurred through the bulk flow. Therefore, the water-wet porous medium yielded the highest recovery factor since oil as the non-wetting phase had access to the pathway of large pore bodies, corresponding to a larger oil relative permeability. However, for the fractionally-wet porous media the oil relative permeability was lower than that in the water-wet media, but less pore bodies were occupied by water compared to the uniformly oil-wet media, resulting in higher relative permeability compared to the latter case. Consequently, the production curve for the fractionally-wet media situated between the water-wet and

oil-wet ones at the early stages of oil recovery. At the late stage of oil recovery through free fall gravity drainage, however, the spreading film flow was the dominant recovery mechanism, and therefore both the water-wet and fractional-wet cases showed similar performance in terms of the oil recovery factor.

Vizika and Duquerroix (1997) investigated the phase distributions, recovery kinetics and sweep efficiency of secondary gas injection process, in the presence of connate water saturation, in unconsolidated porous media exhibiting well controlled wettability: uniformly water-wet, uniformly oil-wet, and a heterogeneous sand-pack consisting of two long water-wet layers separated by a 2-cm thick oil-wet stratum. They used a dual energy CT-scanner to obtain a three-dimensional saturation profile for the water, oil and gas phases. It was observed that the cumulative oil recovery at any time was higher in the water-wet porous media than that in the oil-wet and heterogeneous systems. This was because in the latter two cases, water being the non-wetting phase occupied the large pores, and thereby lowering the permeability to the oil phase. At the later stages of production, in water-wet media the oil recovery was through spreading films, leading to very low residual oil saturation (S_{org}=11%). For the oil-wet porous media, the high capillary retention caused much lower oil recovery (S_{org}=21%). In the heterogeneous sand-pack, while the spreading films under the action of the gravity force assisted in oil production for the lower water-wet layer, the upper layer was isolated by a non-conducting layer. As a result, the recovery efficiency was lower than in the other two cases (S_{org}=24%).

No experimental studies have yet been devoted to describing the effects of heterogeneous wettability conditions of porous media on the flow mechanism and recovery efficiency of the tertiary GAIGI process. This study focuses on the experimental aspects of waterflooding and the tertiary oil recovery by controlled gravity drainage in glass-bead-packed columns with centimeter-scale wettability heterogeneities embedded in a matrix of similar glass bead size distributions. This particular type of heterogeneity configuration is known as Dalmatian, which refers to a special form of distribution of oil-wet and water-wet surfaces, in which one of these two is embedded in a continuum of the other one (Cuiec 1991). Of particular interest in this work is the type of heterogeneity that the oil-wet surfaces are in the form of isolated regions, distributed in the continuous water-wet matrix. From the knowledge of pore-scale trapping mechanisms (Chatzis et al. 1983), we could discern that the reverse case of heterogeneity (water-wet isolated regions embedded

in the oil-wet continuum) is not of interest because the amount of oil trapped over the course of waterflooding is not significant to attract the tertiary recovery processes.

4.3 Experimental Aspects

4.3.1 Heterogeneous and Homogeneous Packed Models

Waterflooding and tertiary oil recovery by the controlled gravity drainage experiments were conducted in glass-bead-packed columns, having a length of 43 cm and a diameter of 2.7 cm. A 1.5 cm layer of fine glass beads with an average size of 214 μm was always placed at the bottom of the packed columns to achieve high capillary pressure conditions, and to gravitationally stabilize the fluid flow. This fine layer, known as the capillary barrier, is expected to impose a high enough bubble pressure to prevent gas breakthrough and, hence, to improve the oil displacement (Dullien et al. 1989).

The wettability heterogeneity in packed columns consisted of an unconsolidated water-wet glass bead continuum (with an average particle size of 717 μm) with regions of oil-wet consolidated glass beads randomly placed in the packed column. The oil-wet regions were created in the following way: first, slightly sintered cores were created from glass beads of the same size as the beads forming the continuum. Consolidating glass beads is essential in having consistent volumes of heterogeneities throughout the experiments. Next, the sintered core samples were cut into smaller pieces (on the order of 3–12 cm^3) whose wettability was altered subsequently using the dry-film technique (Holbrook and Bernard 1958) prior to packing them in a column. These treated pieces were used to form the discontinuous oil-wet regions in a packing with the unconsolidated water-wet glass beads forming the continuum in the packed column. Packed columns with 0, 17, and 38 volume % of heterogeneities were created to explore the impact of the volume fraction of oil-wet heterogeneities in the packing on the recovery factor of the tertiary GAIGI process, evaluated at gas breakthrough.

4.3.2 Wettability Alteration

The wettability of consolidated pieces of glass beads was altered from water-wet to oil-wet conditions through a silylation process. The process included soaking the sintered pieces in a solution of 5 volume % dry-film (dichlorodimethylsilane or DCDMS) in *n*-hexane solvent (Holbrook and

Bernard 1958), followed by draining the dry-film solution. The dry-film treated samples were then placed in a convection oven while on a screen over a water-filled stainless tray, whereby the sintered pieces were exposed to the water vapor as the hexane was evaporating. Afterward, the silane-treated cuttings were dried further to 250 ºC in the absence of water vapor.

Over the course of the silylation process, DCDMS reacts with the silica surface through covalent bonding of chlorine to the hydrogen atoms of the surface hydroxyl groups. This reaction at a glass surface exposes the organic groups at the surface, thereby establishing an oil-wet surface. Depending upon how close the silanol groups are on the surface, the reaction can occur mono- and difunctionally, as shown in Figure 4-6. Moreover, the hydration is essential in the reaction of silane with a silica surface at temperatures below 300 ºC. Under this situation, silane reacts with water molecules on the surface, forming a polymeric species that can later adsorb onto the silica surface through hydrogen bonding (Hair and Tripp 1995). Moreover, if the glass beads were previously dried at high temperatures for the cleaning purpose, they may lose the surface hydroxyl groups; therefore, re-equilibration of the hydroxyl groups is induced by bringing the surface in contact with the water vapor (Takach et al. 1989). It is worth mentioning that the procedure of silylating the glass beads does not affect grain size distribution and the grain surface morphology does not change either, as microscopically observed by Vizika and Lombard (1996).

To examine the performance of the silylation process in wettability alteration, the oil–water contact angle of the treated glass beads was measured by the sessile drop method using a video contact angle system (VCA 2500XE) several times. The average contact angle at equilibrium for the dyed kerosene–water system was estimated at about 141.1° ± 2.1°. Figure 4-7a shows a snapshot of one of the contact angle measurement trials. The contact angles reported here are for the left and right side of the drop shown in this figure. The average magnitude of the measured contact angle shows the hydrophobicity of the treated glass surface. However, the contact angle could not be accurately measured using this technique due to the light reflection on the glass surface during the test. In fact, when dealing with a polished surface for such an experiment, the reflection of the drop image on the surface produces a shadow by which the exact contact points of the three phases of water–oil–solid is covered, making it difficult to draw the angle lines at the proper position, and hence, this causes error in estimating the actual contact angle. We made an attempt to diminish the effect of surface reflection by reducing the intensity of the light on the top of the drop but could not completely eliminate the

light reflection. Therefore, the wettability of the treated sintered glass beads was qualitatively evaluated. When both the water-wet and oil-wet sintered-glass beads were brought in contact with oil and water, oil imbibed spontaneously into the oil-wet porous medium while water imbibed into the water-wet one (see Figure 4-7b). This quantitative technique demonstrated a strong tendency of the treated surface to be wetted by oil compared to the water phase.

Artificial wettability alteration of sintered glass beads using the silylation method, although controllable in terms of producing a considerably uniform oil-wet surface, suffers from a drawback. Through the chemical reaction of silane with the glass surface, even the very small pores and throats are exposed to the treatment, which seems to be less realistic compared to the wettability alteration in natural rocks caused by exposure to crude oil in the presence of connate water saturation (Jia et al. 1991).

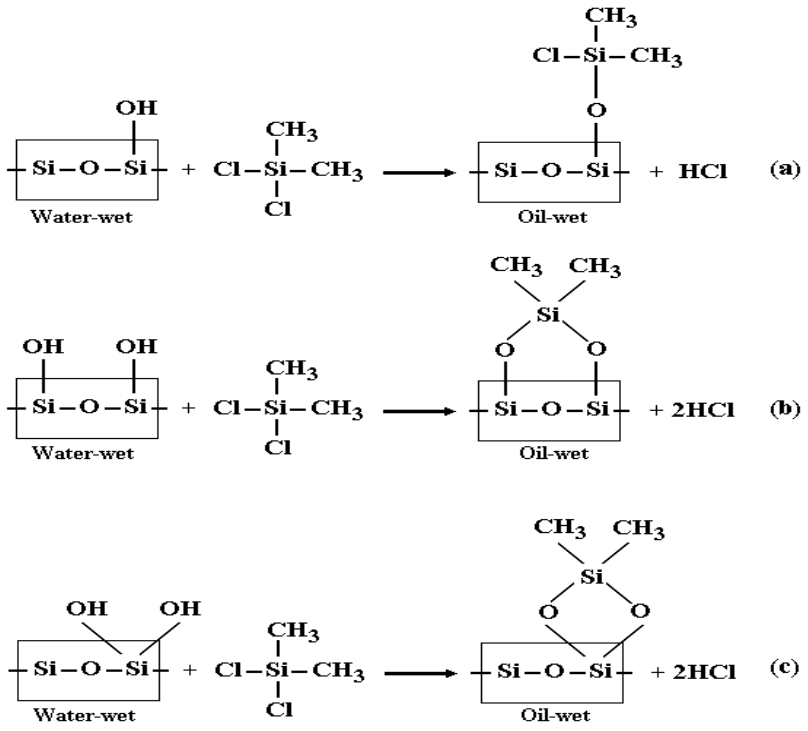

Figure 4-6: Different mechanisms for the reaction of DCDMS with the silica surface (modified from Hair and Tripp 1995)

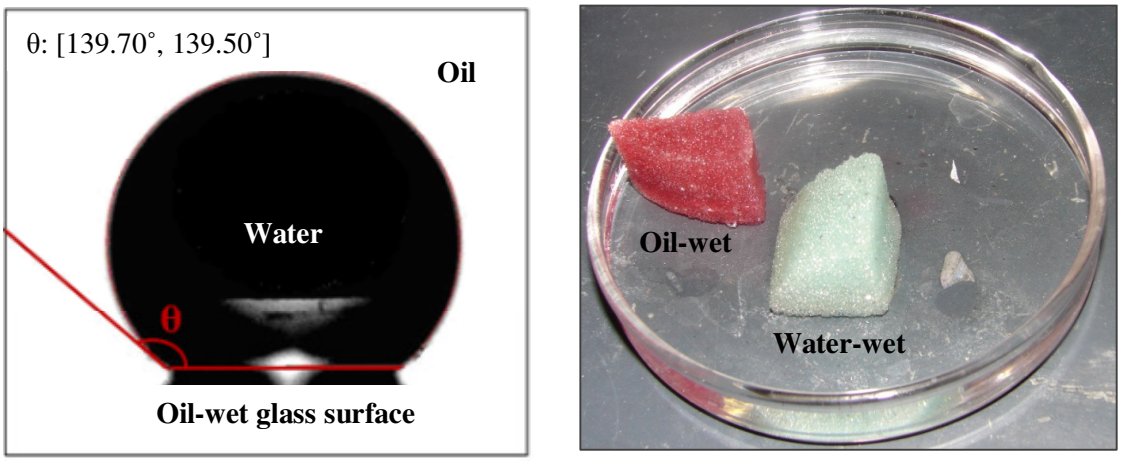

(a) (b)

Figure 4-7: Wettability evaluation for a surface treated to oil-wet:
(a) Oil–water contact angle measurement for an oil-wet glass surface
(b) Spontaneous imbibition of oil (red) in an oil-wet piece of sintered glass beads

4.3.3 Fluids Used in the Experiments

The laboratory fluids used in the experiments were the same ones used in the experimental work described in Chapter 3 and consisted of kerosene, deionized and deaerated water, and air as the gas phase. The fluid properties are shown in Table 3-1.

4.3.4 Experimental Procedure

The experimental procedure for model preparation, waterflooding, and controlled gravity drainage tests can be summarized as follows:

Packing and saturating: for the packing under study, the configuration of the heterogeneities is in the form of randomly placed consolidated oil-wet regions of heterogeneities, embedded in the water-wet matrix. The typical saturating procedure for a porous medium includes flushing trapped air out of the porous medium by carbon dioxide (which is a dissolvable gas in water), followed by injecting several pore volumes (PVs) of deaerated water to dissolve CO_2 and to attain complete saturation. This process is not as efficient in such heterogeneous (in terms of wettability) packed columns. Upon waterflooding a packed column with this form of heterogeneity pattern, water will imbibe into the water-wet continuum because of the greater affinity of water for the water-wet continuum, as compared to that in the oil-wet isolated inclusions, which causes a large extent of gas becoming

trapped in the treated sintered glass bead regions. Therefore, prior to packing the glass bead heterogeneous columns, the following approach was used to saturate the oil-wet pieces. We first placed the oil-wet pieces in an empty vessel, where a vacuum condition was achieved using an aspirator, to purge the air out from the pore spaces. The vacuum was then removed, and water was forced into the pore spaces of the oil-wet pieces through the resultant pressure gradient. Subtracting the mass of oil-wet pieces before and after saturation enabled the estimation of the heterogeneity PV.

After the successful process of saturating the treated sintered pieces, the column was filled with a known volume of water and the saturated oil-wet pieces were randomly placed in the packed model within the continuum of water-wet beads. The PV and porosity of the packing was determined by material balance.

Oil flooding: the water-saturated column was flooded by injecting oil from the top of the packing to displace the water downward to achieve a gravitationally stable displacement. The water was discharged from the outlet at the bottom of the column. A total quantity of about 1.5 PV of oil was injected into the packing to attain the conditions of initial oil and connate water saturation. The volume of the displaced water was measured volumetrically, which was equivalent to the volume of oil in place in the column. From this measurement, the initial oil and connate water saturation was estimated.

Waterflooding: water was introduced from the bottom of the column to displace the oil upward, and, thus, to establish the so-called normal waterflood residual oil saturation condition, S^*_{or}. To provide the conditions of maximum residual oil saturation, the capillary number was kept sufficiently low by keeping the water injection rate at a low value (200 mL/h).

Gravity drainage: the experiments of tertiary oil recovery using the GAIGI process were conducted in the waterflooded columns to recover the oil left behind after the secondary recovery process (i.e., waterflooding). The experiments were started by withdrawing the liquid from the bottom of the column at a constant rate using a metering syringe pump. During this period, the air invaded the porous medium at constant atmospheric pressure from the top of column down to the bottom end until the time of gas breakthrough was attained. A water–oil separator, which was connected to the packed column at one end and the syringe pump at the other end, facilitated the separation of produced oil and water as well as monitoring the cumulative volume of produced oil over time. The volume of produced water up to the time of oil breakthrough was equal to the amount of liquid pumped out by

the syringe pump. After the oil breakthrough, the difference between the separator reading for the volume of produced oil and the amount withdrawn by the pump at any time gave the quantity of water produced versus time. The position of the gas–liquid interface as a function of time was also monitored using a digital camera. A schematic of the experimental setup is similar to the one used for the experiments in models containing permeability heterogeneities as shown in Figure 3-8.

4.4 Results and Discussion

4.4.1 Oilflooding the Heterogeneous Media

The oilflooding of packed columns exhibiting wettability heterogeneity was carried out to displace the water and establish the condition of initial oil in place. A snapshot of the displacement front in the vicinity of an oil-wet region is shown in Figure 4-8. The oilflooding advanced with a relatively stable front in the water-wet matrix until the front hit the oil-wet region ahead and was sucked into it. This was because the oil-phase pressure in the oil-wet zone was less than that in the surrounding water-wet matrix due to capillary pressure difference. This phenomenon caused water bypassing in the matrix primarily; however, further injection of oil with the assist of the capillary barrier (whose function is explained in §4.3.1) increased the oil pressure which in turn resulted in sweeping more water from the matrix. After injection of about 1.5 PV of oil, on average, a connate water saturation of 9.3%, 7.4% and 9.1% was attained in the packings containing 0, 17 and 38% volume fraction of heterogeneities, respectively.

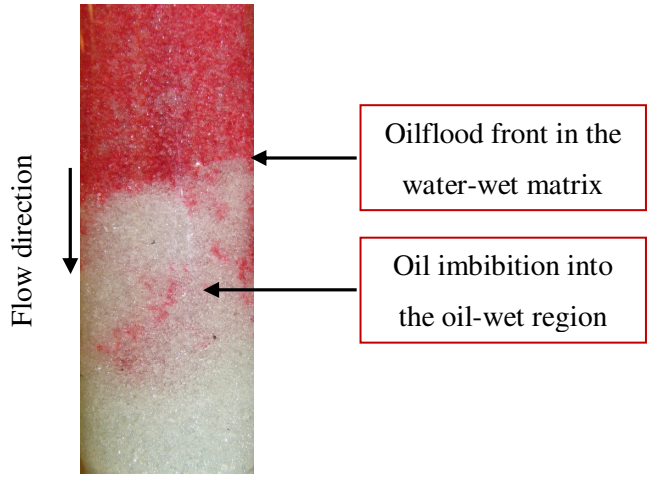

Figure 4-8: Oilflooding a heterogeneous glass bead column containing oil-wet inclusions

4.4.2 Effect of Wettability Heterogeneities on the Magnitude of Waterflood Residual Oil

The packed columns at the initial oil saturation condition were subjected to secondary recovery by waterflooding. The rate at which waterflooding was implemented corresponds to a capillary number (the ratio of viscous/capillary forces, Equation 3-1) equal to $N_{Ca} = 2.97 \times 10^{-6}$. The Bond number (the ratio of gravity/capillary forces, Equation 3-2) for the porous media and the types of fluids employed was calculated to be $N_B = 8.58 \times 10^{-3}$. Under such operating conditions of small capillary number and Bond number values, waterflooding leads to the entrapment of oil as a result of both the buoyancy and capillary forces. Therefore, from the correlation of the residual non-wetting phase saturation as a function of capillary and bond number, introduced by Morrow and Songkran (1981) and Morrow et al. (1988), the residual oil saturation during the waterflooding was expected to be about 14% of the PV of a homogeneous porous medium. The experimentally measured average value for normal waterflood residual oil saturation in the homogeneous packed columns was 13.2 ± 2.2% PV, which is slightly below the estimated values based on the correlation by Morrow and Songkran (1981). Considering the standard deviation of ±2.2% PV, the measured amount of residual oil is within an expected range. The visualization experiments in a uniformly water-wet, glass-etched micromodel showed that oil is trapped in the pore bodies as a single blob and in the form of clusters occupying several pores as shown in Figure 4-9. Chatzis et al. (1983) studied the magnitude of residual oil saturation for different types of porous media, including homogeneous sphere packings with wide and narrow bead-size distribution, two-component sphere packings, and multicomponent mixtures of beads. For these types of porous media, the reported residual non-wetting phase saturation was in the range of 14–16% PV. Therefore, our experimentally measured values of residual oil saturation are comparable to the literature data.

Waterflooding packed columns with wettability heterogeneities results in an even higher magnitude of residual oil saturation values compared to the homogeneous media. The residual oil saturation values of 23.1 ± 2.3 and 33.3 ± 2.8% PV were obtained for the packed columns with 17% and 38% oil-wet heterogeneity levels, respectively. Figure 4-10 illustrates the plot of waterflood residual oil saturation versus the fraction of oil-wet heterogeneities in the packings for the entire set of experiments. This figure shows that the waterflood residual oil saturation varies linearly with the volume fraction of oil-wet regions in the packings, as anticipated on the basis of the pore-scale

trapping mechanisms (Chatzis et al. 1983). During the capillary-dominated infiltration of water into a porous medium containing isolated oil-wet inclusions (embedded in a water-wet matrix), the water imbibes preferably the water-wet continuum and displaces most of the oil presented there (i.e., only 15% of PV of residual oil is left in the water-wet part of the packing in the form of isolated oil blobs). However, the injected water entirely bypasses the oil-wet regions because water is a non-wetting phase with respect to oil present in the oil-wet regions. Consequently, it cannot penetrate into the pore spaces of the oil-wet regions under the prevailing conditions. As a result, most of the oil is bypassed in the oil-wet regions, which accounts for 85% PV in the form of continuous oil patches (see Figure 4-11). Therefore, the extent of residual oil saturation corresponding to a particular heterogeneity level can be estimated by the following equation:

$$S^{*}_{or,\ predicted} = [0.85x + 0.15(1-x)] \times 100 \tag{4-4}$$

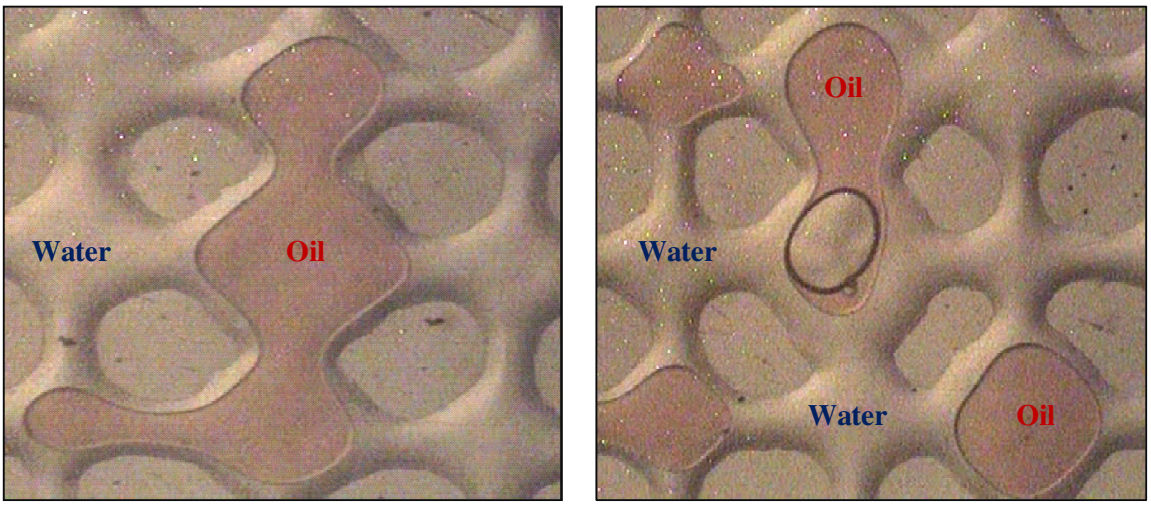

(a) (b)

Figure 4-9: Oil trapped upon waterflooding, (a) in cluster of pores, (b) in single pore bodies (water-wet glass-etched micromodel)

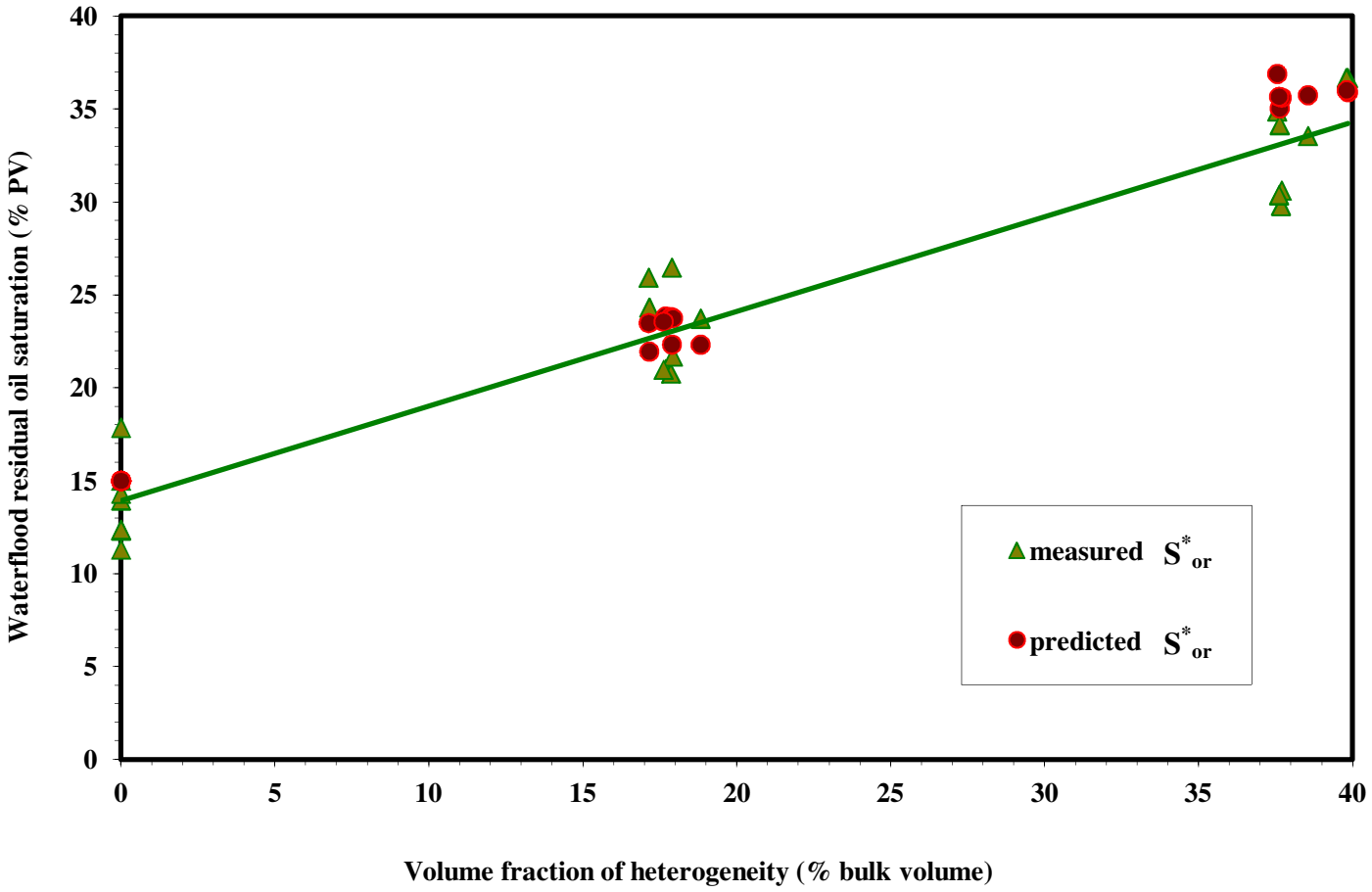

Figure 4-10: Waterflood residual oil saturation at different wettability heterogeneity levels

where x is the fraction of PV in the packing contributed by the heterogeneities. As shown in Figure 4-10, the residual oil saturation values were predicted to be 23.1 and 35.8% PV, with prediction errors of 0.1 and 6.9%, for the heterogeneity levels of 17% and 38%, respectively, showing that the waterflood residual oil saturations have been well- predicted.

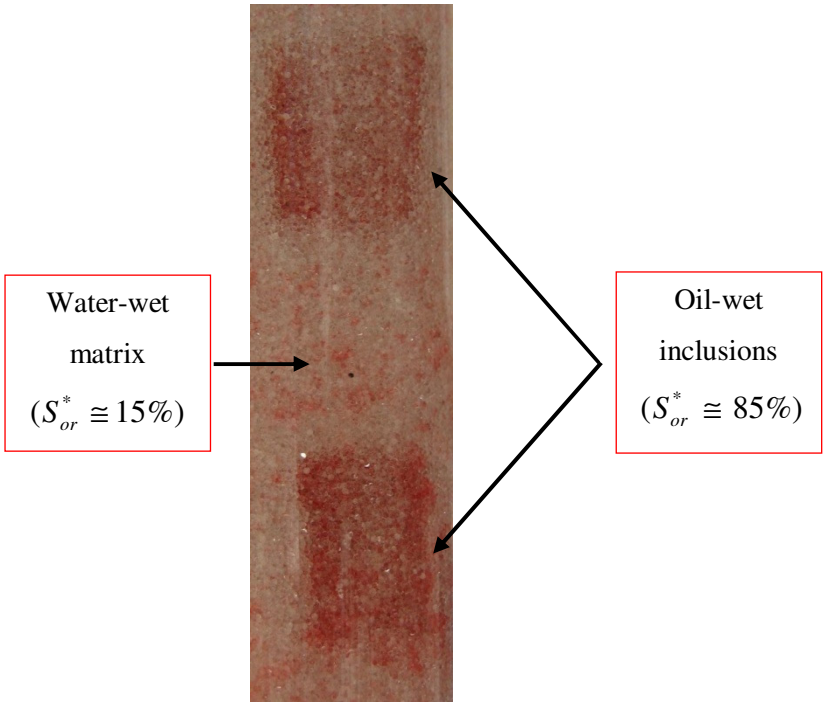

Figure 4-11: Distribution of waterflood residual oil in a heterogeneous porous medium

4.4.3 Experimental Results of the Tertiary Gravity Drainage Process

The packed columns, at the state of waterflood residual oil, were subjected to the GAIGI experiments at five different levels of withdrawal rates and at three different levels of heterogeneity fractions (volume basis). The GAIGI test for each individual experiment was terminated at the time when the entire oil bank was produced, and the gas phase arrived at the capillary barrier interface at the bottom of the column. The gas breakthrough time was selected as the ending point for all of the experiments to keep consistency in analyzing the test results. A summary of experimental conditions and results for all of the runs performed randomly at different heterogeneity levels and withdrawal rates is given

in Table 4-1. Higher values of recovery factors were achieved during the tertiary recovery process of oil from heterogeneous porous media compared to the homogeneous media. In addition, the oil recovery factor decreased as the liquid withdrawal rate from the waterflooded reservoir was increased, at the same level of wettability heterogeneity.

Table 4-1: Summary of the experimental results for the GAIGI experiments in packed columns at different fractions of wettability heterogeneity and withdrawal rates[†]

experiment number	H	ϕ	PV_M	PV_H	S_{or}^*	Q_L	$RF_{g.bkt}$	V_{pg}	N_{gv}	S_{org}
7	0.00	39.77	103.0	0.0	12.33	3.2	67.72	0.344	850.3	3.98
8	0.00	39.35	103.2	0.0	13.95	3.2	66.67	0.339	864.5	4.65
4	0.00	38.89	98.0	0.0	17.86	6.4	62.29	0.713	410.6	6.73
11	0.00	40.43	104.3	0.0	12.37	20.0	44.96	2.270	129.0	6.81
14	0.00	39.89	104.7	0.0	11.30	64.0	0.00	8.503	34.4	11.30
2	17.89	40.69	84.5	9.9	26.48	3.2	76.40	0.377	684.7	6.25
3	18.82	35.16	83.0	9.7	23.73	6.4	63.64	0.788	327.6	8.63
5	17.15	37.66	87.0	9.6	24.33	8.0	62.13	0.954	270.6	9.21
13	17.62	37.54	87.5	12.2	20.97	64.0	20.57	9.230	28.0	16.66
1	37.55	36.47	65.0	29.6	34.88	4.2	77.88	0.491	445.6	7.72
6	39.80	33.97	62.0	26.6	36.68	8.0	68.31	1.076	203.3	11.63
9	37.62	36.58	67.5	27.1	34.15	12.0	66.87	1.591	137.4	11.31
10	37.69	36.69	67.5	28.2	30.62	20.0	53.92	2.807	77.9	14.11
12	37.61	36.53	67.3	28.2	30.38	64.0	39.30	10.435	21.0	18.44

[†]H: heterogeneity (% bulk volume)
ϕ: porosity (%)
PV_M: pore volume of matrix (mL)
PV_H: pore volume of heterogeneity (mL)
S_{or}^*: waterflood residual oil saturation
Q_L: liquid withdrawal rate (mL/h)
$RF_{g.bkt}$: oil recovery factor at gas breakthrough (%S_{or}^*)
V_{pg}: average gas–liquid interface pore velocity (m/day)
N_{gv}: gravity number
S_{org}: reduced residual oil saturation

To observe the effects of the experimental variables on the oil recovery factor more clearly through plots, they were combined into a dimensionless form. For the enhanced oil recovery (EOR) process under study, the gravity number incorporates the majority of the variables influencing the fluid flow in a porous medium. This dimensionless number shows the relative magnitude of gravity forces compared to the viscous forces in the three-phase flow. The gravity number is defined by Equation 3-4, assuming that the pressure gradient within the gas phase is negligible.

The absolute permeability of the packings were measured using the steady-state method at values of 393.4 ± 3.2, 347.7 ± 3.0 and 294.8 ± 1.5 Darcy for the three cases of 0, 17, and 38 volume % heterogeneity levels in the packing, respectively. The overall permeability of the heterogeneous packings is reduced to some extent, corresponding to the volume of heterogeneities embedded in the packing, as a result of slight consolidation during the sintering process.

The pore velocity of the gas–liquid (G–L) interface, V_{pg}, was calculated from the experimental data of gas–liquid interface position, extracted from the photos taken periodically during each experiment. Figure 4-12 shows some sample photos in time sequence (at t = 0, 2, 4, 7, and 9 h) for the interface advancement in a set of experiments, which were run at the same withdrawal rate of 8.0 mL/h but at three different heterogeneity levels. The photos show smooth interfaces along the horizontal direction for all of the heterogeneity levels, demonstrating a gravitationally stable GAIGI process. This behavior becomes more lucid when plotting the G–L interface positions versus time, as shown in Figure 4-13, for the two sets of experiments carried out at 3.2 and 8.0 mL/h withdrawal rates. For clarity purposes, the rest of the results have been omitted from Figure 4-13. The linear advancement of the G–L interface demonstrates that the displacement front proceded in a stable manner with respect to G–L interface advancement. At a particular withdrawal rate, the three interface position curves corresponding to the three different heterogeneity levels are expected to collapse into a single curve. However, because of the differences in the waterflood residual oil saturation along with the variations in the PV of packings with dissimilar volumes of sintered inclusion, three distinct curves have been found when plotting the experimental data.

With Equation 3-4, fluid physical properties (see Table 3-1), and the pore velocity data calculated from plots like those shown in Figure 4-13, the gravity numbers were estimated for all of the experiments, and are listed in Table 4-1. Figure 4-14 illustrates the plot of oil recovery factor at gas breakthrough as a function of gravity number for the three levels of heterogeneities tested. This figure

reveals a strong correlation of recovery factor with the gravity number, especially at the lower ranges of the gravity number. Such a correlation was previously established for homogeneous porous media (Chatzis and Ayatollahi 1993). Figure 4-14 shows that the recovery factor trend is similar for the three cases of heterogeneity levels. However, the curves are shifted upward as the magnitude of heterogeneity increases. This indicates a greater oil recovery factor in heterogeneous media in comparison to the homogeneous media. To describe such behavior, one needs to consider the pore-scale mechanism of the GAIGI process in both homogeneous and heterogeneous porous media.

Let us consider first a homogeneous water-wet porous medium at waterflood residual oil conditions. In such a porous medium, the surfaces of solid particles and the pore wedges are covered by water and some pore bodies contain residual oil blobs. When an inert gas invades a pore with residual oil present, thin film layers of oil will form between the connate water and the gas in the invaded pores, as illustrated in Figure 3-12. These spreading films of oil contribute to oil flow in the gas-invaded pores by gravity drainage, thus creating an oil bank ahead of the macroscopic G–L interface by oil segregation. In addition to the film flow, the gravity-assisted drainage of oil from the column involves residual oil reconnection at the leading front of the oil bank. Therefore, the oil bank grows over time as more of the residual oil is being reconnected with the downward flowing oil bank, as it invades into the waterflooded part of the column. Because the oil has a lower density than water, it naturally accumulates ahead of the G–L interface (see Figure 4-12), thereby, only water is produced before the arrival of the oil bank to the production end. The oil production will commence when the oil bank arrives at the production end and will continue up until the time that gas breaks through the capillary barrier near the bottom of the column. Therefore, water-wetness conditions and the positive spreading coefficient of oil over water are both responsible for the formation of continuous oil films in the pores invaded by the gas. In fact, the water layer on the solid surface acts as a “lubricant”, which significantly increases the oil relative permeability in three-phase flow (Dong et al. 1995; Dong and Chatzis 2003).

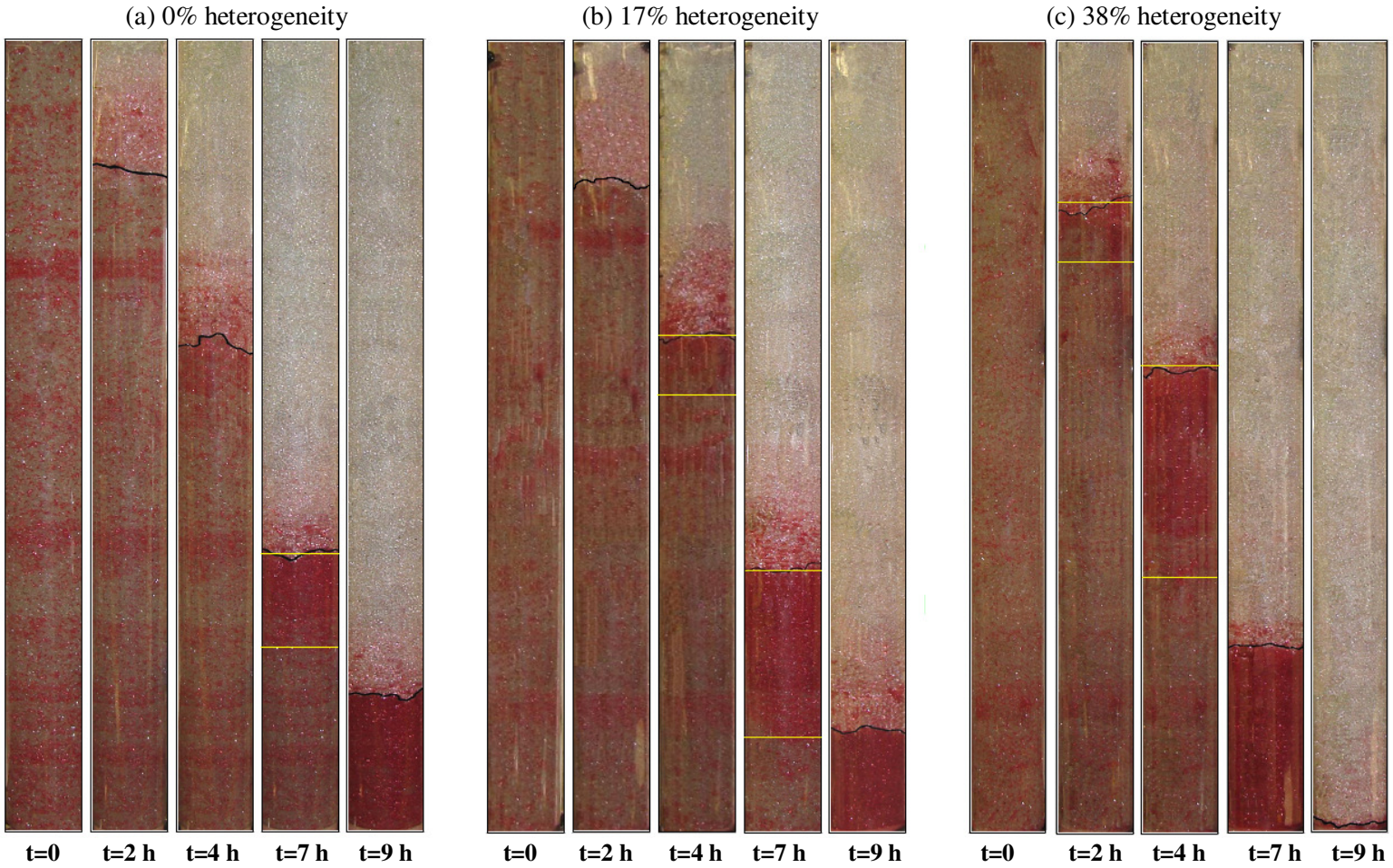

Figure 4-12: Time-lapse photographs of the oil bank size (shown by yellow lines) and gas–liquid interface positions in the set of experiments run at 8.0 mL/h withdrawal rate

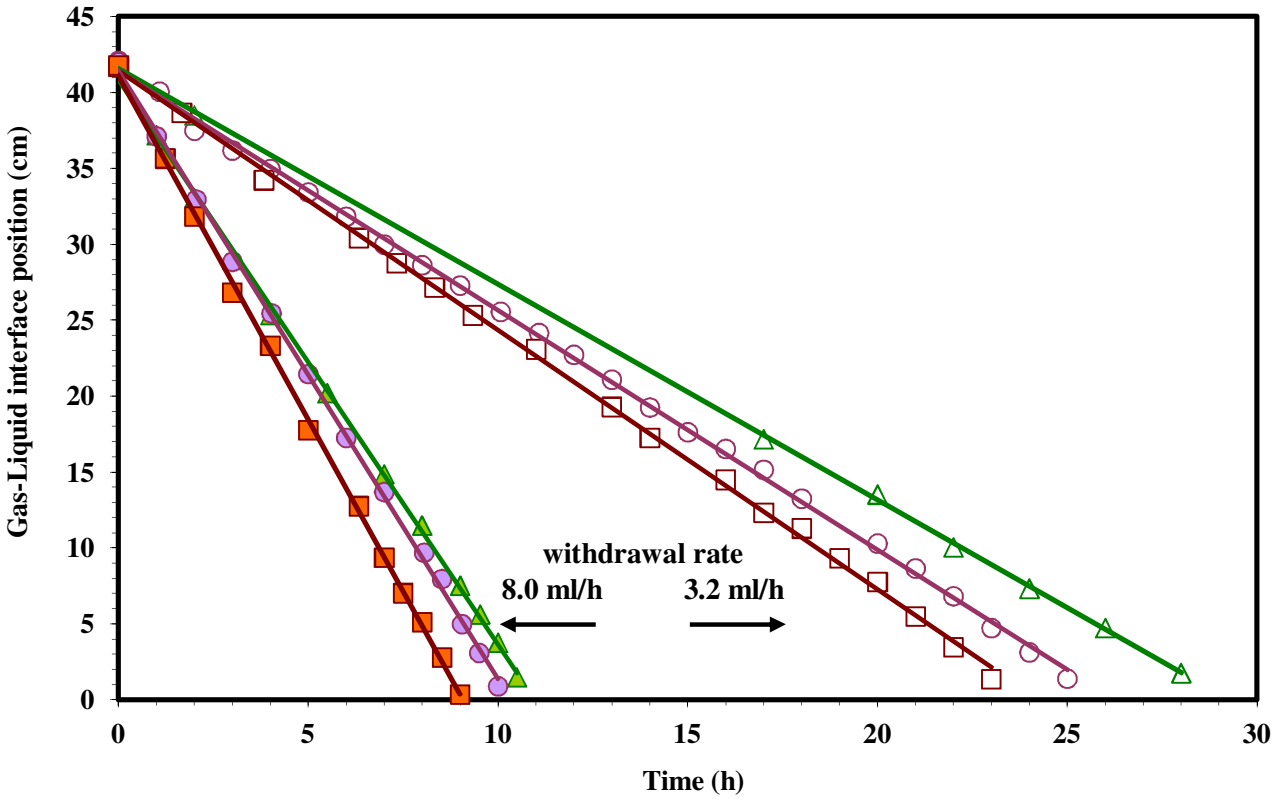

Figure 4-13: Comparison of the gas–liquid interface positions during the GAIGI tests in packing containing different levels of wettability heterogeneity running at two different withdrawal rates (the data are given in Table A.6 and A.7).

(Δ) 0% Heterogeneity, 3.2 mL/h withdrawal rate (○) 17% Heterogeneity, 3.2 mL/h withdrawal rate (□) 38% Heterogeneity, 3.2 mL/h withdrawal rate (▲) 0% Heterogeneity, 8.0 mL/h withdrawal rate (●) 17% Heterogeneity, 8.0 mL/h withdrawal rate (■) 38% Heterogeneity, 8.0 mL/h withdrawal rate

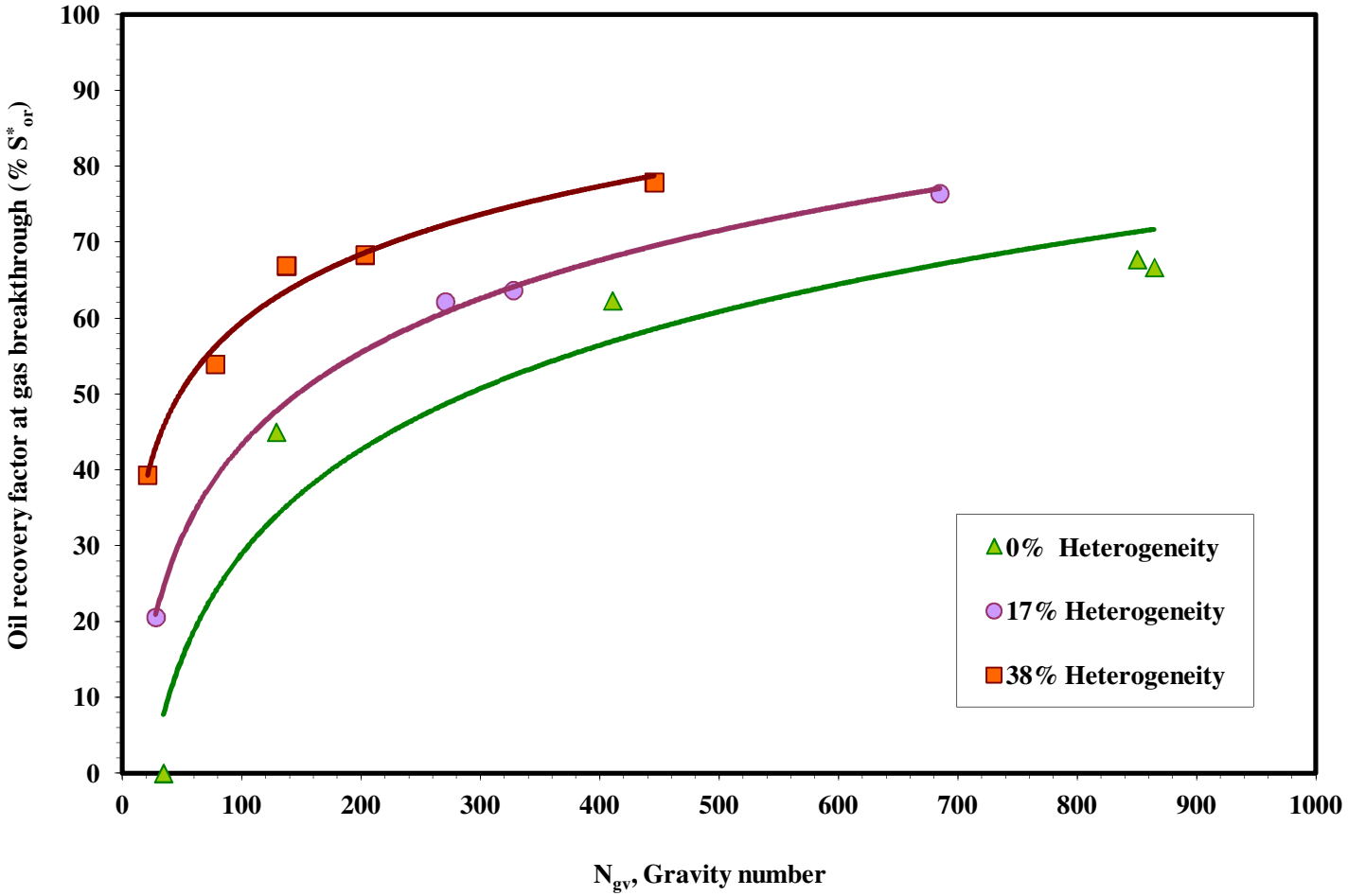

Figure 4-14: Correlation of the oil recovery factor at gas breakthrough with the gravity number for packings containing different levels of wettability heterogeneity

Now, let us consider the gas invasion and gravity drainage in a waterflooded column with macroscopic-scale wettability heterogeneities. The inert gas first invades the water-wet continuum, which spans throughout the packed column with wettability heterogeneities. Therefore, initially the spreading of oil will occur as it does in homogeneous porous media when gas invades the water-wet part of the column. However, once the oil films and the invading gas contact the oil-wet regions, the significant volume of oil present there is reconnected immediately. Consequently, the oil bank will form much earlier and grow faster in a column having wettability heterogeneities. This phenomenon was visually observed during the experiments, and it can be distinguished when comparing the snapshots captured at the same run time for different heterogeneity levels in Figure 4-12. This figure reveals that, in the case of 38 volume % heterogeneities, the oil bank formation commenced after a short time from the start of the GAIGI process and the oil bank production terminated after about 9 h, while for the case of homogeneous porous media, we did not observe oil bank formation until about 7 h after the beginning of liquid withdrawal. In other words, for equivalent operating conditions (e.g., withdrawal rate), the time of oil breakthrough and, hence, the time of gas breakthrough are shorter for a heterogeneous media with respect to the breakthrough times in a homogeneous media.

Another point with respect to Figure 4-14 is the effect of the liquid withdrawal rate on the GAIGI process performance for all cases of heterogeneity fractions. In the experiments conducted at low flow rates (corresponding to large gravity numbers), the favorable condition of larger gravity forces in comparison to the viscous pressure gradient facilitated the development of an oil bank through gravity-assisted drainage of oil and, hence, a higher oil recovery factor. However, when the liquid is pumped out of a porous medium at high rates, the gas phase propagates too fast and a significant quantity of residual oil can be bypassed by the gas phase and appear as an “isolated” phase in the gas-invaded zone. Nonetheless, because of the spreading of some of the remnant oil (whose extent depends upon how fast the gas phase invades the system), the oil blobs will reconnect; some of the bypassed residual oil will be produced up to the breakthrough time through film flow and oil leakage mechanisms. In a heterogeneous medium with isolated oil-wet inclusions, the oil production is mainly controlled by the leakage; a higher oil recovery factor is attained in comparison to a homogeneous system subjected to the same withdrawal rate because of the occurrence of huge amounts of waterflood residual oil. Therefore, the minimum gravity number beyond which the oil bank formation and production occurs is smallest for the most heterogeneous case: gravity numbers corresponding to about 29, 16, and 6 for three heterogeneity levels of 0, 17, and 38 volume %, respectively (calculated

from the fitted lines in Figure 4-15). Having the critical values for gravity number, one can estimate the maximum pumping rate below which the oil bank formation occurs for a particular waterflooded porous medium.

On the basis of the above-mentioned discussions, it is evident that the variation in the waterflood residual oil saturation is the main reason for achieving dissimilar oil recovery factors through the GAIGI process at different heterogeneity levels. This conclusion along with the similarity in the trends of the oil recovery factor at gas breakthrough versus the gravity number for all three levels of heterogeneity (see Figure 4-14) prompted us to normalize the oil recovery factor. Therefore, the normalized oil recovery factor (RF^*) was defined as the fraction of oil produced at gas breakthrough divided by the maximum attainable oil recovery factor through the GAIGI process, which is essentially very close to the waterflood residual oil saturation

$$RF^* = \frac{S_{or}^* - S_{org}}{S_{or}^* - S_{org}^{min}} \tag{4-5}$$

where S_{or}^* is the waterflood residual oil saturation, S_{org} is the reduced residual oil saturation after the GAIGI process, and S_{org}^{min} is the minimum attainable residual oil saturation after the GAIGI process. Figure 4-16 illustrates the plot of the normalized oil recovery factor at gas breakthrough versus the gravity number for the whole set of experiments run at different heterogeneity levels. This figure demonstrates that the normalized oil recovery factor is correlated to the gravity number through the following equation for all three levels of heterogeneity:

$$RF^* = -6.033\, N_{gv}^{-0.6857} + 0.8398 \tag{4-6}$$

This correlation was found to fit the experimental data satisfactorily, with an R^2 value equal to 0.85. Equation 4-6 could be applied to predict the normalized oil recovery factor at gas breakthrough (and hence the oil recovery factor) for different heterogeneity levels, given the operating conditions of the GAIGI process and the characteristics of porous media.

The proposed correlation between the normalized oil recovery factor and the gravity number was validated, having the experimental data of the GAIGI process in homogeneous packings with average bead size of 507 μm taken from section 3.4, and is shown in Figure 4-16 by triangle markers. This figure reveals that the model was successful in satisfactorily estimating the oil production through the

GAIGI process, as the trend for the model closely follows that of both sets of the experimental results. In addition, the oil recovery factor at gas breakthrough is independent of the glass bead size for a packing with relatively uniform bead size distribution. When the experimental results are reported in dimensionless form, one can use them in another scale for comparison purposes or primary assessment of the process at the field scale.

4.4.4 Reduced Residual Oil Saturation after the GAIGI Process

Aside from the economical considerations for evaluating the profitability of any tertiary oil recovery process, the amount and rate of oil recovery are considered as the major criteria for assessment of a particular process. However, the amount of oil left behind by the tertiary processes is also important because it is not usually economical to add another stage for improving oil recovery. As the tertiary process is terminated, the reservoir is brought to the end point of its production life. Therefore, the residual oil saturation is among the most important parameters that are being considered in evaluating the performance of recovery processes.

In this study, the amount of oil trapped upon the GAIGI process (known as reduced residual oil saturation, S_{org}) at the time of gas breakthrough was estimated given the values of waterflood residual oil and the volume of oil recovered in the separator through the GAIGI process. Owing to the dependence of reduced residual oil saturation on a variety of parameters, among which are absolute permeability and withdrawal rate, S_{org} was plotted against the gravity number to include all of the experimental variables, as shown in Figure 4-17a, for the three cases of volume fractions of wettability heterogeneity. This figure demonstrates a similar correlation of S_{org} and N_{gv} for all three fractions of wettability heterogeneity at high values of the gravity number, showing the promising feature of the GAIGI process in recovering a significant amount of oil trapped upon waterflooding in heterogeneous media, comparable to the homogeneous water-wet media. For the lower values of the gravity number, the gas phase propagates very rapidly. Therefore, the formation of spreading films (which are responsible for achieving low reduced residual oil saturation) diminishes, and the leakage mechanism contributes the most to the oil production, especially for heterogeneous media. In a homogeneous water-wet medium, the favorable wettability condition facilitates the progress in the formation of the spreading film, even though the gas invades very quickly at high withdrawal rates. As a result, the uniform wettability condition results in lower reduced residual oil saturation values compared to the heterogeneous cases. In Figure 4-17b, the results of S_{org} versus N_{gv} are shown for the

GAIGI process carried out in heterogeneous porous media with permeability heterogeneity (large permeability inclusions randomly distributed in a continuum of smaller permeability) but of uniform wettability. Having the same configuration of heterogeneity distribution as the present work, both plots of the waterflood residual oil saturation versus the volume fraction of heterogeneities and the oil recovery factor versus the gravity number show similar trends. However, the reduced residual oil saturations at a given gravity number tend to be independent of the volume fraction of the permeability heterogeneity as long as the wettability of the medium is uniformly water-wet.

The more intense effect of wettability heterogeneities on the performance of the GAIGI process in comparison to that of the pore structure heterogeneities has been further verified in panels a and b of Figure 4-18. This figure illustrates the plot of S_{org} versus N_{gv} for the two cases of wettability and permeability heterogeneity at two levels of volume fraction of heterogeneities, i.e., 17 and 38%, respectively. While both the wettability and pore structure heterogeneities cause a significant amount of oil being trapped upon secondary recovery, the latter type of heterogeneity is less detrimental to the tertiary gravity drainage process. The oil continuity is assured by the presence of spreading oil films over the water layer (which covers the water-wet surfaces throughout the porous medium) for both permeability heterogeneity fractions. Consequently, unlike the wettability heterogeneity, the occurrence of the pore structure heterogeneity plays a less significant role on the reduced residual oil saturations. On the other hand, in media with wettability heterogeneity, the oil can remain as a residual wetting phase in the oil wet regions, which eventually results in a higher reduced residual oil saturation. This is the reason why the two residual curves do not coincide. Essentially, almost all of the residual oil in the water-wet media is recoverable during the GAIGI process, provided that the average permeability of the porous media and the drainage time are sufficiently high (Chatzis et al. 1988; Kantzas et al. 1988a, b).

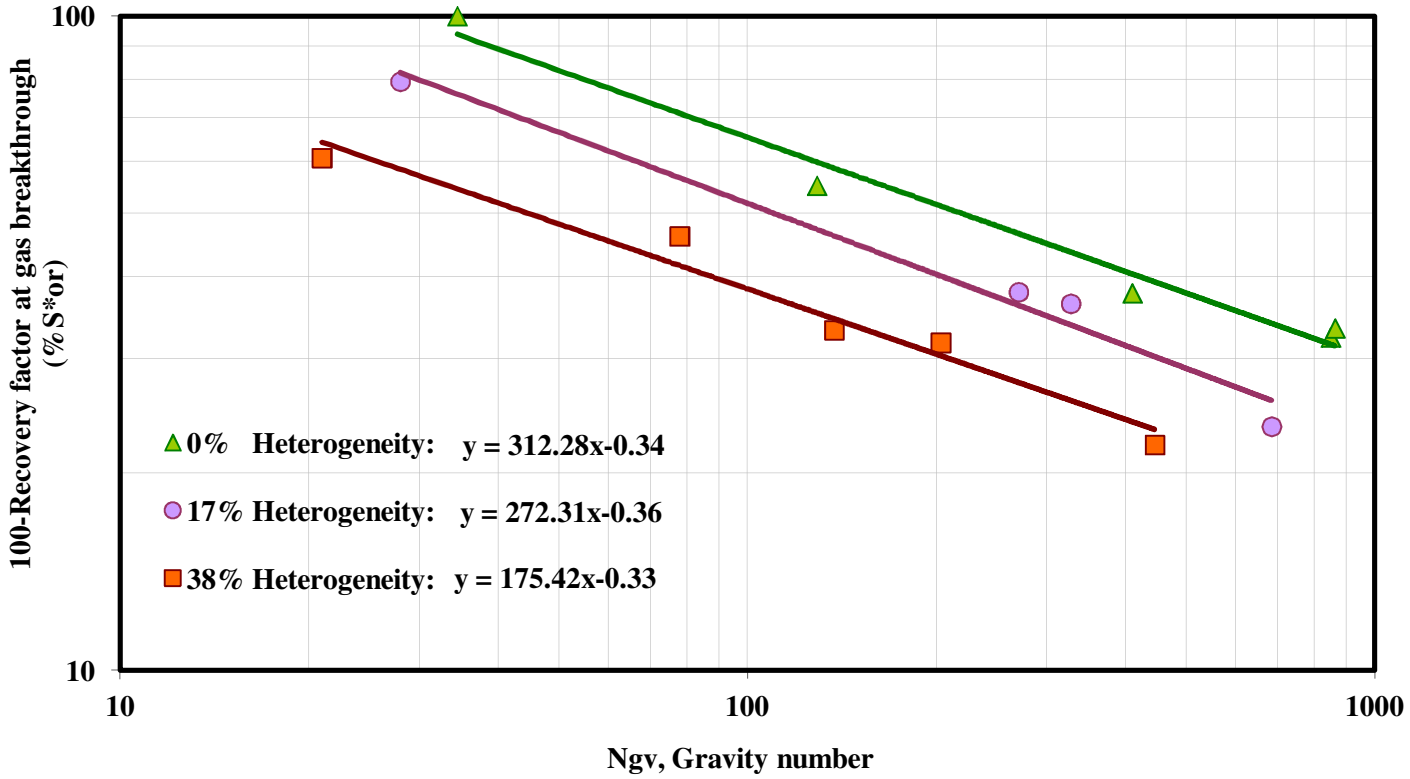

Figure 4-15: Logarithmic-scale correlation of the recovery factor at gas breakthrough with the gravity number for packings of different levels of wettability heterogeneity

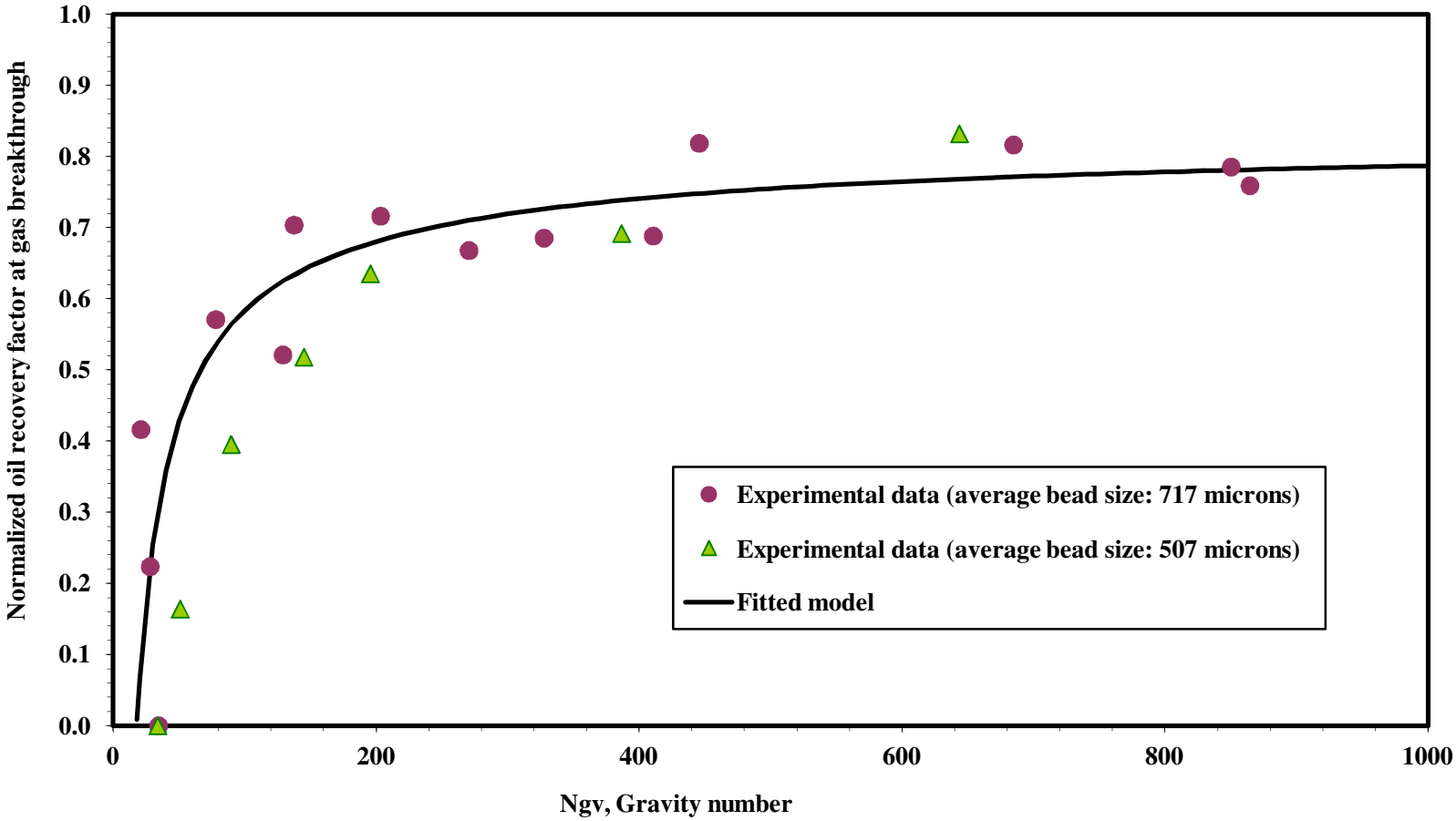

Figure 4-16: Correlation of the normalized oil recovery factor at gas breakthrough and the gravity number for all experimental runs

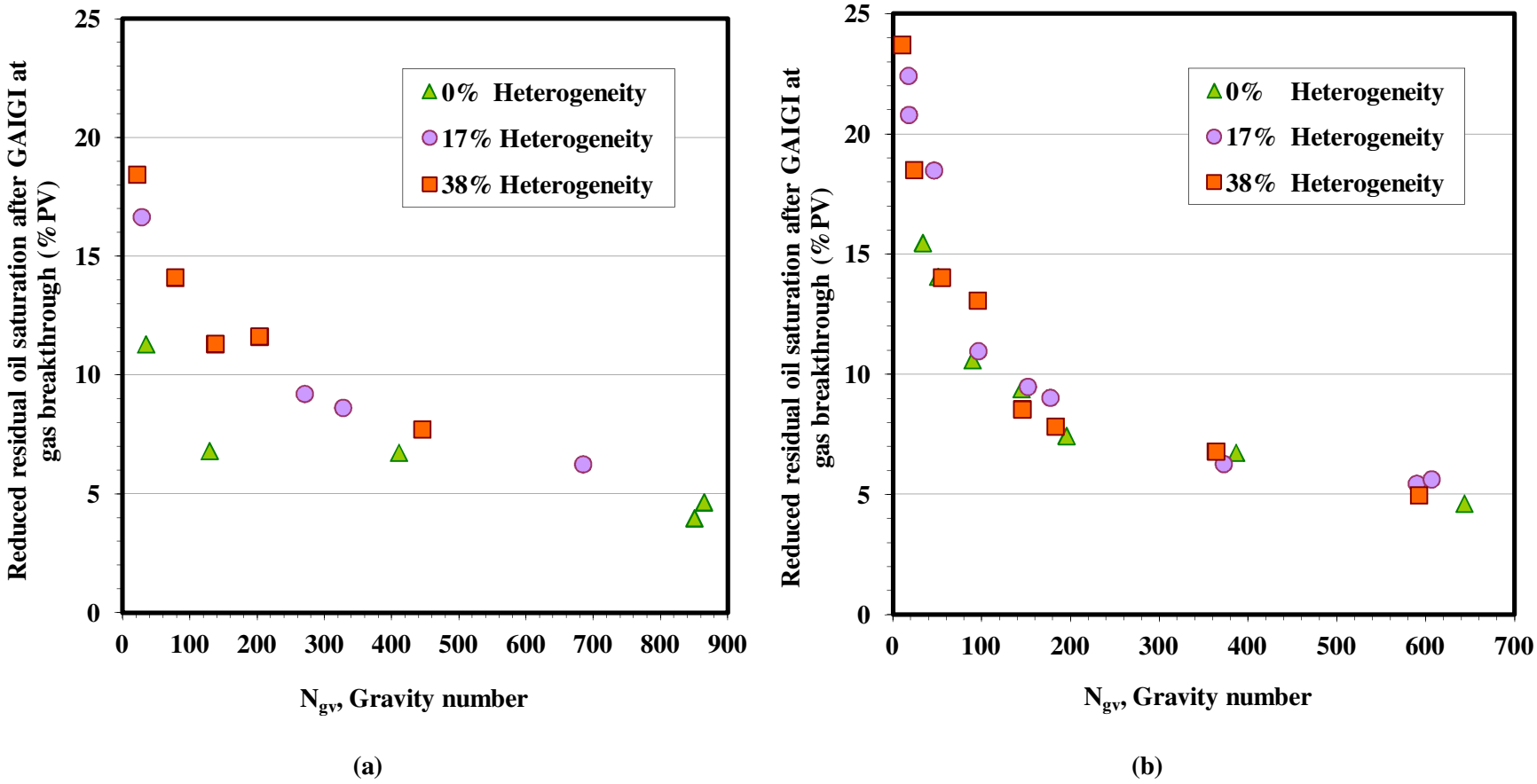

Figure 4-17: Comparison of reduced residual oil saturation at gas breakthrough in packings containing different fractions of (a) wettability and (b) permeability heterogeneity after being depleted by the GAIGI process

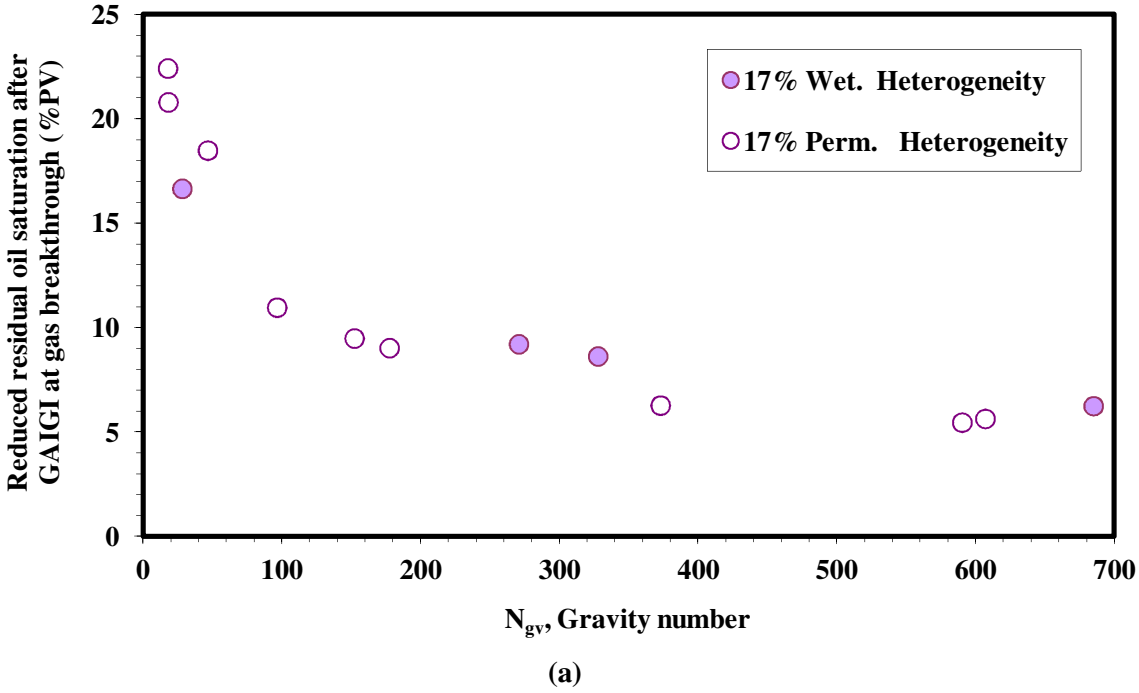

(a)

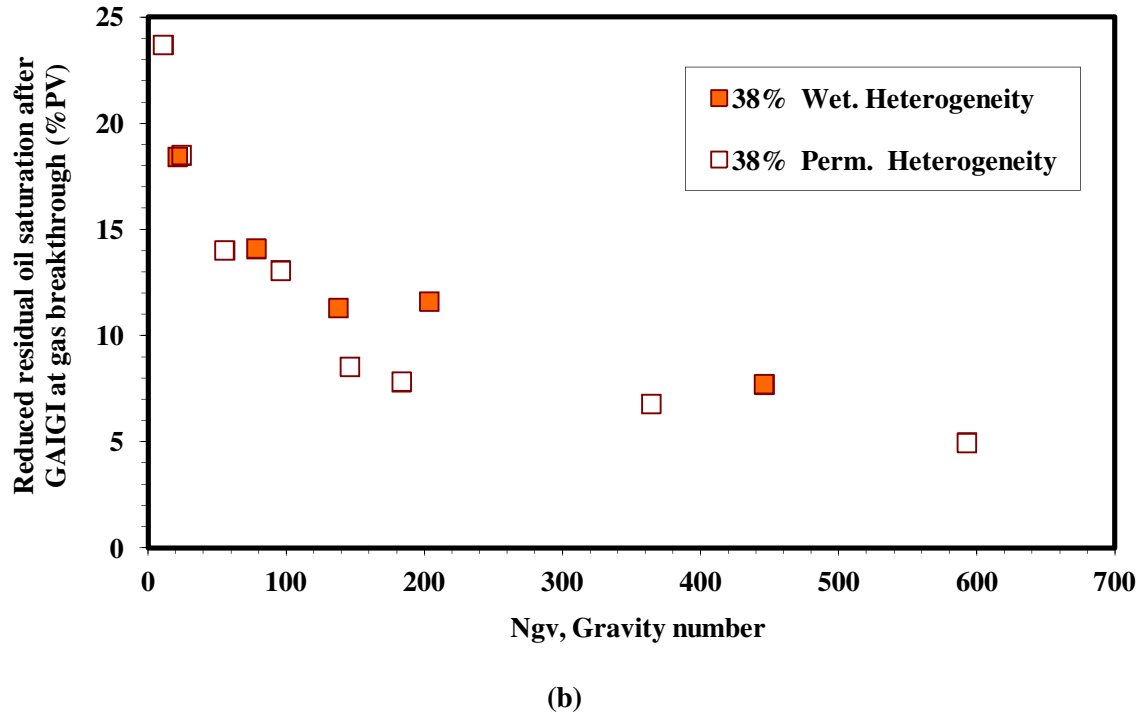

(b)

Figure 4-18: Reduced residual oil saturation at gas breakthrough in packings containing different fractions of wettability or permeability heterogeneity after being depleted by the GAIGI process: (a) 17% Heterogeneity (b) 38% Heterogeneity

4.5 Conclusions

Waterflooding and controlled gravity drainage tests were carried out in the heterogeneous glass bead packed columns consisting of water-wet continuum with oil-wet inclusions. Upon waterflooding, a significant amount of oil was bypassed in the oil-wet zones because of the capillary effects at the boundary of the regions exhibiting different wetting states. Over the course of the GAIGI process in the heterogeneous porous media, an oil bank was formed at the early stages of the process due to the occurrence of a large amount of the waterflood residual oil. This early-formed oil bank grew in size by reconnecting the residual oil ganglia in the water-wet matrix and the continuous oil-phase in the oil-wet regions. Therefore, the GAIGI process was found to be very efficient in sweeping waterflood residual oil from both homogeneous and heterogeneous porous media. However, the analysis of reduced residual oil saturations showed that the amount of S_{org} is slightly higher in the heterogeneous porous media because some oil is trapped in the oil-wet regions due to capillarity effects. Finally, the oil recovery factor at gas breakthrough was very well correlated with gravity number for all three cases of volume fractions of heterogeneities tested.

Chapter 5

Conclusions and Future Work

5.1 Conclusions

This chapter presents the conclusions drawn from the experimental study of waterflooding and the gravity-assisted inert gas injection process in two types of heterogeneous porous media, namely, heterogeneity in pore structure and heterogeneity in wettability. The configuration of heterogeneities studied here was in the form of randomly distributed high permeability isolated regions enclosed by low permeability continuum for the former case of heterogeneity, and in the form of randomly distributed oil-wet inclusions in the water-wet matrix for the latter case of heterogeneity. The liquid withdrawal rate and volume fraction of heterogeneities were the two major parameters whose impacts on the GAIGI process were demonstrated. The following main conclusions can be drawn:

i. The magnitude of waterflood residual oil saturation in heterogeneous porous media exhibiting permeability and wettability heterogeneities is significantly higher than that in homogeneous porous media. The pore-scale trapping mechanism explains that the amount of trapped oil upon waterflooding is proportional to the fraction of heterogeneities (large-pore-size regions for the case of permeability heterogeneities, and oil-wet isolated regions in the case of wettability heterogeneity). The experimental data verified this linear proportionality.

ii. Unlike waterflooding, gas invasion occurs both in the continuum as well as in the isolated regions for both cases of heterogeneous porous media tested. In addition, the occurrence of high residual oil saturation after waterflooding heterogeneous porous media facilitates the

early formation of an oil bank. Consequently, the GAIGI process improves the poor performance of waterflooding in heterogeneous reservoirs.

iii. The oil recovery factor at gas breakthrough correlates satisfactorily with the gravity number for homogeneous porous media as well as the heterogeneous media. A similar trend was observed for all three cases of heterogeneity levels. This similarity enabled the development of a mathematical analysis that predicts quite well the oil recovery factor for heterogeneous media up to gas breakthrough.

iv. Comparison of the reduced residual oil saturation after the GAIGI process in both types of heterogeneous porous media showed that effect of permeability heterogeneity was less detrimental to oil recovery by gravity drainage. The reason was that despite the presence of pore structure heterogeneities, the media were uniformly water-wet, assuring the oil continuity through spreading oil films throughout the porous media.

v. The dimensionless groups were used to characterize the operating parameters of the gravity drainage process at the field scale. Accordingly, the GAIGI process appears to be feasible for the reservoirs with an average permeability larger than 1 Darcy. An alternative oil recovery process is suggested that is a combination of controlled and free fall gravity drainage. The total required time for the controlled and free-fall gravity drainage process to attain a certain oil recovery factor is significantly lower than the required time for the controlled gravity drainage alone to give the same oil recovery factor, even at permeability values less than 1 Darcy.

5.2 Future work

When this project was started, an important goal was to determine three-phase relative permeability curves from saturation data collected during tertiary gravity drainage experiments. A considerable amount of time and resources were spent on attempting to collect three-phase saturation data by means of the RI (Resistivity Index) and NMR (Nuclear Magnetic Resonance) methods. Unfortunately, the preliminary results of the RI measurements for a two-phase system (air-0.001M KCl solution) showed that this method is not suitable for the low ranges of saturation. Accordingly, the application of RI method for the GAIGI process scheme was found to be inappropriate in view of the fact that both the gas and transition zones contain very low amounts of water and oil. Also, for

this method to be feasible, the water-phase continuity should be maintained throughout the porous media to provide a conductive path for the electrical current. This condition exists in the water-wet porous media while in the porous media exhibiting wettability heterogeneities there is no water film continuity in the oil-wet inclusions. Therefore, the water saturation in the oil-wet regions cannot be detected using the RI method. Another problem with applying this technique for our study is its limitation to detect only the water-phase. Thus, the RI technique is a suitable choice where only the saturation of water is needed, or for the case that only two fluids are present in the porous media. For the type of multiphase flow problem under study, we needed to measure the saturation profile for all three phases, which is not possible by this method.

The NMR method was also unsuccessful because of two main reasons. First, low contrast in the diffusion rates of water and oil prevented differentiation of signals for the two fluids. Second, the machine interior core diameter allowed for accommodation of a packed column of small diameter (less than 1 cm) which made it challenging to create a randomly distributed configuration of heterogeneity. Although we could not carry out the saturation distribution measurement using NMR during dynamic displacements, because of technical limitations, we did measure the saturation distribution at the end of the GAIGI process. If in the future NMR imaging tools become available, it is suggested to continue this research for monitoring oil saturation, as a function of location and time, and develop models for oil relative permeability.

Making improvements in glass bead sintering methods without significantly affecting the permeability of sintered material compared to the permeability of the matrix will possibly help in better quantifying the wettability heterogeneity effects on the GAIGI process.

To apply the dimensional analysis in the present work, it is necessary to study other factors which influence the process. The oil viscosity, column length and the degree of permeability contrasts are three significant factors which should be studied further. More experiments need to be carried out to incorporate the effect of these factors into the dimensional analysis and make it more general.

References

Adamson, A.W., Physical Chemistry of Surfaces, 5th ed., Wiley-Interscience Inc., New York, (1960)

Agbalaka, C., Dandekar, A.Y., Patil, S.L., Khataniar, S., and Hemsath, J.R., "The Effect of Wettability on Oil Recovery: A Review", presented at the SPE Asia Pacific Oil and Gas Conference and Exhibition, Perth, Australia, 20-22 October (2008)

Ahmed, T., Hydrocarbon Phase Behavior, Contribution in Petroleum Geology and Engineering, Vol. 7, Gulf Publishing Company, (1989)

Amott, E., "Observations Relating to the Wettability of Porous Rock", *Transactions AIME,* (1959) 216, pp. 156–162

Amyx, J.W., Bass, D.M., and Whiting, R.L., Petroleum Reservoir Engineering, Physical Properties, McGrow-Hill Book Company Inc., (1960)

Anderson, W.G., "Wettability Literature Survey – Part 1: Rock/Oil/Brine Interactions and the Effects of Core Handling on Wettability", *Journal of Petroleum Technology*, (1986a), pp. 1125-1144

Anderson, W.G., "Wettability Literature Survey – Part 2: Wettability Measurement", *Journal of Petroleum Technology*, (1986b), pp. 1246-1262

Araujo, Y. C., Araujo, M., Guzmán, H., and Moya, G., "Effect of the Spreading Coefficient on Two-Phase Relative Permeability", SPE 65385, presented at the SPE International Symposium on Oilfield Chemistry, Houston, Texas, 13–16 February (2001)

Ayatollahi, S.S., "Experimental and Theoretical Studies on Gravity Assisted Inert Gas Injection for the Recovery of Waterflood Residual Oil in Homogeneous and Layered Porous Media", PhD thesis, University of Waterloo, Waterloo, ON, Canada (1994)

Bertin, H., Hugget, A., and Robin, M., "Two-Phase Flow through Orthogonal Composite Cores with Wettability Heterogeneity", *Journal of Petroleum Science and Engineering*, 1998, 20, pp. 185–188

Blunt, M., Zhou, D., and Fenwick, D., "Three-Phase Flow and Gravity Drainage in Porous Media", *Transport in Porous Media*, (1995), 20, pp. 77-103

Blunt, M., "Pore Level Modeling of the Effects of Wettability", *SPE Journal*, (1997), 2(4), pp. 494-510

Bradford, S.A., and Leij, F.J., "Fractional Wettability Effects on Two-and Three-Fluid Capillary Pressure-Saturation Relations", *Journal of Contaminant Hydrology*, (1995), 20, pp. 89-109

Brigham, W.E., "Mixing Equations in Short Laboratory Cores", *SPE Journal*, (1974), 14(1), pp. 91–99

Brown, R.J.S. and Fatt, I., "Measurements of Fractional Wettability of Oilfield Rocks by the Nuclear Magnetic Relaxation Method", *Transactions of the American Institute of Mining, Metallurgical and Petroleum Engineers*, (1956), 207, pp. 262-264

Buckley, S.E. and Leverett, M.C., "Mechanism of Fluid Displacement in Sands," *Petroleum Transactions, AIME*, (1942), 146, pp. 107-116

Buckley, J.S., Takamura, K., and Morrow, N.R., "Influence of Electrical Surface Charges on the Wetting Properties of Crude Oils", *SPE Reservoir Engineering*, (1989), 4(3), pp. 332-340

Buckley, J.S., and Morrow, N.R., "An Overview of Crude Oil Adhesion Phenomena", in: Physical Chemistry of Colloids and Interfaces in Oil Production, H. Toulhoat, and J. Lecourtier, (eds.), Éditions Technip, Paris, (1992), pp. 39-45

Burcik, E.J., Properties of Petroleum Reservoir Fluids, IHRDC, Boston, (1979)

Carlson, L.O., "Performance of Hawkins Field Unit under Gas Drive-Pressure Maintenance Operations and Development of an Enhanced Oil Recovery Project", SPE paper 17324, presented at the SPE Enhanced Oil Recovery Symposium, Tulsa, Oklahoma, 16-21 April (1988)

Caruana, A., and Dawe, R.A., "Flow Behaviour in the Presence of Wettability Heterogeneities", *Transport in Porous Media*, (1996), 25, pp 217–233

Catalan, L., "Gravity drainage of Waterflood Residual Oil Assisted by Inert Gas Injection", PhD thesis, University of Waterloo, Department of Chemical Engineering, Waterloo, ON, Canada, (1992)

Catalan, L., Dullien, F.A.L., and Chatzis, I., "The Effect of Wettability and Heterogeneities on the Recovery of Waterflood Residual Oil with Low Pressure Inert Gas Injection Assisted by Gravity Drainage", *SPE Advanced Technology Series*, (1994), 2(2), pp. 140-149

Chatzis, I., Morrow, N.R., and Lim, H.T., "Magnitude and Detailed Structure of Residual Oil Saturation", paper 10681, *SPE Journal*, (1983), 23(2), pp. 311-326

Chatzis, I., Kantzas, A., and Dullien, F.A.L., "On the Investigation of Gravity Assisted Inert Gas Injection Using Micromodels, Long Berea Cores, and Computer Assisted Topography", SPE paper 18284 presented at the 1988 SPE Annual Technical Conference and Exhibition, Houston, 2-5 October (1988)

Chatzis, I., and Ayatollahi, S., "The Effect of Production Rate on the Recovery of Waterflood Residual Oil Under Gravity Assisted Inert Gas Injection", Paper No. 32, presented at the 5th Petroleum Conference of the south Saskatchewan section, the Petroleum Society of CIM, Regina, Saskatchewan, October 18-19 (1993)

Chatzis, I., and Ayatollahi, S.S., " Investigation of the GAIAI process in stratified porous media for the recovery of waterflood residual oil", presented at the sixth Petroleum Conference of the south Saskatchewan section, the Petroleum Society of CIM, held in Regina, Saskatchewan, October 16-18 (1995)

Chow, R.S., and Takamura, K., "Electrophoretic Mobilities of Bitumen and Conventional Crude-in-Water Emulsions Using the Laser Doppler Apparatus in the Presence of Multivalent Cations", *Journal of Colloid and Interface Science*, (1988), 125(1), pp. 212-225

Correâ, A.C.F., and Firoozabadi, A., "Concept of Gravity Drainage in Layered Porous Media", *SPE Journal*, (1996), **1** (1), pp. 101-111

Cuiec, L.E., "Evaluation of Reservoir Wettability and Its Effect on Oil Recovery", in: Interfacial Phenomena in Petroleum Recovery, Morrow, N. R., ed., Marcel D., New York, (1991), pp. 319-375

Dawe, R.A., Wheat, M.R., and Bidner, M.S., "Experimental Investigation of Capillary Pressure Effects on Immiscible Displacement in Lensed and Layered Porous Media", *Transport in Porous Media*, (1992), 7, pp 83–101

Dawe, R.A., and Grattoni, C.A., "Experimental Displacement Patterns in a 2×2 Quadrant Block with Permeability and Wettability Heterogeneities – Problems for Numerical Modeling", *Transport in Porous Media*, (2008), 71, pp. 5–22, DOI 10.1007/s11242-007-9108-5

Deng, Y., " Experimental and Theoretical Studies of Drainage Type Unstable Immiscible Displacements in Porous Media in a Gravity Field", PhD thesis, University of Waterloo, Department of Chemical Engineering, Waterloo, ON, Canada, (1996)

DiCarlo, D.A., Sahni, A., and Blunt, M.J., "Three-Phase Relative Permeability of Water-Wet, Oil-Wet, and Mixed-Wet Sandpacks", *SPE Journal*, (2000), 5(1), pp. 82-91

Dixit, A.B., McDougall, S.R., and Sorbie, K.S., "Analysis of Relative Permeability Hysteresis Trends in Mixed-wet Porous Media Using Network Models", SPE paper 39656, presented at the 1998 SPE/DOE Improved Oil Recovery Symposium, Tulsa, Oklahoma, 19-22 April, (1998)

Donaldson, E.C., Thomas, R. D., and Lorenz, P.B., "Wettability Determination and Its Effect on Recovery Efficiency", *SPE Journal*, (1969), 9(1), pp. 13-20

Donaldson, E.C. and Siddiqui, T. K., "Relationship between the Archie Saturation Exponent and Wettability", *SPE Formation Evaluation*, (1989), 4(3), pp. 359-362

Dong, M., Dullien, F.A.L., and Chatzis, I., "Imbibition of Oil in Film Form over Water Present Edges of Capillaries with an Angular Cross Section", *Journal of Colloid and Interface Science*, (1995), 172, pp. 21-36

Dong, M., and Chatzis, I., "Oil Layer Flow along the Corners of Non-Circular Capillaries by Gravity Drainage", *Journal of Canadian Petroleum Technology*, (2003), 42(2), pp. 9-11

Dullien, F.A.L., Chatzis, I., and Kantzas, A., "Laboratory Studies of Macroscopic and Microscopic Mechanisms of Immiscible Gas Drive Gravity Drainage Recovery", proceedings of the 3rd International Symposium on Enhanced Oil Recovery, Maracaibo, Venezuela, February 19-22 (1989)

Dullien, F.A.L., Catalan, L., Chatzis, I., and Collins, A., "Recovery of Waterflood Residual Oil with Low Pressure Inert Gas Injection, Assisted by Gravity Drainage from Water-Wet and Oil-Wet Cores", presented at the CIM/AOSTRA 1991 Technical Conference held in Banff, (1991)

Dumoré, J.M., and Schols, R.S., "Drainage Capillary-Pressure Functions and the Influence of Connate Water", *SPE Journal*, (1974), 14(5), pp. 437-444

Dumoré, J.M., "Stability Considerations in Downward Miscible Displacements", *SPE Journal*, 1964, 4(4), pp. 356 – 362

Essley, P. L., Hancock, G.L., and Jones, K.E, "Gravity Drainage Concepts in a Steeply Dipping Reservoir", paper SPE 1029-G, presented at the Petroleum Conference on Production and Reservoir Engineering, Tulsa, Oklahoma, 20-21 March (1958)

Farouq Ali, S.M., "Heavy Oil—Evermore Mobile", *Journal of Petroleum Science and Engineering*, (2003), 37, pp. 5-9

Fassihi, M.R., and Gillham, T.H., "The Use of Air Injection to Improve the Double Displacement Processes", SPE paper 26374, presented at the SPE Annual Technical Conference and Exhibition, Houston, Texas, 3-6 October (1993)

Grattoni, C.A., and Dawe, R.A., "Gas and Oil Production from Waterflood Residual Oil: Effects of Wettability and Oil Spreading Characteristics, *Journal of Petroleum Science and Engineering*, (2003), 39, pp. 297–308

Hagoort, J., "Oil Recovery by Gravity Drainage", *SPE Journal*, (1980), 20(3), pp. 139-150

Hair, M.L., and Tripp, C.P., "Alkylchlorsilane Reactions at the Silica Surface", *Colloids and Surfaces A: Physiochemical and Engineering Aspects*, 1995, 105, pp. 95-103

Harkins, W.D., "A General Thermodynamic Theory of the Spreading of Liquids to Form Duplex Films and of Liquids or Solids to Form Monolayers", *Journal of Chemical Physics*, (1941), 9(7), pp. 552-568

Helland, J.O., and Skjæveland, S.m., "Three-Phase Capillary Pressure Correlation For Mixed-Wet Reservoirs", SPE paper 92057, presented at the SPE International Petroleum Conference held in Mexico, Puebla, Mexico, 7-9 November, (2004)

Hill, S., "Channeling in Packed Columns", *Chemical Engineering Science*, (1952), 6(1), pp. 247-253

Hirasaki, G.J., "Wettability: Fundamentals and Surface Forces", *SPE Formation Evaluation*, (1991), 6(2), pp. 217-226

Holbrook, O.C., and Bernard, G.G., "Determination of Wettability by Dye Adsorption", SPE 896-G *Petroleum Transactions, AIME* (1958), 213, pp. 261-264

Jadhawar, P.S. and Sarma, H.K., "Numerical Simulation and Sensitivity Analysis of Gas-Oil Gravity Drainage Process of Enhanced Oil Recovery", *Journal of Canadian Petroleum Technology*, (2010), 49(2), pp. 64-70

Jerauld, G.R., "Prudhoe Bay Gas/Oil Relative Permeability", *SPE Reservoir Engineering*, (1997), 12(1), pp. 66-73

Jia, D., Buckley, J.S., and Morrow, N.R., "Control of Core Wettability with Crude Oil", SPE paper 21041, presented at the SPE International Symposium on Oilfield Chemistry, Anaheim, California, 20-22 February (1991)

Johnston, J.R., "Weeks Island Gravity Stable CO_2 Pilot", SPE paper 17351, presented at the SPE Enhanced Oil Recovery Symposium, Tulsa, Oklahoma, 16-21 April (1988)

Kalaydjian, F.J.M., "Performance and Analysis of Three-Phase Capillary Pressure Curves for Drainage and Imbibition in Porous Media", SPE paper 24878, presented at the SPE Annual Technical Conference and Exhibition, Washington, DC, 4-7 October (1992)

Kalaydjian, F.J.M., Moulu, J.C., and Vizika, O., "Three-Phase Flow in Water-Wet Porous Media: Determination of Gas-Oil Relative Permeabilities under Various Spreading Conditions", SPE paper 26671 presented at the 1993 SPE Annual Technical Conference and Exhibition, Houston, TX, 3-6 October (1993)

Kantzas, A., A Theoretical and experimental study of gravity assisted inert gas injection as a method of oil recovery, PhD thesis, University of Waterloo, Waterloo, ON, Canada (1988)

Kantzas, A., Chatzis, I., and Dullien, F.A.L., "Enhanced Oil Recovery by Inert Gas Injection", SPE/DOE 17379 presented at the 1988 SPE/DOE Enhanced Oil Recovery Symposium, Tulsa, OK, 17-20 April (1988a)

Kantzas, A., Chatzis, I., and Dullien, F.A.L., "Mechanisms of Capillary Displacement of Oil by Gravity Assisted Inert Gas Injection", SPE paper 17506, presented at the 1988 SPE Rocky Mountain Regional Meeting, Casper, WY, 11-13 May (1988b)

Kantzas, A., Nikakhtar, B., de Wit, P., Pow, M, and Jha, K.M., "Design of a Gravity Assisted Immiscible Gas Injection Program for Application in a Vuggy Fractured Reef, *Journal of Canadian Petroleum Technology*, (1993), 32(10), pp. 15-23

Katz, D.L., "Possibilities of Secondary Recovery for the Oklahoma City Wilcox Sand", *Trans. AIME*, (1942), 146, pp. 28-53

Keller, A. A., and Chen, M., "Effect of Spreading Coefficient on Three-Phase Relative Permeability of Nonaqueous Phase Liquids", *Water Resources Research*, (2003), 39(10), pp. 1288-1305, doi: 10.1029/2003WR002071

Kiriakidis, D.G., Mitdsoulis, E., and Neale, G.H., "Computer Simulation of Immiscible Displacement in a Porous Medium Containing a Region of Different Wettability", *Journal of Canadian Petroleum Technology*, (1993), 32(6), pp. 21-25

Kulkarni, M.M., and Rao, D.N., "Experimental Investigation of Various Methods of Tertiary Gas Injection", SPE paper 90589, presented at the SPE Annual Technical Conference and Exhibition, Houston, Texas, 26-29 September (2004)

Kulkarni, M.M., and Rao, D.N., "Experimental Investigation of Miscible and Immiscible Water-Alternating-Gas (WAG) Process Performance", *Journal of Petroleum Science and Engineering*, (2005), 48, pp. 1–20

Laroche, C., "Secondary and Tertiary Gas Injection Experiments in Heterogeneous Wettability Micromodels", SPE 52067-STU, presented at the 1998 SPE European Petroleum Conference, The Hague, The Netherlands, 20-22 October (1998)

Laroche, C., Vizika, O., and Kalaydjian, F., "Wettability Heterogeneities in Gas Injection: Experiments and Modeling", *Petroleum Geoscience*, (1999), 5, pp. 65-69

Leverett, M.C., "Capillary Behavior in Porous Solids", *Petroleum Transactions AIME*, (1941), 142, pp. 152-169

Levorsen, A.I., Geology of Petroleum, W.H. Freeman and Company, San Francisco, (1967)

Lewis, O.J., "Gravity Drainage in Oil Fields", *Petroleum Transactions AIME*, (1944), 155, pp. 133-154

Link, P.K., Basic Petroleum Geology, Oil & Gas Consultants Intern/al Publications, (1982)

Maeda, H., and Okatsu, K., "EOR Using Thin Oil Film Drainage Mechanism in Water Wet Oil Reservoir", SPE paper 116532, presented at the SPE Asia Pacific Oil & Gas Conference and Exhibition, Perth, Australia, 20-22 October (2008)

Mani, V. and Mohanty, K. K., "Effect of the Spreading Coefficient on Three-Phase Flow in Porous Media", *Journal of Colloid and Interface Science*, (1997), 187, pp. 45–56

Marcelle-De Silva, J., and Dawe, R.A., "Effects of Permeability and Wettability Heterogeneities on Flow in Porous Media", SPE paper 81164, presented at the SPE Latin American and Caribbean Petroleum Engineering Conference held in Port-of-Spain, Trinidad, West Indies, 27-30 April, (2003)

Masalmeh, S.K., "Studying the Effect of Wettability Heterogeneity on the Capillary Pressure Curves Using the Centrifuge Technique", *Journal of Petroleum Science and Engineering*, (2002), 33, pp. 29-38

Masalmeh, S.K., "The Effect of Wettability Heterogeneity on Capillary Pressure and Relative Permeability", *Journal of Petroleum Science and Engineering*, (2003), 39, pp. 399-408

McDougall, S.R., and Sorbie, K.S., "The Impact of Wettability on Waterflooding: Pore-Scale Simulation", *SPE Reservoir Engineering*, (1995), 10(3), pp. 208-213

McKean, H. C. and Dawe, R.A., "Numerical Simulations of Displacements Containing a Lens Heterogeneity", *Journal of Canadian Petroleum Technology*, (1990), 29(6), pp. 88-93

Mirzaei, M., DiCarlo, D., Ashouripashaki, M., Dehghanpour, H., and Aminzadeh, B., "Prediction of Three-Phase Gravity Drainage from Two-Phase Capillary Pressure Curves", SPE paper 129945, presented at the 2010 SPE Improved Oil Recovery Symposium, Tulsa, Oklahoma, 24-28 April (2010)

Morgan, W.B., and Pirson, S. J., "The Effect of Fractional Wettability on the Archie Saturation Exponent", Trans. SPWLA, Fifth Annual Logging Symposium, Midland, TX, USA, 13-15 May (1964)

Morrow, N.R., and McCaffery F.G., "Displacement Studies in Uniformly Wetted Porous Media", in Wetting, Spreading and Adhesion, J.F. Padday (ed.), Academic Press, New York, (1978), pp. 289-319

Morrow, N.R. and Songkran, B., "Effect of Viscous and Buoyancy Forces on Non-Wetting Phase Trapping in Porous Media", in: Surface Phenomena in Enhanced Oil Recovery, D.O. Shah (ed.), Plenum Press, New York, (1981), pp. 387-411

Morrow, N.R., Chatzis, I., and Taber, J.J., "Entrapment and Mobilization of Residual Oil in Bead Packs", *SPE Reservoir Engineering*, 1988, 3(3), pp. 927-934

Morrow, N.R., "Wettability and Its Effect on Oil Recovery", *Journal of Petroleum Technology*, (1990), 42(12), pp. 1476-1484

Moss, A.K., and Jing, X.D., "Resistivity Index and Capillary Pressure Characteristics of Reservoir Sandstone in Different Wettability Conditions", Society of Core Analysis Conference, Paper Number 9945, (1999)

Motealleh, S., "Mechanistic Study of Menisci Motion within Homogeneously and Heterogeneously Wet Porous Media", Ph.D. Thesis, the University of Texas at Austin, Austin, TX, USA (2009)

Muggeridge, A.H., Jackson, M.D., Agbehi, O., Al-Shuraiqi, H., and Grattoni, C.A., "Quantifying Bypassed Oil in the Vicinity of Discontinuous Shales during Gravity-Dominated Flow", SPE paper 94134, presented at SPE Europec/EAGE Annual Conference, Madrid, Spain, June 13-16 (2005)

Muskat, M., Physical Principles of Oil Production, McGraw Hill, Boston, MA, (1949)

Nahara, G. M., Pozzi, A. L., and Blackshear, T. H., "Effect of Connate Water on Gas- Oil Relative Permeabilities for Water-Wet and Mixed-Wet Berea Rock", *SPE Advanced Technology Series*, (1993), 1(2), pp. 114-122

Nenniger, E., and Storrow, J.A., "Drainage of Packed Beads in Gravitational and Centrifugal-force Fields", *AIChE*, (1958), 4(3), 305-316

Nutting, P.G., "Some Physical and Chemical Properties of Reservoir Rocks Bearing on the Accumulation and Discharge of Oil", In: Problems of Petroleum Geology, Wrather, W.E., and Lahee, F.H., (eds.), AAPG, Tulsa, (1934)

Øren, P.E., Billiotte, J., and Pinczewski, W.V., "Mobilization of Waterflood Residual Oil by Gas Injection for Water-Wet Conditions", *SPE Formation Evaluation*, (1992), 25(7), pp. 70–78

Øren, P.E. and Pinczewski, W.V., "Effect of Wettability and Spreading on Recovery of Waterflood Residual Oil by Immiscible Gasflooding", *SPE Formation Evaluation*, (1994), 9(3), pp. 149–156

Pavone, D., Bruzzi, P., and Verre, R., "Gravity Drainage at Low Interfacial Tensions", 5th European Symposium on Improved Oil Recovery, April (1989)

Pedrera, B., Bertin, H., Hamon, G., and Augustin, A., "Wettability Effect on Oil Relative Permeability During a Gravity Drainage", SPE paper 77542, presented at the SPE/DOE 13th Symposium on Improved Oil Recovery, Tulsa, OK, April 13 – 17 (2002)

Piper, L.D., Morse, R.A., "Criteria for Displacement by Gas versus Water in Oil Reservoirs", SPE 10870, SPE Unsolicited Paper (1982)

Radler, M., and Bell, L., "US Energy Demand Growth Slows on Economic Sluggishness", *Oil & Gas Journal*, July (2011), 109(14), pp. 24-36

Rao, D.N., Girard, M., and Sayegh, S.G., "The Influence of Reservoir Wettability on Waterflood and Miscible Flood Performance", *Journal of Canadian Petroleum Technology*, 1992, 31(6), pp. 47-55

Rao, D.N., "Gas Injection EOR — A New Meaning in the New Millennium", *Journal of Canadian Petroleum Technology*, (2001), 40(2), pp. 11-18

Rao, D.N., Ayirala,S.C., Kulkarni, M.M., and Sharma, A.P., "Development of Gas Assisted Gravity Drainage (GAGD) Process for Improved Light Oil Recovery", SPE paper 89357, presented at the SPE/DOE 14th Symposium on Improved Oil Recovery, Tulsa, Oklahoma, 17-21 April (2004)

Rapoport, L.A., "Scaling Laws for Use in Design and Operation of Water-Oil Flow Models", *Petroleum Transactions AIME*, (1955), 204, pp. 143-150

Riazi, M., Alizadeh, A.H., and Haghighi, M., "Experimental Study of Gravity Drainage during Gas Injection in Carbonate Rocks", Canadian International Petroleum Conference, Calgary, Alberta, 13-15June (2006)

Sajadian, V.A., and Tehrani D.H., "Displacement Visualization of Gravity Drainage by Micromodel", SPE paper 49557, presented at the 8th Abu Dhabi International Petroleum Exhibition and Conference, Abu Dhabi, U.A.E, 11-14 November (1998)

Schechter, D.S., Guo, B., "Mathematical Modeling of Gravity Drainage after Gas Injection into Fractured Reservoirs", SPE paper 35170, presented at the Permian Basin Oil and Gas Recovery Conference, Midland, Texas, 27-29 March (1996)

Shook, M., Li, D., Lake, L.W., "Scaling Immiscible Flow through Permeable Media by Inspectional Analysis", *In-Situ,* (1992) 16(4), pp. 311–349

Skauge, A., Eleri, O. O., Graue, A., and Monstad, P., "Influence of Connate Water on Oil Recovery by Gravity Drainage", SPE/DOE paper 27817, presented at the SPE/DOE 9th Symposium on Improved Oil Recovery, Tulsa, OK, April 17 – 20 (1994)

Skauge, A., "Comparing Core Analysis Data to Field Observations for Gravity Drainage Gas Injection", paper SCA-9904, in 1999 International Symposium Proceedings, Society of Core Analysts, (1999)

Skauge, A., and Paulsen, S., "Rate Effects on Centrifuge Drainage Relative Permeability", SPE paper 63145, presented at the SPE Annual Technical Conference and Exhibition, Dallas, Texas, 1-4 October (2000)

Stahl, R.F., Martin, W.A., and Huntington, R.L., "Gravity Drainage of Liquids from Unconsolidated Wilcox Sands", *Trans. AIME*, (1943), 151, pp. 138-146

Sweeney, S. A., and Jennings Jr., H. Y., "Effect of Wettability on the Electrical Resistivity of Carbonate Rock from a Petroleum Reservoir", *J. Phys. Chem.*, (1960), 64, pp. 551–553

Szymkiewicz, A., Helmig R., and Kuhnke H., "Two-Phase Flow in Heterogeneous Porous Media with Non-Wetting Phase Trapping", *Transport in Porous Media*, (2010), 86(1), pp. 27-47, doi: 10.1007/s11242-010-9604-x

Takach, N.E., Bennett, L.B., Douglas, C.B., Andersen, M.A., and Thomas, D.C., "Generation of Oil-Wet Model Sandstone Surfaces", SPE paper 18465, presented at the SPE International Symposium on Oilfield Chemistry in Houston, TX, February 8-10 (1989)

Takamura, K., and Chow, R.S., "A Mechanism for Initiation of Bitumen Displacement from Oil Sand", *Journal of Canadian Petroleum Technology*, (1983), 22, pp. 20-30

Takamura, K., Loahardjo, N., Winoto, W., Buckley, J., Morrow, N.R., Kunieda, M., Liang, Y., and Matsuoka, T.: "Spreading and Retraction of Spilled Crude Oil on Seawater", Chapter in Crude Oil/Book 2, published by InTech - Open Access, scheduled publication date: March 2012

Templeton, E.E. Nielsen, R.F., and Stahl, C.D., "A Study of Gravity Counterflow Segregation", *SPE Journal*, (1962), 2(2), pp. 185-193

Terwilliger, P.L., Wiley, L.E., Hall, H.N., Bridges, P.M., and Morse, R.A., An Experimental and Theoretical Investigation of Gravity Drainage Performance, *Trans. AIME*, (1951), 192, pp. 285-296

Tsakiroglou, C.D., and Fleury, M., "Resistivity Index of Fractional Wettability Porous Media", *Journal of Petroleum Science and Engineering*, (1999), 22, pp. 253-274

Vizika, O., and Lombard J.M., "Wettability and Spreading: Two Key Parameters in Oil Recovery with Three-Phase Gravity Drainage", *SPE Reservoir Engineering,* (1996), 11(1), pp. 54-60

Vizika, O., and Duouerroix, J.P., "Gas Injection and Heterogeneous Wettability: What Is the Relevant Information That Petrophysics Can Provide", paper SCA-9708, presented at the 1997 International Symposium, Calgary, 7-10 September (1997)

Wylie, P.L., and Mohanty, K.K., "Effect of Wettability on Oil Recovery by Near-Miscible Gas Injection", *SPE Reservoir Evaluation & Engineering*, (1999), 2(6), pp. 558-564

Appendix A

Table A. 1: Oil recovery factor versus time for three levels of permeability heterogeneity and withdrawal rate of 2.0 mL/h

0% heterogeneity		17% heterogeneity		38% heterogeneity	
time (h)	oil recovery factor ($\%S_{or}^{*}$)	time (h)	oil recovery factor ($\%S_{or}^{*}$)	time (h)	oil recovery factor ($\%S_{or}^{*}$)
0.00	0.00	0.00	0.00	0.00	0.00
37.58*	0.00	31.95*	0.00	26.63*	0.00
39.30	22.08	33.87	18.22	28.91	17.42
40.26	33.12	34.45	23.56	29.59	21.97
41.64	50.00	35.10	28.89	30.18	26.52
42.04	55.84	35.67	34.22	31.83	38.64
42.41	60.39	36.10	37.78	32.43	43.18
42.85	66.23	36.67	42.67	33.02	47.73
43.12†	69.48	37.17	47.11	33.55	51.14
		37.80	52.44	34.22	56.06
		38.38	57.78	34.69	59.09
		38.98	62.67	35.27	63.64
		39.56	68.00	35.77	67.05
		40.50†	76.00	36.61	73.48
				37.13	76.89
				37.63	80.68
				37.97†	83.33

*time of oil breakthrough
†time of gas breakthrough

Table A. 2: Oil recovery factor versus time for three levels of permeability heterogeneity and withdrawal rate of 6.4 mL/h

0% heterogeneity		17% heterogeneity		38% heterogeneity	
time (h)	oil recovery factor ($\%S_{or}^{*}$)	time (h)	oil recovery factor ($\%S_{or}^{*}$)	time (h)	oil recovery factor ($\%S_{or}^{*}$)
0.00	0.00	0.00	0.00	0.00	0.00
12.00*	0.00	9.85*	0.00	8.07*	0.00
12.61	23.17	10.17	8.89	9.80	38.08
12.83	31.10	10.35	12.44	9.98	42.31
12.98	37.20	10.57	17.78	10.15	46.15
13.20	43.90	10.72	21.78	10.33	50.00
13.39	51.22	11.01	28.89	10.50	53.46
13.46†	53.66	11.23	34.22	10.67	57.31
		11.38	38.67	11.00	65.38
		11.63	45.78	11.17	70.00
		11.98	54.22	11.32†	73.46
		12.13	58.22		
		12.28†	61.78		

*time of oil breakthrough
†time of gas breakthrough

Table A. 3: Oil recovery factor versus time for three levels of permeability heterogeneity and withdrawal rate of 12.0 mL/h

0% heterogeneity		17% heterogeneity		38% heterogeneity	
time (h)	oil recovery factor ($\%S_{or}^{*}$)	time (h)	oil recovery factor ($\%S_{or}^{*}$)	time (h)	oil recovery factor ($\%S_{or}^{*}$)
0.00	0.00	0.00	0.00	0.00	0.00
6.47*	0.00	5.15*	0.00	4.45*	0.00
6.76	22.84	5.48	16.74	4.82	16.43
6.80	25.93	5.64	23.53	5.00	22.73
6.86	30.25	5.73	27.60	5.17	28.67
6.90†	33.33	5.83	31.67	5.34	34.97
		5.93	36.65	5.49	40.91
		6.15	47.51	5.67	47.55
		6.25†	52.49	5.83	54.20
				5.92	57.69
				5.93†	58.04

Table A. 4: Gas–liquid interface position for packed column containing different levels of permeability heterogeneity and withdrawal rate of 3.2 mL/h

0% Heterogeneity		17% Heterogeneity		38% Heterogeneity	
time (h)	Gas–liquid interface position (cm)	time (h)	Gas–liquid interface position (cm)	time (h)	Gas–liquid interface position (cm)
0.0	42.0	0.0	42.0	0.0	41.7
2.00	37.5	4.00	34.5	2.00	38.3
5.00	32.0	17.00	14.6	4.00	33.7
7.25	28.7	19.00	11.3	5.00	31.8
13.00	20.6	21.00	7.3	7.08	28.5
15.00	17.6	23.50	3.6	9.00	25.8
17.00	14.9			11.08	22.6
18.00	13.3			13.00	18.0
20.00	10.6			15.00	15.8
22.00	7.9			16.50	12.5
24.00	5.4			18.50	8.9
25.00	3.8			21.03	4.2
26.00	2.2			22.50	1.4

Table A. 5: Gas–liquid interface position for packed column containing different levels of permeability heterogeneity and withdrawal rate of 6.4 mL/h

0% Heterogeneity		17% Heterogeneity		38% Heterogeneity	
time (h)	Gas–liquid interface position (cm)	time (h)	Gas–liquid interface position (cm)	time (h)	Gas–liquid interface position (cm)
0.0	41.8	0.0	42.0	0	42
1.00	37.2	1.00	37.2	1.3	37.1
2.00	33.1	2.80	32.7	2.00	33.8
3.00	29.6	3.08	29.9	3.00	29.6
4.10	26.3	4.50	25.8	4.00	27.3
5.00	23.7	6.02	21.8	5.00	24.3
7.10	18.6	7.00	18.1	5.50	22.3
8.00	15.9	8.03	15.6	6.50	18.6
10.50	8.2	9.03	11.8	7.00	16.5
12.00	4.4	10.00	8.4	8.00	13.6
13.00	1.3	10.55	6.0	9.43	9.0
		11.67	2.2	10.00	6.4
		12.17	0.5	11.00	2.1

Table A. 6: Gas–liquid interface position for packed column containing different levels of wettability heterogeneity and withdrawal rate of 3.2 mL/h

0% Heterogeneity		17% Heterogeneity		38% Heterogeneity	
time (h)	Gas–liquid interface position (cm)	time (h)	Gas–liquid interface position (cm)	time (h)	Gas–liquid interface position (cm)
0.00	41.8	0.00	42.1	0.00	41.7
2.00	38.5	1.08	40.1	1.67	38.7
17.00	17.2	2.00	37.5	3.83	34.2
20.00	13.5	3.00	36.2	6.33	30.4
22.00	10.1	4.00	35.0	7.33	28.8
24.00	7.3	5.00	33.4	8.33	27.2
26.00	4.7	6.00	31.8	9.33	25.3
28.00	1.8	7.00	30.0	11.00	23.1
		8.00	28.6	13.00	19.3
		9.00	27.3	14.00	17.3
		10.07	25.6	16.00	14.5
		11.08	24.2	17.00	12.3
		12.00	22.7	18.00	11.3
		13.00	21.1	19.00	9.3
		14.00	19.3	20.00	7.8
		15.00	17.6	21.00	5.5
		16.00	16.5	22.00	3.5
		17.00	15.2	23.00	1.4
		18.00	13.3		
		20.00	10.3		
		21.00	8.7		
		22.00	6.8		
		23.00	4.7		
		24.00	3.1		
		25.00	1.4		

Table A. 7: Gas–liquid interface position for packed column containing different levels of wettability heterogeneity and withdrawal rate of 8.0 mL/h

0% Heterogeneity		17% Heterogeneity		38% Heterogeneity	
time (h)	Gas–liquid interface position (cm)	time (h)	Gas–liquid interface position (cm)	time (h)	Gas–liquid interface position (cm)
0.00	41.8	0.00	42.0	0.00	41.8
1.00	40.8	1.00	41.0	1.23	40.6
2.00	39.8	2.05	40.0	2.00	39.8
3.00	38.8	3.00	39.0	3.00	38.8
4.00	37.8	4.03	38.0	4.00	37.8
5.50	36.3	5.00	37.0	5.00	36.8
7.00	34.8	6.00	36.0	6.33	35.5
8.00	33.8	7.00	35.0	7.00	34.8
9.00	32.8	8.05	34.0	7.50	34.3
9.53	32.3	8.52	33.5	8.00	33.8
10.00	31.8	9.05	33.0	8.52	33.3
10.50	31.3	9.50	32.5	9.00	32.8
		10.00	32.0		